JUSTUS-LIEBIG-
UNIVERSITÄT
GIESSEN

Plasmodium falciparum Glucose 6-Phosphate Dehydrogenase-6-Phosphogluconolactonase. Characterisation of Redox-Related Networks as Contribution to the Development of Novel Intervention Strategies

by

Mailu Boniface Mwongela

from

Mombasa, Kenya

A thesis submitted to the Faculty of Biology and Chemistry (FB 08) in partial fulfilment for the requirements of the Doctor of Science Degree of Justus-Liebig-University Giessen, Germany

September 2008

Declaration

I declare that this thesis is my original work and that it has not been previously presented in this or any other university for any degree.

Dedication

This thesis is dedicated to my daughter Lynn Ndimu Mwongela, my son Liam Musyimi Jnr III[rd] Mwongela, my wife Grace C. Mwangome and the entire Musyimi family.

You all inspire my life to live the dream.

I Have a Dream. . . . . .

(Martin Luther King Jnr, August 28th, 1963)

The thesis was presented to the faculty of Biology and Chemistry of the Justus-Liebig University Giessen, Germany for examination on the 11th September 2008 and the thesis defence was on the 5th November 2008.

The thesis defence jury was composed of

Prof. Dr. Gabriele Klug
Institute for Microbiology and Molecular Biology
Interdisciplinary Research Centre (IFZ)
Heinrich-Buff-Ring 26-32
35392 Giessen
Germany

Prof. Dr. Med. Katja Becker
Institute for Nutritional Biochemistry
Interdisciplinary Research Centre (IFZ)
Heinrich-Buff-Ring 26-32
35392 Giessen
Germany

Prof. Dr. Rudolf Geyer
Institute of Medical Biochemistry
Friedrichstr. 24
35392 Giessen
Germany

Acknowledgements

Many individuals have contributed to the overall research achievements reported herein. My sincere gratitude goes to my supervisors, Prof. Dr. med Katja Becker and Prof. Dr. Gabrielle Klug. I would like to especially thank Prof. Katja Becker who apart from her guidance and hosting me in her research group, shared with me her wide experience in redox metabolism of the malaria parasite *Plasmodium falciparum*. I extend my heartfelt and sincere thanks for her excellent supervision, fruitful ideas, valuable advice and encouragement during the period of my study.

I am greatly indebted to all distinguished members of Prof Becker's research group both past and present members (2005-2008), who assisted me with invaluable counsel in the course of this study. Specifically many thanks go to Dr. Stefan Rahlfs who was my officemate and collaborator in all the studies, Dr. Rimma Iozef (once a chemist like me) who cloned the human 6-PGL and was a great source of inspiration and encouragement, Marina Fischer for the hands on experience on enzyme assays, Elisabeth Fischer for the great experience in *P. falciparum* cell culture, Beate Hecker thanks for your help and experience in IDO assays and gel filtration, Michaela Stumpf with the help of your magic hands we have *Pf*GluPho crystals, Kathleen Zocher thanks for your protein modelling experience, Ulrike B Z for the help with graphics, Sabine Ettinger and Santhosh Maddila for their wonderful contribution in the characterisation of *Pf*GluPho and Tim Bostick for helping in proofreading my manuscripts. To my fellow Ph.D colleagues K Buchholz, N Hiller, A Röseler, E Jortzik, S Koncarevic, K Sebastian thank you all. To all the other members of the group Doris, Antje and Raphael I appreciate the help I recived from you in the couse of this study.

It would have been an uphill task to carry out this research without the assistance of the Deutscher Akademischer Austausch Dienst (DAAD) who helped finance not only my stay in Germany throughout my study period but also the four months language course in Marburg.

Above all I am greatly indebted to my parents Mr. and Mrs. D. M. Musyimi and all my brothers, sisters and their families for their sacrifices, encouragement, patience, support and understanding during the course of this study. I extend my heartfelt and sincere thanks to Dr. P.L. M. Githua and Dr. M. N. Mwangome for their relentless support and encouragement throughout the course of this study.

Finally my heart felt gratitude to my wife Grace C. Mwangome, my daughter Lynn Ndimu Mwongela and my son Liam Musyimi Jnr III Mwongela for their sacrifices, patience, understanding and encouragement throughout this study.

List of Publications

Buchholz K, **Mailu B M**, Schirmer R H, Becker K. **(2007)**. Structure based drug development against malaria. *Frontiers in Drug Design and Discovery*, **3**: 225-255.

Rahlfs S, Koncarevic S, Iozef R, **Mailu B M**, Savvides S N, Schirmer R H, Becker K. **(2008)**. Myristoylated adenylate kinase 2 of *Plasmodium falciparum* forms a heterodimer with myristoyl transferase. *Mol. Biochem. Parasitol*. **In press**.

Sturm N, **Mailu B M**, Jortzik E, Koncarevic S, Deponte S, Rahlfs S, Forchhammer K, Becker K. **(2008)**. Identification of proteins targeted by the thioredoxin superfamily in *Plasmodium falciparum*. *PLoS Pathogens* **Submitted.**

Austin C J D, **Mailu B M**, Maghzal G J, Sanchez-Perez A, Rahlfs S, Zocher K, Arthur J, Becker K, Stocker R, Hunt N H, Ball H J. **(2008)**. Recombinant mouse Indoleamine 2,3-dioxygenase like protein (rmIDO-2) utilise cytochrome b5 for optimal activity. *Biochemistry J*. **Submitted.**

Mailu B M, Rahlfs S, Becker K. **(2008)**. Heterologous overexpression and characterisation of glucose 6-phosphate dehydrogenase-6-phosphogluconolactonase from *Plasmodium falciparum*. **In preparation.**

Conferences and Scientific Meetings

Mailu B M, Rahlfs S, Austin C J D, Hunt N H, Becker K. **(2006)**. Further optimisation of the heterologous overexpression of mouse indoleamine 2, 3-dioxygenase. *22 Jahrestagung der Deutschen Gesellschaft für Parasitologie*, Wien, February 2006.

Mailu B M, Rahlfs S, Austin C J D, Hunt N H, Becker K. **(2006)**. Optimisation of the heterologous overexpression of mouse indoleamine 2, 3-dioxygenase. *Second joint Ph.D Students Meeting of the Collaborative Research Centres SFB 544 Heidelberg and SFB 630 Würzburg*, Heidelberg, November 2006.

Austin C J D, **Mailu B M**, Sanchez-Perez A, McQuillan J, Astelbauer F, Rahlfs S, Aurther J, Becker K, Ball H J, Hunt N H. **(2007)**. Indoleamine 2, 3-dioxygenase like protein 1 (INDOL 1). A novel heme containing tryptophan catabolising enzyme. *IUPAC Conference*, Turin Italy, July 2007.

Mailu B M, Hiller N, Fritz-Wolf K, Rahlfs S, Becker K. **(2007)**. Interference with redox active proteins as a basis for the design of antimalarial drugs. *Drug Development Seminar*, Tübingen, April 2007.

Mailu B M, Rahlfs S, Becker K. **(2008)**. Glucose 6-phosphate dehydrogenase-6-phosphogluconolactonase from *Plasmodium falciparum*. *Jahrestagung der Deutschen Gesellschaft für Parasitologie*, Hamburg, March 2008.

Summary

Plasmodium parasites are developing unacceptable levels of resistance to one drug after another and many insecticides are no longer useful against mosquitoes transmitting the disease. Years of vaccine research have produced few hopeful candidates and although scientists are redoubling the search, an effective vaccine is at best years away. Therefore there is need for identification of new drug targets and alternative antimalarial regimes. In response to this dire situation the study aimed at evaluating the pentose phosphate pathway of the malaria parasite *P. falciparum* in particular the bifunctional enzyme glucose-6-phosphate dehydrogenase-6-phosphogluconolactonase, understanding the kynurenine pathway of tryptophan metabolism in particular the enzymes indoleamine 2,3-dioxygenase (1 and 2) and unravelling more knowledge about the thioredoxin system networks in search for a new potential drug target and new drug alternatives.

The first two steps of the pentose phosphate pathway in *Plasmodium falciparum* are catalysed by the enzyme glucose 6-phosphate dehydrogenase-6-phosphogluconolactonase (*Pf*GluPho) which is a unique bifunctional enzyme exclusively found in the genus *Plasmodium*. In spite of the importance of the role this enzyme plays in the parasite's pentose phosphate pathway as well as in overcoming oxidative stress, the characteristics of *Pf*GluPho are still a mystery. For the first time *Pf*GluPho has been successfully cloned, heterologously overexpressed and purified to homogeneity. The recombinant enzyme was found to be a hexamer which exhibits lower K_m values that favour substrate turnover by the parasite enzyme when compared to the human homologue. The steady state kinetics of *Pf*GluPho's glucose-6-phosphate dehydrogenase (*Pf*GluPho's G6PD) demonstrates that the enzyme follows an ordered sequential mechanism with $NADP^+$ being the leading substrate. Three novel inhibitors of *Pf*GluPho's G6PD which are active at the lower micromolar range were identified and found to be non-competitive with respect to glucose-6-phosphate and $NADP^+$. The study offers the first clear documentation of the cloning, heterologous overexpression, biochemical as well as kinetic characterisation, crystallisation and the first novel inhibitors of *Pf*GluPho.

For 30 years, the established dogma regarding tryptophan catabolism was that the first step of the kynurenine pathway, the cleavage of the 2,3–double bond of the indole ring of tryptophan was performed by two enzymes, indoleamine 2,3-dioxygenase-1 (IDO-1) and tryptophan 2,3-dioxygenase (TDO). Recently, indoleamine 2,3-dioxygenase-2 (IDO-2) a third enzyme capable of performing this reaction has been discovered. Reported here is a study of the kinetic activity, pH stability, oligomeric structure as well as secondary structural features of recombinant mouse IDO-2 in direct comparison with mouse IDO-1. A screen for new more potent inhibitors of IDO-1 which lack the indole core and avoid the liability arising from the use of indole derivatives which have been reported to be neuroactive gave rise to compound 55D11 (K_i 0.05 μM) which is more potent than the already existing IDO inhibitors. A structure activity study was done using various derivatives of compound 55D11 to determine

the elements that could be modified to increase potency. The study clearly demonstrates that IDO-1 and IDO-2 differ significantly in terms of their affinity for substrates as well as structure.

The malarial parasite *Plasmodium falciparum* possesses a functional glutathione and thioredoxin system comprising the redox-active proteins thioredoxin (Trx), glutaredoxin (Grx), and plasmoredoxin (Plrx) which all belong to the thioredoxin superfamily and share the active site motif Cys-X-X-Cys. A better understanding of the role of these members of the thioredoxin superfamily in *P. falciparum* as well as other systems could be achieved if more was known about their target proteins. Using thioredoxin affinity chromatography prepared by immobilising mutants of the redoxins lacking the resolving cysteine at the active site on $CNBr^-$ activated sepharose, target proteins of *P. falciparum* cell extract were trapped. The covalently linked proteins were eluted with dithiothreitol and analyzed by matrix assisted laser desorption ionization time of flight (MALDI-TOF). Twenty one potential targets were identified for plasmoredoxin. Besides confirming known interacting proteins, potential target candidates involved in processes such as; protein biosynthesis, energy metabolism and signal transduction were identified. Further confirmations of the interaction of plasmoredoxin and the target proteins were done using BIAcore surface plasmon resonance experiments.

Zusammenfassung

Der Malaria-Parasit *Plasmodium* entwickelt bemerkenswert hohe Resistenzen gegenüber einem Medikament nach dem anderen. Außerdem verlieren viele Insektizide, die gegen die Überträger-Moskitos eingesetzt werden, an Wirkung. Jahrelange Forschung an Impfstoffen gegen Malaria hat bisher nur wenige hoffnungsvolle Kandidaten erbracht und obwohl Wissenschaftler Ihre Bemühungen verstärken, ist eine effektive Impfung bestenfalls immer noch Jahre entfernt. Deshalb sind dringend neue Zielmoleküle für die Medikamenten-entwicklung zu identifizieren, die zu alternativen Behandlungsmethoden führen können. Diese Situation vor Augen, waren es Ziele dieser Arbeit, i) das bifunktionelle Enzym Glukose-6-Phosphatdehydrogenase-6-Phosphogluconolactonase aus dem Pentosephosphat-weg des Parasiten als potentielles Wirkungsziel zu bestätigen, ii) den Kynurenin-Stoffwechselweg, insbesondere die Enzyme Indolamin 2,3-Dioxygenase (1 und 2) der Maus als Modell näher zu charakterisieren und iii) mehr über das Redox-Netzwerk des Malariaparasiten zu erfahren, um neue mögliche Zielmoleküle aufzuzeigen.

Die ersten zwei Schritte des Pentosephosphatweges werden in *Plasmodium falciparum* durch das Enzym Glukose-6-Phosphatdehydrogenase-6-Phosphogluconolactonase (*Pf*GluPho) katalysiert. Dieses ist ein einzigartiges bifunktionelles Enzym, das bisher nur in *Plasmodien* gefunden wurde. Obwohl diesem Enzym im Pentosephosphatweg des Parasiten und damit auch in der Bekämpfung oxidativen Stresses eine enorme Bedeutung zukommt, ist das Enzym aus *P. falciparum* nicht besonders gut charakterisiert, da es bisher nicht kloniert werden konnte. Zum ersten Mal konnte *Pf*GluPho jetzt kloniert und überexprimiert werden und das Genprodukt konnte bis zur Reinheit gebracht werden. Es wurde gezeigt, dass das rekombinante Enzym als Hexamer vorliegt, welches niedrigere Km-Werte im Vergleich zu seinen humanen Orthologen aufweist, die einen bevorzugten Substratumsatz durch das parasitäre Enzym aufzeigen. Kinetische Untersuchungen zeigen, dass der Glukose-6-Phosphatdehydrogenase (G6PD)-Teil von *Pf*GluPho einem geordneten Mechanismus folgt, bei dem $NADP^+$ das erste Substrat ist. Drei neue Inhibitoren, die den G6PD-Teil des Enzym im unteren mikromolaren Konzentrationsbereich hemmen, konnten gefunden werden und zeigten sich gegenüber Glukose-6-Phosphat und $NADP^+$ als nicht-kompetitiv. Somit zeigt diese Arbeit die Klonierung, heterologe Expression, biochemische und kinetische Charakterisierung von *Pf*GluPho auf, sowie darüberhinaus die Kristallisation und erste, neue Inhibitoren.

Seit 30 Jahren ist es ein etabliertes Dogma, dass im Tryptophan-Katabolismus der erste Schritt des Kynurenin-Stoffwechselweges die 2,3-Doppelbindung des Indolringes des Tryptophans durch zwei Enzyme gespalten werden kann: einerseits durch Indolamin 2,3-Dioxigenase (IDO), anderseits durch Tryptophan 2,3-Dioxigenase (TDO). Kürzlich konnte mit IDO-2 ein drittes Enzym in der Maus und im Menschen entdeckt werden, das in der Lage ist, diese Reaktion zu vollziehen. In dieser Arbeit sind Daten zur Kinetik, pH-Stabilität, zu oligomeren Strukturen, sowie Besonderheiten der Sekundärstruktur von rekombinanter IDO-2

der Maus im direkten Vergleich mit rekombinanter IDO-1 der Maus erhoben worden. Die Suche nach neuen, effektiveren Inhibitoren für IDO-1, die den Indolkern nicht mehr besitzen und somit weniger neurotoxisch sein könnten, führte zu 55D11 (K_i 0,05 µM), einer Substanz aus einer öffentlichen Sammlung von Naturstoffen. Zahlreiche Derivate von 55D11 wurden untersucht, um Molekülreste zu zeigen, die verändert werden können und die Aktivität noch erhöhen. Die Untersuchungen zeigen, dass sich IDO-1 und IDO-2 eindeutig hinsichtlich ihrer Affinität zu Substraten, aber auch in ihrer Struktur unterscheiden.

Der Malaria-Parasit *Plasmodium falciparum* besitzt ein funktionelles Glutathion-, sowie ein Thioredoxin-System, die unter anderem aus den redox-aktiven Proteinen Thioredoxin (Trx), Glutaredoxin (Grx) und Plasmoredoxin (Plrx) bestehen, die alle zur sogenannten Thioredoxin-Superfamilie gehören und das Motiv Cys-X-X-Cys im aktiven Zentrum besitzen. Wenn mehr Interaktionspartner dieser Redoxproteine bekannt wären, könnte die jeweilige Rolle der Redoxine in ihrem Netzwerk besser verstanden werden. Deshalb wurden Thioredoxin-Affinitätschromatographien an $CNBr^-$-aktivierter Sepharose durchgeführt. Hierzu wurden immobilisierte Mutanten der Redoxine, denen das sogenannte „*resolving cysteine*“ aus ihrem aktiven Zentrum fehlt, mit Zellextrakt aus *P. falciparum* versetzt. Kovalent an die Fängerproteine (Redoxine) gebundene Reaktanden wurden mit Dithiothreitol eluiert und mittels (Maldi-ToF) analysiert. Einundzwanzig potentielle Zielproteine wurden für Plasmoredoxin als mögliche Interaktionspartner identifiziert. Neben bekannten Interaktionspartnern waren darunter auch Kandidaten, die eine mögliche Redoxregulierung der Proteinbiosynthese, des Energiemetabolismus sowie der Signaltransduktion in *Plasmodium* vermuten lassen können. Weitere Untersuchungen, um diese Wechselwirkungen zu bestätigen, wurden mit Plasmoredoxin und einigen seiner potentiellen Interaktionspartner mithilfe von BIACORE Oberflächen-Resonanzexperimenten durchgeführt.

Table of Contents

List of Figures

List of Tables

List of Abbreviations

aa	amino acid	FP	ferri/ferroprotoporphyrin IX
ATP	adenosine triphosphate	FAD	flavin adenine dinucleotide
ATP-Ribose	adenosine triphosphate-ribose		
ALA	δ-aminolevulinic acid	g	gram
APS	ammoniumpersulfate	Gly	glycine
BSA	bovine serum albumin	HMS	hexose monophosphate shunt
		His	histidine
cpm	counts per minute		
Ci	Curie	IDO	indoleamine 2,3-dioxygenase
Cys	cysteine	IC	inhibitory concentration
		IFNγ	interferon-gamma
Da	Dalton	ITNs	insecticide treated nets
Φ	Dalziel constant ($1/k_{cat}$)	IPTG	isopropyl-β-D-thiogalactopyranoside
^{o}C	degree centigrade		
DeoxyG6P	deoxyglucose-6-phosphate		
DNA	deoxyribonucleic acid	kDa	kilodalton
DNase	deoxyribonuclase	KA	kynurenic acid
dNTP	deoxyribonucleotide triphosphate	l	liter
DDT	dichlorodiphenyl trichloroethane	LB	Luria-Bertani media
DMSO	dimethylsulfoxide	K_m	Michaelis constant
DTT	1, 4-dithiothreitol	µg	microgram
H_2O_{dd}	double distilled water and	µl	microliter
autoclaved	autoclaved	µM	micromolar
		mg	milligram
EMP	Embden Meyerhof Parnas	ml	milliliter
E. coli	*Escherichia coli*	mM	millimolar
et al	*et alii* and others	mU	milliunits
EDTA	ethylene diamine tetraacetic acid	min	minute
		M	molar (mol/l)
		MW	molecular weight

nm	nanometer
Ni-NTA	nickel nitrilotriacetic acid
$NADP^+$	nicotinamide adenine dinucleotide phosphate (oxidised)
NADPH	nicotinamide adenine dinucleotide phosphate (reduced)
NMDA	*N*-methyl-*D*-aspartate
OD	optical density
p-DMAB	*p*-dimethylaminobenzaldehyde
PPP	pentose phosphate pathway
PMSF	phenylmethylsulfonylflouride
6-PGL	6-phosphogluconolactonase
6-PG-δ-L	6-phosphoglucono-δ-lactone
6-PGn	6-phosphogluconolactonate
6-PGD	6-phosphogluconolactonate dehydrogenase
*Pf*GluPho	*Plasmodium falciparum* glucose-6-phosphate dehydrogenase-6-Phosphogluconolactonase
PCR	polymerase chain reaction
PVDF	polyvinyl difluoride
QA	quinolinic acid
RBC	red blood cells
ROS	reactive oxygen species
rpm	revolutions per minute
RNA	ribonucleic acid
SDS	sodium dodecyl sulphate
SOD	superoxide dismutase
SDS-PAGE	sodium dodecyl sulphate polyacrylamide gel electrophoresis
TB	terrific Broth medium
Trx	thioredoxin
TrxR	thioredoxin reductase
TDO	tryptophan 2,3 dioxygenase
TNF	tumor necrosis factor
U	enzyme activity (µmol/min)
WHO	World Health Organisation

1 Introduction

1.1 Malaria

Malaria is a life-threatening parasitic disease transmitted by mosquitoes. The term malaria is derived from the Italian word "mal'aria", which means 'bad air', from the early association of the disease with marshy areas. In 1880, Charles Louis Alphonse Laveran discovered that the real cause of malaria was a single cell parasite called *Plasmodium*. Later Dr. Ronald Ross discovered that the parasite was transmitted from one person to another through the bite of a mosquito and the Italian professor Giovanni Battista Grassi subsequently showed that human malaria could only be transmitted by female *Anopheles* mosquitoes which require blood to nurture their eggs.

Today more than 2 billion people (approximately 40% of the world's population) are at risk of contracting malaria with 300-660 million clinical cases of malaria and over 1.3 million deaths reported to occur per annum [Snow *et al*., 2005]. Ninety per cent of deaths due to malaria occur in Africa south of the Sahara mostly among young children where malaria kills an African child every 30 seconds. Many children who survive an episode of severe malaria may suffer from learning impairments or brain damage [Snow *et al*., 2004]. Pregnant women and their unborn children are also particularly vulnerable to malaria, which is a major cause of perinatal mortality, low birth weight and maternal anaemia.

There are four *Plasmodium* species that infect humans (*Plasmodium vivax*, *Plasmodium malariae*, *Plasmodium ovale* and *Plasmodium falciparum*) and can be distinguished by morphology. *Plasmodium ovale* and *P. malariae* are not lethal and are rare, most commonly found in parts of Africa and Papua New Guinea. *Plasmodium vivax* and *P. falciparum* are the two most prevalent species worldwide and *P. falciparum* causes the most deadly type of malaria infection. *Plasmodium falciparum* malaria is endemic in Africa, accounting in large part for the extremely high mortality in this region. South and East Asia, South America, the Caribbean, and the Middle East also experience *P. falciparum* malaria. There are also worrying indications of the spread of *P. falciparum* malaria into new regions of the world and its reappearance in areas where it had been eliminated. *Plasmodium vivax* is typically nonlethal and endemic in India, Latin America, and parts of the Eastern Mediterranean [Daily, 2006].

Malaria has a broad distribution in both the subtropics and tropics, with many areas of the tropics where the temperature and rainfall are most suitable for the development of the malaria causing *Plasmodium* parasites in *Anopheles* mosquitoes being endemic for the disease. The countries of sub-Saharan Africa account for the majority of all malaria cases. Malaria once occurred widely in temperate areas, including Western Europe and the United States, but it receded with economic development and public health measures. The disease was finally eliminated in the United States between 1947 and 1951 through a campaign that included household spraying of the residual insecticide dichlorodiphenyl trichloroethane (DDT) throughout the southeastern states [Zucker, 1996].

The Global Malaria Eradication Programme was launched by the WHO in 1955 [WHO, 1999] and depended on two key tools: chloroquine for treatment and prevention and DDT for vector control. Implementation of these tools had a substantial impact in some areas, particularly areas with relatively low transmission rates, such as India and Sri Lanka [WHO, 1999]. Despite these successes, the campaign foundered in the face of lost political will and the emergence of chloroquine resistant *Plasmodium* parasites and DDT resistant *Anopheles* mosquitoes. Global eradication was officially abandoned as a goal in 1972 [Brito, 2001]. Furthermore, the campaign never attempted to eradicate malaria in most parts of Africa, where malaria transmission is intense.

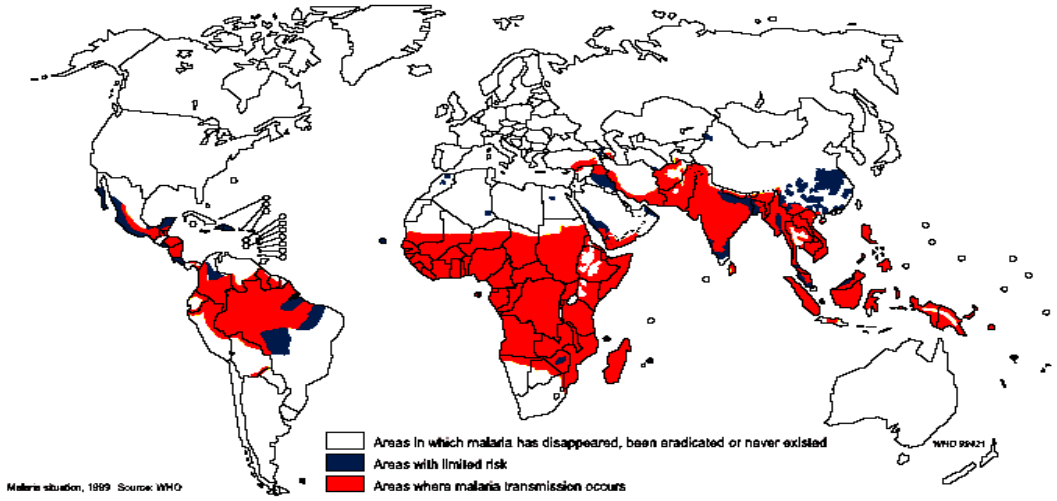

Figure 1: Global distribution of malaria [WHO, 2007]

Since the Global Malaria Eradication Programme ended, the burden of malaria increased substantially in many parts of the world, and the resurgence of malaria has sometimes been dramatic, such as the epidemics in Sri Lanka (1968–1969) and in Madagascar (1987–1988) [Roberts *et al*., 2000]. Childhood deaths in Africa due to malaria have increased relentlessly as chloroquine resistant *Plasmodium* parasites spread across the continent [Snow *et al*., 2001]. The rapid emergence of *Plasmodium* parasites resistant to sulfadoxine pyrimethamine (Fansidar®) soon after this drug replaced chloroquine as first-line therapy in many parts of Africa can be described as a disaster in Africa [White *et al*., 1999].

Vector control intervention using insecticide treated nets (ITNs) or long lasting insecticide treated nets (LLINs) has been reported to reduce clinical episodes of malaria caused by *P. falciparum* and *P. vivax* infections by 50 % on average (range 39–62 %), as well as reducing the prevalence of high density parasitemia. ITNs reduce child mortality due to malaria by an average 18 % (range 14–29 %) in sub-Saharan Africa [WHO, 2007; Killeen *et al*., 2007; Clarke *et al*., 2001; Lengeler, 2004]. The general implication is that 5.5 lives could be saved per year for every 1000 children under 5 years of age. Although ITNs are a success in terms of vector control interventions there are many teething problems that have to be overcome before their potential can be fully realised. For instance in most malaria endemic

countries, ITN coverage is still below agreed targets. This has lead to the ITNs use to be limited to young children and pregnant women who are the most vulnerable groups. Currently, most mosquito nets are made of polyester and rarely last long. They are therefore easily compromised due to their poor physical condition under field situations. Besides, the cost of ITNs is still beyond the reach of communities living in areas where malaria is endemic [WHO, 2007].

Science still has no magic bullet for malaria, the *Plasmodium* parasites are developing unacceptable levels of resistance to one drug after another and many insecticides are no longer useful against mosquitoes transmitting the disease. Years of vaccine research have produced few hopeful candidates and although scientists are redoubling the search, an effective vaccine is at best years away. In response to this dire situation, the global community is now taking steps to deliver more effective interventions throughout Africa and other malaria endemic areas, including drug combinations with artemisinin derivatives and anti-vector measures. The dramatic success of these measures in a few specific areas, such as Kwa Zulu-Natal in South Africa [Barnes *et al*., 2005], Eritrea [Nyarango *et al*., 2006] and the Tanzanian island of Zanzibar [Bhattarai *et al*., 2007], has inspired a new call for global eradication. Achieving this ambitious goal depends on the development of new tools to treat, prevent, and monitor malaria.

1.1.1 Life Cycle of *Plasmodium* Parasite

Among the four *Plasmodium* species (*P. falciparum*, *P. vivax*, *P. ovale* and *P. malariae*) that cause malaria in humans, *Plasmodium falciparum* is the most virulent. This species causes the vast majority of deaths from malaria and is also distinguished by its ability to bind to endothelium during the blood stage of the infection and to sequester in organs, including the brain. *Plasmodium vivax* is less deadly but highly disabling; it is common in tropical areas outside Africa (most Africans lack the Duffy blood group antigen that is expressed on the surface of erythrocytes and is a necessary receptor for *P. vivax* invasion of these cells). The ability of *P. vivax* and also *P. ovale* to remain dormant for months as hypnozoites in the liver makes infection with these parasites difficult to eradicate. *Plasmodium malariae* does not form hypnozoites, but it can persist for decades as an asymptomatic blood stage infection. A fifth species, *P. knowlesi*, which was originally described as a malaria parasite of long tailed macaque monkeys, also naturally infects humans in some areas, such as Malaysia [Singh *et al*., 2004].

Infection of the human host with a *Plasmodium* parasite begins with the bite of an infected *Anopheles* mosquito that inoculates the individual with sporozoites (Figure 2). The number of sporozoites normally inoculated is usually more than 25. These motile forms of the parasite rapidly access the blood stream and then the liver, where they invade hepatocytes. The asymptomatic liver stage of infection lasts about 6 days, with each sporozoite yielding tens of thousands of merozoites that then invade and develop within erythrocytes. Once inside the erythrocyte, the parasite lies within the erythrocyte cytosol enveloped by its own plasma

membrane and a surrounding parasitophorous vacuolar membrane. Within the erythrocytes, the merozoites develop from small ring forms to the trophozoites feeding stages after about 24 hours of invasion. Approximately 36 hours after merozoites invasion repeated nuclear division takes place to form schizonts or the segmenter form. This then ruptures and releases merozoites (at least 8-20 per schizont every 48 hours or 72 hours for *P. malariae*). Merozoites released from erythrocytes can invade other red blood cells and continue the cycle of 10 fold parasite multiplication, with extensive red blood cell distraction. The asexual reproduction of the parasites in the red blood cells (called schizogony or merogony) and the release of infectious offsprings (merozoites) when the red blood cells lyse are responsible for the pathogenesis of the disease and infected individuals manifest diverse symptoms affecting different organ systems. In some cases, the merozoites enter red blood cells but do not divide. Instead they differentiate into male and female gametocytes (the crescents of Laveran). When ingested by the female mosquito, the male gametocyte divides into eight flagellated microgametes, which escape from the enclosing red blood cells (exflagellation). These swim to the macrogamete, one microgamete fertilises the macrogamete, and the resultant motile zygote (the ookinete) moves between or through cells of the stomach wall. This encysted zygote, resembling a wart on the outside of the mosquito stomach is an oocyst. Through asexual multiplication, threadlike sporozoites are produced in the oocyst, which burst and release sporozoites into the body cavity of the mosquito. These sporozoites quickly find their way to the salivary glands. When the female mosquito feeds again, the transmission cycle is complete. The mosquito becomes infectious to its next blood meal donor approximately two weeks after ingesting gametocytes, a time frame that is influenced by the external temperature. Development of *P. vivax* within the mosquito can occur at a lower environmental temperature than that required for the development of *P. falciparum*, explaining the preponderance of *P. vivax* infections outside tropical and subtropical regions.

During its peripatetic existence, the unicellular malaria causing parasite uses a toolkit of more than 5,000 genes [Gardner *et al*., 2002] to undergo dramatic metamorphoses that are suited to the numerous environments and barriers it encounters. These changes include the development, at different points in its life cycle, of motile, invasive, encysted, intracellular, sexual, and dormant forms. These distinct forms of the parasite help enable it to complete its full life cycle (Figure 2), during which it must pass through the mosquito midgut and salivary glands; localise and penetrate skin vessels; perforate and traverse macrophages and several hepatocytes prior to enveloping itself in an intrahepatocytic vacuole; and attach to and reorient itself on the surface of erythrocytes prior to invasion. Each of the developmental stages represents a potential target at which the life cycle can be interrupted. Vaccines, drugs, and anti-vector measures are being developed to prevent infection, disease, and transmission. Despite numerous potential targets, the most widely used old compound (quinine, isolated from Cinchona bark in 1820) and the best new compound (artemisinin, purified from *Artemisia annua* in 1972) for treatment are both derived from ancient herbal therapies. Further, progress with developing a vaccine is incomplete. These limitations stem, in part,

from the fact that since its discovery in 1880 the parasite has been slow to reveal its secrets, including its metabolic pathways and its antigens that are targeted by protective immunity [Greenwood *et al*., 2008]. However, recent advances in determining the genome sequences for humans, *Anopheles* mosquitoes, and *Plasmodium* parasites have raised hopes that developing new interventions might be feasible.

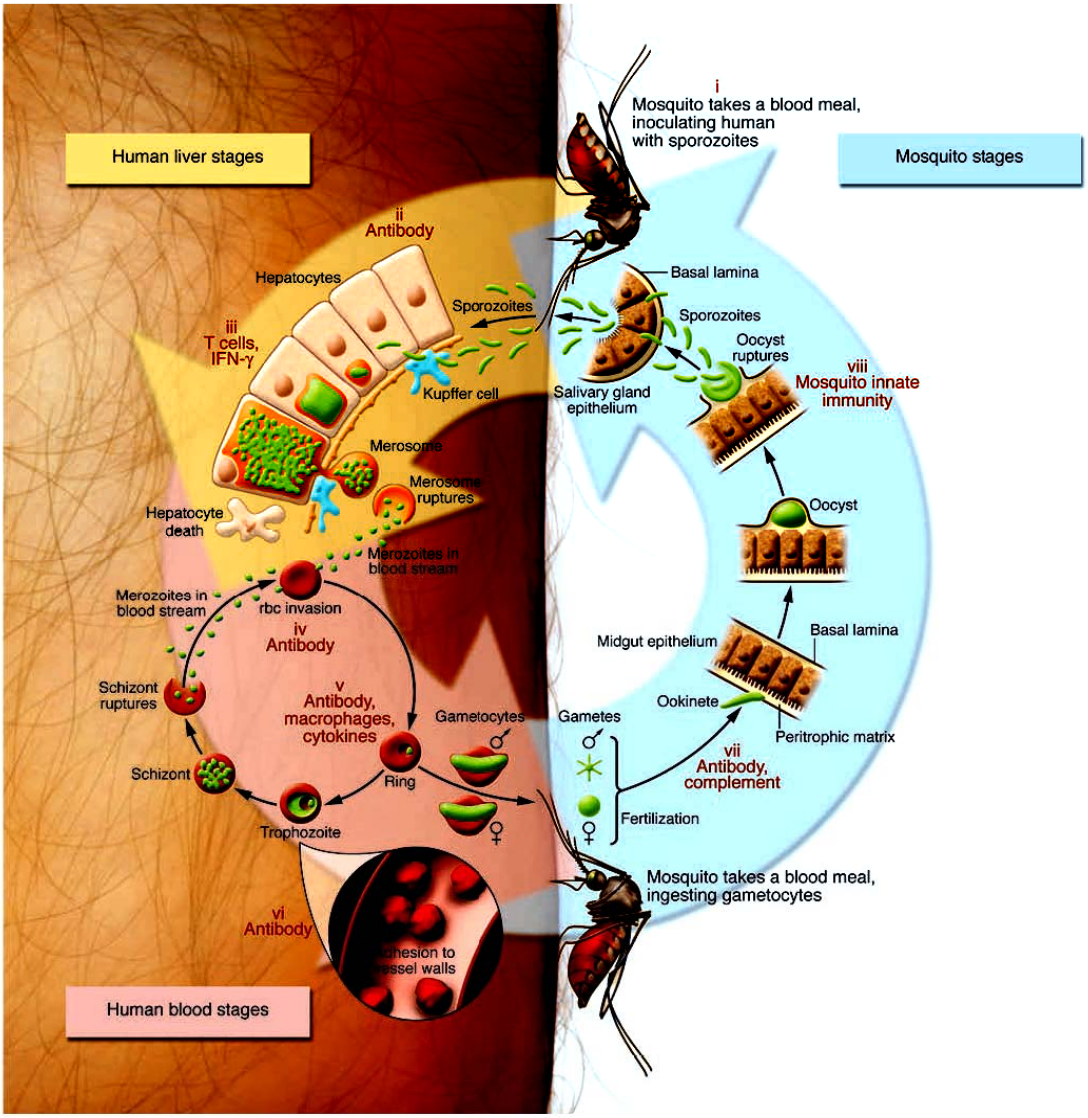

Figure 2: Life cycle of *Plasmodium* parasite [Greenwood *et al*., 2008]

1.1.2 Oxidative Stress and Antioxidant Defense in Malaria Parasites

Malaria parasites are continuously exposed to oxidative and nitrosative stress. Such stress might be classified as exogenous or endogenous. Exogenous stress is produced by the immune response of the host. Endogenous stress on the other hand could either be as a result of the high metabolic rate of the rapidly growing and multiplying parasite which generates large quantities of toxic redox active byproducts or degradation of host haemoglobin by the parasite [Becker *et al*., 2005]. Haemoglobin represents the major source of amino acids for *Plasmodium*, but its degradation in an acidic food vacuole results in the production of toxic

free haem (ferri/ferroprotoporphyrin IX; FP) and reactive oxygen species (ROS) [Tilley *et al*., 2001]. Most of the FP is sequestered into a crystalline form, known as haemozoin or malaria pigment [Egan *et al*., 2002; Slater and Cerami, 1992]. Alternative detoxification pathways, including FP degradation [Zhang *et al*., 1992; Loria *et al*., 1999], reaction with glutathione [Ginsburg *et al*., 1998], and the binding to FP binding proteins [Harwaldt *et al*., 2002; Campanale *et al*., 2003], may also contribute to FP detoxification. However, even if a small amount (e.g. 0.5 %) of the FP escapes the neutralisation processes, it could cause redox damage to the host's proteins and membranes, inhibit parasite enzymes and lyse erythrocytes [Tilley *et al*., 2001].

In order to maintain a redox equilibrium, malaria parasites are equipped with a range of antioxidant defense mechanism namely a complete glutathione system comprising of NADPH highly active glutathione reductase (GR), glutathione (GSH) and different glutaredoxin like proteins [Becker *et al*., 2003; Becker *et al*., 2004] as well as a functional glutathione dependent glyoxylase system and a glutathione S-transferase (GST) with peroxidase activity. Besides this a complete thioredoxin (Trx) system comprising of NADPH thioredoxin reductase (TrxR), different thioredoxin like proteins and thioredoxin dependent peroxidase (TPx) [Rahlfs and Becker, 2001; Muller, 2004] is present. In addition to the thioredoxin and glutaredoxin systems, two functional superoxide dismutase (SOD) and two lipoamide dehydrogenase like proteins are also present [Becker *et al.,* 2005]. Notably, *Plasmodium* possesses neither a classical catalase nor a classical glutathione peroxidase [Sztajer *et al*., 2001]. Some of the enzymes responsible for the maintenance of redox equilibrium have been studied in functional and structural detail over the last few years and represent promising targets for the development of novel antimalarial drugs [Becker *et al*., 2004].

1.2 Rationale of the Study

Science still has no magic bullet for malaria, the *Plasmodium* parasites are developing unacceptable levels of resistance to one drug after another and many insecticides are no longer useful against mosquitoes transmitting the disease. Years of vaccine research have produced few hopeful candidates and although scientists are redoubling the search, an effective vaccine is at best years away. In response to this dire situation I explored the pentose phosphate pathway of the malaria parasite *P. falciparum* in particular the bifunctional enzyme glucose-6-phosphate dehydrogenase-6-phosphogluconolactonase, the kynurenine pathway enzymes indoleamine 2,3-dioxygenase (1 and 2) and the thioredoxin networks in search for a new potential drug target and new drug alternatives.

1.2.1 Glucose-6-Phosphate Dehydrogenase

Glucose serves as the preferred energy source for mammalian cells and for many of the parasitic organisms they harbour. The Embden-Meyerhof-Parnas [EMP] or glycolytic pathway is responsible for oxidation of glucose to pyruvate with concomitant production of

ATP. Glucose is also metabolised by a second route, the pentose phosphate pathway [PPP] also known as the hexose monophosphate shunt [HMS]. The PPP occurs in the cytosol and is classically divided into two major branches: non-oxidative and oxidative. In the non oxidative branch the pathway catalyses the interconversion of three-, four-, five-, six- and seven carbon sugars in a series of nonoxidative reactions that can result in the synthesis of five carbon sugars for nucleotide biosynthesis or the conversion of excess five carbon sugars into intermediates of the glycolytic pathway. The oxidative branch on the other hand is involved in the generation of reductive equivalents in the form of NADPH and ribose 5-phosphate whose derivatives are components of RNA and DNA, as well as ATP, NADH and FAD. While the role of EMP has been extensively investigated in many parasites, the PPP has been relatively neglected although the pathway does play a crucial role both in the metabolism of *P. falciparum* and in its relationship with the human host.

1.2.1.1 Glucose-6-Phosphate Dehydrogenase and the Pentose Phosphate Pathway

Glucose-6-phosphate dehydrogenase (G6PD) is a cytoplasmic so called "house keeping" enzyme that catalyses the first and rate limiting step of the PPP [Ruwende and Hill, 1998]. This pathway is an important source of NADPH that is required for several biosynthetic reactions and is essential for maintaining adequate intracellular levels of the reduced form of glutathione [Becker *et al*., 2004]. The reduced form of glutathione is essential for the reduction of hydrogen peroxide and oxygen radicals and the maintenance of haemoglobin and other red blood cell proteins in the reduced state [Cappellini and Fiorelli, 2008]. Since red blood cells do not contain mitochondria, the PPP is their only source of NADPH; therefore, defence against oxidative damage is dependent on NADPH production by G6PD [Luzzatto *et al*., 2001].

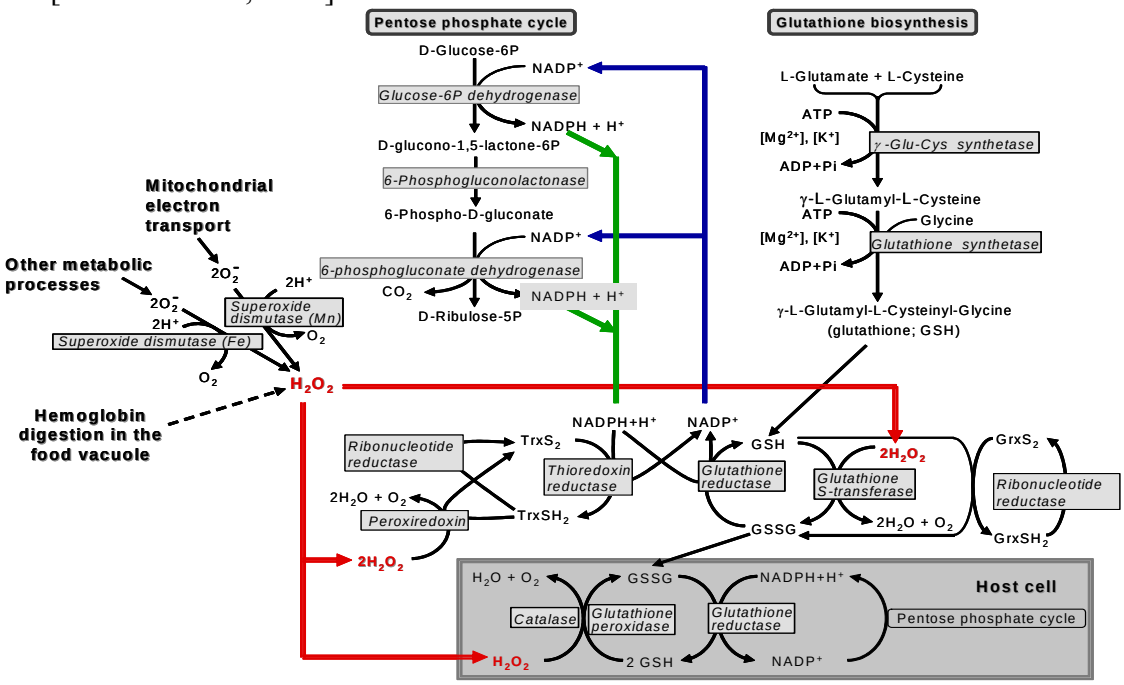

Figure 3: Pentose phosphate pathway and defence against oxidative stress in infected red blood cells [Becker *et al*., 2004].

The HMS catalysed by G6PD is also an important source of ribose which is essential for production of nucleotide coenzymes, the replication of nucleic acids and therefore cell division [Sodiende, 1992]. The biological importance of G6PD is underlined by the fact that this enzyme is present in all cells, however its concentration varies in different tissues [Battistuzzi *et al*., 1985] and in the red blood cells (RBC) it operates at only 1-2 % of its maximum potential even under induced oxidative stress [Gaetani *et al*., 1974].

1.2.1.2 G6PD Deficiency and Malaria

The G6PD deficiency is the most common human enzyme defect which is widely distributed across the globe. A conservative estimate is that at least 400 million people carry a mutation in the G6PD gene causing the deficiency. Since 1967 when the WHO made an initial recommendation for the characterisation of the G6PD deficiency, more than 400 biochemical variants of it have been characterised according to their physicochemical properties (such as thermostability and chromatographic behaviour), kinetic properties (involving substrates glucose-6-phosphate, NADP and substrate analogues) and pH dependence [Beutler, 1984]. These variants of the G6PD deficiency can be grouped into five classes according to their enzyme activity and clinical manifestations [WHO, 1989] or classified as sporadic or polymorphic [Luzzatto *et al*., 2001]. The G6PD deficiency can be caused by a reduction in the number of enzyme molecules, a structural difference in the enzyme causing a qualitative change, or both. Examination of G6PD variants shows that, in most cases, the G6PD deficiency is due to enzyme instability, implying that amino acid substitutions or mutations at different locations can destabilise the enzyme molecule. Many single point mutations or amino acid substitutions have been recorded repeatedly in different parts of the world, suggesting that their origin is unlikely to be from a common ancestor and that they are therefore probably new mutations that have arisen independently [Mason *et al*., 1995; Hirono *et al*., 1997; Vulliamy *et al*., 1998].

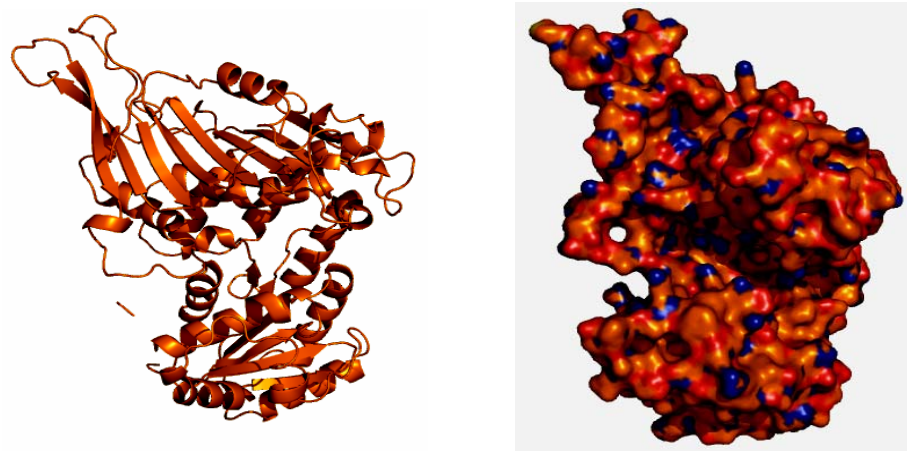

Figure 4: Human G6PD structure [Au *et al*., 2000].

The inheritance of the G6PD deficiency shows a typical X-linked pattern, which was identified through favism as having a higher incidence in males than in females, long before

the G6PD deficiency was identified as the cause. Males are hemizygous for the G6PD gene and can, therefore, have normal gene expression or be G6PD deficient. Females, who have two copies of the G6PD gene on each X chromosome, can have normal gene expression or be heterozygous. In some populations, in which the frequency of the G6PD deficient allele is very high, homozygous females are not rare. Heterozygous females are genetic mosaics as a result of X chromosome inactivation (in any cell, one X chromosome is inactive, but different cells randomly inactivate one chromosome or the other) and the abnormal cells of a heterozygous female can be as deficient for G6PD as those of a G6PD deficient male; therefore, such females can be susceptible to the same pathophysiological phenotype [Beutler *et al*., 1962]. Although heterozygous women have on average less severe clinical manifestations than G6PD deficient males, some develop severe acute haemolytic anaemia [Lim *et al*., 2005].

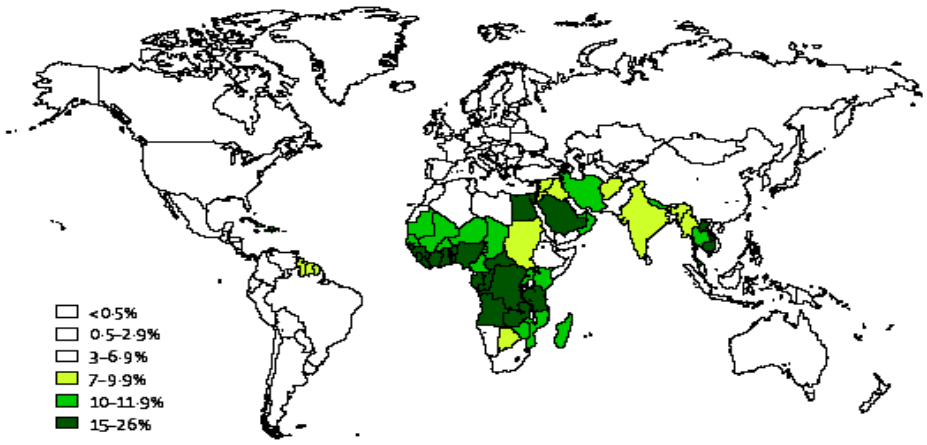

Figure 5: World distribution of G6PD deficiency [WHO, 1989].

The highest prevalence of G6PD deficiency is reported in Africa, southern Europe, the Middle East, Southeast Asia, and the central and southern Pacific islands; however, because of fairly recent migration, G6PD deficiency is nowadays quite prevalent in North and South America and in parts of northern Europe [Frank, 2005]. Two apparent exceptions to the geographical rule with clear explanations exist. These are southern Europe and North America. Whereas malaria was only eradicated in southern Europe during the 20th century; in North America, the defect is confined to immigrants from regions where malaria is found, and the descendants of these immigrants [Greene, 1993].

The geographical distribution of malaria is remarkably similar to that of the G6PD deficiency. Based on this observation Motulsky [1961], Siniscalco *et al*., [1961], Allison [1960] and Allison and Clyde [1961] suggested over 45 years ago the malaria hypothesis of G6PD deficiency that states "G6PD deficiency is one of the polymorphisms that confers resistance to infection by *P. falciparum* malaria" a generally well accepted notion which has recently been supported by Luzzatto and Bienzle [1979] and Ruwende and Hill [1998]. This hypothesis has been verified through various studies:

a) Although epidemiologic evidence indicates that the highest G6PD deficiency gene frequencies are present among populations living where malaria disease is endemic [Luzzatto and Battistuzzi, 1985; Siniscalco *et al*., 1966], the relationships or connections between G6PD deficiency and malaria disease have been questioned [Luzzatto and Battistuzzi, 1985; Kidson and Gorman, 1962]. Early studies designed to assess this connection were somewhat contradictory and could not give conclusive evidence [Martin *et al*., 1979; Oo M *et al*., 1995; Bienzle *et al*., 1972; Guggenmoos-Holzmann *et al*., 1981]. This led to the suggestion that an additional factor, perhaps oxidative stress [Greene, 1993; Martin, 1980], may be required for G6PD deficiency to confer immunity to malaria. The malaria parasite appears to be sensitive to oxidative stress [Becker *et al*., 2004] and it has been suggested that the eating of fava beans and the G6PD deficiency synergistically protects against malaria [Greene 1993; Clark *et al*., 1984; Golenser *et al*., 1988]. However it is difficult to explain protection against malaria on this basis in sub-Saharan Africa where fava beans are not cultivated.

b) Decreased parasitemia among patients with G6PD deficiency when compared with normal individuals was originally reported by Allison [1960] and Allison and Clyde [1961] and has been confirmed in a number of studies [Luzzatto and Battistuzzi, 1985; Gilles *et al*., 1967; Kar *et al*., 1992]. A number of negative studies have also been reported but are considered to be flawed [Greene, 1993]. Although one study indicated that protection extended only to heterozygous females [Bienzle *et al*., 1972], this conclusion has not been borne out in other investigations and it seems likely that hemizygous males are also protected [Greene, 1993]. However, based on the disputed finding that it is heterozygotes that are resistant to malaria, an interesting explanation was devised. It was suggested that when deficient cells are parasitised, the parasite G6PD is eventually induced, but it requires several cycles in deficient host cells. Heterozygotes, who have a mixture of normal and deficient cells, would host the parasite in normal cells often enough to prevent the induction of the enzyme [Luzzatto *et al*., 1986; Usanga and Luzzatto, 1985]. However, subsequent data from the same group of investigators indicated that in reality, the G6PD activity of the host cells did not influence the expression of the parasite enzyme [Kurdi-Haidar and Luzzatto, 1990]. Ruwende and colleagues have recently been able to reveal that the G6PDH A– allele (the most prevalent in Africa) is associated with a reduction in the risk of severe *P. falciparum* malaria, for female heterozygotes and male hemizygotes (46 % and 58 %, respectively) [Ruwende *et al*., 1995].

c) Studies in heterozygotes for G6PD deficiency, in which two populations of RBCs coexist, show that more parasites are present in the cells with normal enzyme activity than in the deficient cells. In an elegant investigation of the number of parasites in the RBCs of patients heterozygous for G6PD deficiency, Luzzatto *et al*., [1969] showed

that more parasites (2-80 times more) could be found in G6PD sufficient cells than in G6PD deficient ones.

d) *In vitro* studies show that malaria parasite growth was slower in G6PD deficient than in normal cells [Luzzatto *et al*., 1986; Roth and Schulman 1988; Usanga and Luzzatto 1985; Roth *et al*., 1983]. Cappadoro *et al*., [1998] were also able to show that G6PD deficient RBCs infected with parasites undergo phagocytosis by macrophages at an earlier stage of parasite maturation than do normal RBC with parasitic infection, which could be a further protective mechanism against malaria.

At the molecular level the most likely explanation attributes the G6PD deficiency protection mechanism against malaria to reduced multiplication in deficient RBC, probably as a result of the intracellular accumulation of toxic oxidised substances such as oxidised glutathione and haemozoin [Turrini *et al*., 1993; Miller *et al*., 1984; Golenser *et al*., 1988]. However there is some evidence that infected RBCs are more susceptible to haemolysis as a result of increased methaemoglobin and release of ferriheme a known cytolytic agent [Janney *et al*., 1986], and that in addition they are more readily phagocytosed by cells of the reticuloendothelial system as a result of the RBC changes (i.e. methaemoglobin and heinz body formation, membrane damage) that are associated with oxidative stress imposed by the parasite infection [Turrini *et al*., 1993].

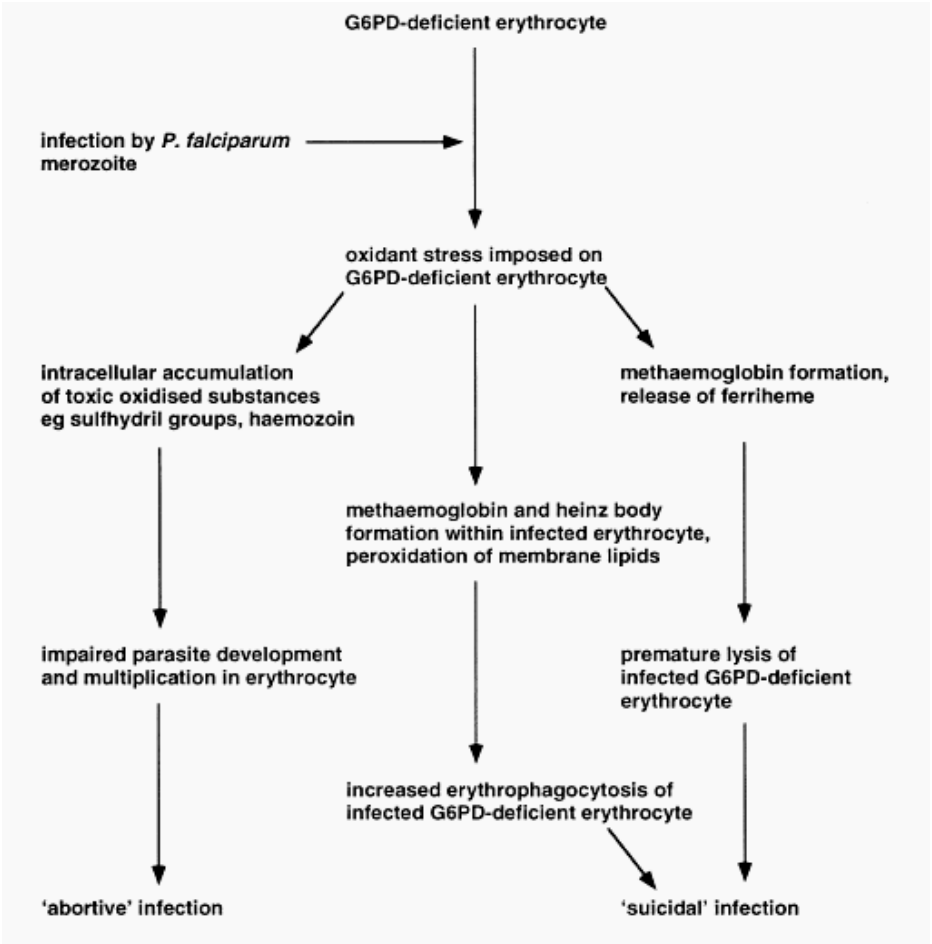

Figure 6: Possible protective mechanisms of the G6PD deficiency against severe malaria [Ruwende and Hill, 1998].

When a gene that has some potential for decreasing fitness achieves a high frequency in some populations, it is necessary to assume that in those populations it also confers a survival advantage. Thus, a balance is achieved between the advantage (resistance to malaria) and the disadvantage (lowered resistance to oxidative stress) conferred by a gene, and this is designated a balanced polymorphism. Evidence from a variety of sources has led to the conclusion that the advantage conferred by this gene is resistance to *P. falciparum* malaria [Beutler, 1994].

In most areas with a prevalence of the G6PD deficiency, several polymorphic alleles are found [Cappellini *et al*., 1996; Martinez di Montemuros *et al*., 1997]. Tropical regions of Africa where malaria is endemic are one exception, where the variant G6PD A– accounts for about 90 % of G6PD deficiency. G6PD A– is also frequent in North and South America, in the West Indies, and in areas where people of African origin are present [Martinez di Montemuros *et al*., 1997; Cappellini *et al*., 1994]. The second most common variant is G6PD Mediterranean, which is present in all countries surrounding the Mediterranean Sea [Luzzatto *et al*., 2001], and is also widespread in the Middle East, including Israel [Kurdi-Haidar *et al*., 1990; Karimi *et al*., 2003]. In several populations, such as the countries around the Persian Gulf, G6PD A– and G6PD Mediterranean coexist at polymorphic frequencies [Bayoumi *et al*., 1996]. Other polymorphic variants are the Seattle and Union variants, which have been reported in southern Italy, Sardinia [Fiorelli *et al*., 1989; De Vita *et al*., 1989], Greece, the Canary Islands [Cabrera *et al*., 1996], Algeria, Germany, and Ireland. G6PD Union was also reported in China [Perng *et al*., 1992], and G6PD Maewo which by molecular analysis was shown to be G6PD Union is polymorphic in the corresponding island in the Vanuatu archipelago [Ganczakowski *et al*., 1995].

1.2.1.3 Glucose-6-Phosphate Dehydrogenase-6-Phosphogluconolactonase from *P. falciparum*

More than 41 years ago Langer *et al*., [1967] demonstrated the existence of G6PD activity in *P. berghei*, but the inability to confirm these findings through several subsequent investigations [Sherman, 1979] coupled with the clear documentation and reproducible findings on the existence of the second enzyme (6-phosphogluconolactonase) of the PPP [Fletcher *et al*., 1977] reaffirmed the theory that disputed the existence of the complete PPP in the *Plasmodium* parasite and suggested that the parasite made use of the host G6PD enzyme to carry out the initial step of the PPP [Eckman and Eaton, 1979]. The presence of *P. falciparum* G6PD activity was first reported 14 years later by Hempelmann and Wilson [1981]. A slow moving band on acrylamide gels which corresponded to a high molecular weight compared to the RBC G6PD was identified to be that of *P. falciparum* G6PD [Hempelmann and Wilson, 1981; Ling and Wilson, 1988; Kurdi-Haidar and Luzzatto, 1990]. Further studies on the enzyme lead not only to its identification and partial purification but also showed that the enzyme was present at similar levels in both G6PD deficient and normal host cells [Ling and Wilson, 1988; Kurdi-Haidar and Luzzatto, 1990]. Suggesting that parasite

G6PD activity was expressed independently from induction and adaptation to deficient cells [Kurdi-Haidar and Luzzatto, 1990].

The nucleotide sequence encoding the enzyme has been cloned and sequenced [Shahabuddin *et al*., 1994; O'Brien *et al.,* 1994]. The primary structure as predicted from the gene sequence was found to be remarkably different from any of the 50 or so other G6PDs whose structure is known or inferred. The deduced protein has a subunit molecular weight of 107 kDa. The C- terminal part (residues 311-911) is clearly homologous to other described G6PDs [Jeffery *et al*., 1993]. The 310 amino acid protein sequence of the N-terminal region clearly differs from most eukaryotic and prokaryotic G6PDs and shows 6-phosphogluconolactonase (6PGL) activity [Scopes *et al*., 1997]. Genes encoding very similar enzymes have also been found in four other *Plasmodium* parasites namely, *P. berghei*, *P. yoelii*, *P. chabaudi* and *P. knowlesi* [Clark *et al*., 2003]. Thus the first two steps of the PPP in *Plasmodium* are catalysed by a unique bifunctional enzyme named glucose-6-phosphate dehydrogenase-6-phosphogluconolactonase (GluPho) [Clark *et al*., 2001; Scopes *et al*., 1997] which is exclusively found in *Plasmodium* species.

A unique feature of *Pf*GluPho is the 62 amino acid insert (within the G6PD part) found between the structurally predicted $NADP^+$ and G6P binding site that has no similarity found to date. Similar inserts which differ in size and sequence are present in other *Plasmodium* GluPho and have nevertheless been demonstrated to be essential for GluPho activity [Clark *et al*., 2003].

Figure 7: Sequence comparison of inserts within five *Plasmodium* GluPho proteins and human G6PD. Completely conserved amino acids are shaded black, highly conserved amino acids are shaded grey and insertion sequences are italicised. Potential N-glycosylation sites are underlined [Clark *et al*., 2003].

Further studies to determine if the unique structural features of *Pf*GluPho have any biological significance may be useful in understanding the role *Pf*GluPho plays in the PPP and in overcoming oxidative stress. Particularly because PPP activity in infected RBCs is greatly increased (78 fold) compared to non infected ones, and the parasite PPP is responsible for 82 % of this activity [Atamna *et al*., 1994]. RNA-mediated gene silencing of *Pf*GluPho in cell culture has demonstrated an arrest of the parasite life cycle at the trophozoite stage.

Immediate transcript enhancement of thioredoxin reductase suggests that the *Pf*GluPho plays a role in the response of the parasite to oxidative stress [Crooke *et al*., 2006].

In the battle to eradicate malaria effectively, new drug targets are needed. An essential feature for a molecule to be considered as a potential drug target is that it must be distinguishable from its homologues in the human host. The enzyme *Pf*GluPho might prove valuable in this respect, as mammals do not express this bifunctional enzyme and do not express insertion sequences within their two monofunctional proteins.

1.2.2 Tryptophan Metabolism: Kynurenine Pathway

Tryptophan is an essential amino acid that is required in several physiological processes in addition to protein synthesis. Dietary tryptophan enters the liver through the hepatic portal system, where it has been demonstrated to induce protein synthesis [Sidransky, 1976]. Excess tryptophan can be delivered to the bloodstream, where it can be taken up by tissues and used in protein synthesis or in the synthesis of serotonin and melatonin. The dietary intake of tryptophan correlates with the ratio of tryptophan to large neutral amino acids in the plasma and with brain serotonin levels [Fernstrom and Wurtman, 1972]. Thus acute depletion of tryptophan has effects on mood and aggression through causing low serotonin levels [Young and Leyton, 2002]. An alternative fate for L-tryptophan is catabolism through the kynurenine pathway. Named after the pivotal metabolite kynureneine, the first and rate-limiting step in the pathway is the oxidative cleavage of the 2,3-double bond of the indole ring of tryptophan via the incorporation of molecular oxygen or a superoxide anion, a reaction that converts tryptophan to N-formylkynurenine, which is quickly catabolised to kynurenine [Shane and Stocker, 1999].

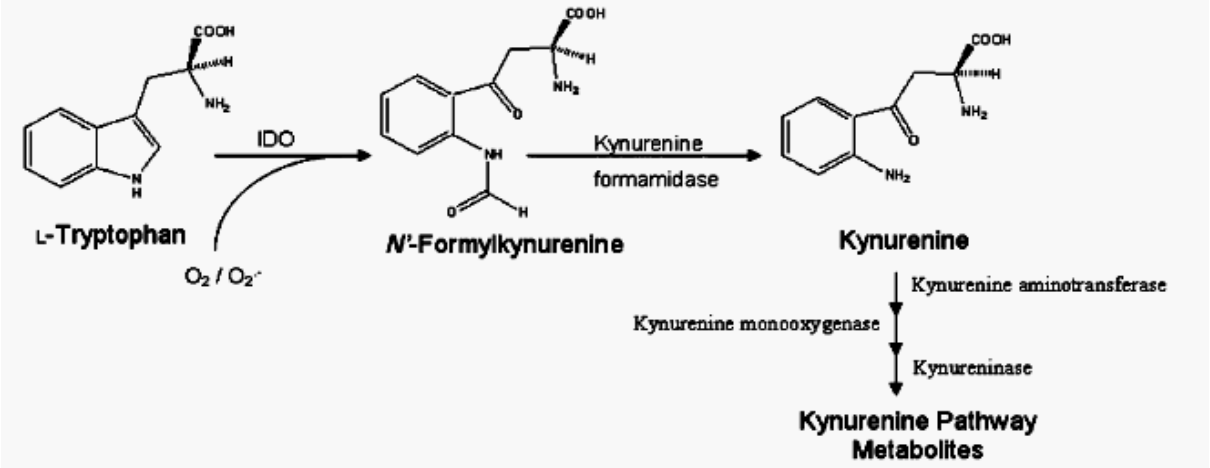

Figure 8: Initial steps of the kynurenine pathway. The heme containing enzymes TDO, IDO-1 and IDO-2 are capable of catalysing this reaction [Austin *et al*., 2008].

The first and rate limiting step in the kynurenine pathway is performed by either of the two enzymes, tryptophan 2,3 dioxygenase (TDO) and indoleamine 2,3-dioxygenase (IDO). The first of these, TDO an enzyme whose activity can be induced by dietary tryptophan and steroid hormones [Schimke *et al*., 1965; Knox, 1966], was first described in 1937 [Kotake and

Masayama, 1937]. It is a heme-containing protein mostly expressed in the liver and it is able to metabolise L- but not D-tryptophan [Schutz *et al*., 1972; Bender, 1989].

Indoleamine 2,3-dioxygenase (IDO-1) is the second enzyme able to open the indole ring of tryptophan. Its existence was suspected for a long time because a large percentage of patients with rheumatoid arthritis, tuberculosis, leukaemia, Hodgkin's disease and bladder tumours excreted exceptionally large amount of kynurenine into the urine without having an induced TDO in the liver. The enzyme was firstly described by Hayaishi *et al*. in the early 1960s in the rabbit intestine as a heme-containing protein (42,000 MW) able to catalyse the incorporation of superoxide anion into the pyrrole moiety of indole [Hayaishi *et al*., 1984]. The name indoleamine 2,3-dioxygenase originates from the proposed importance of the enzyme in the metabolism of the indoleamines 5-hydroxytryptamine (5-HT), tryptamine and melatonin [Hirata and Hayaishi, 1975; Yoshida and Hayaishi, 1987].

In fact, while TDO specifically acts on L-tryptophan, IDO-1 may open the indole ring of the amines, D-tryptophan, L- or D-5-OH-tryptophan, but it is not active on scatole, indole or indole acetic acid. Furthermore, while TDO is predominantly located in the liver, IDO-1 is present in most mammalian organs, including intestine, placenta, lung, blood mononuclear phagocytes, epididymis, endocrine and central nervous systems [Watanabe *et al*., 1981]. IDO-1 is normally highly expressed in inflammatory states with interferon-gamma (IFNγ) and tumor necrosis factor (TNF) playing key mediatory roles in its expression [Takikawa *et al*., 1999; Fujigaki *et al*., 2001]. Induction of IDO-1 in endothelial cells by IFNγ has been shown to inhibit the growth of various infectious agents, including *Toxoplasma gondi*, *Clamydia psittaci*, *C. trachomatis*, *Enterococci*, *Staphylococcus aureus*, herpes simplex virus, measles virus and cytomegalovirus [MacKenzie *et al*., 2007; Schroten *et al*., 2001; Daubener *et al*., 2001; Pfefferkorn, 1984] through tryptophan depletion.

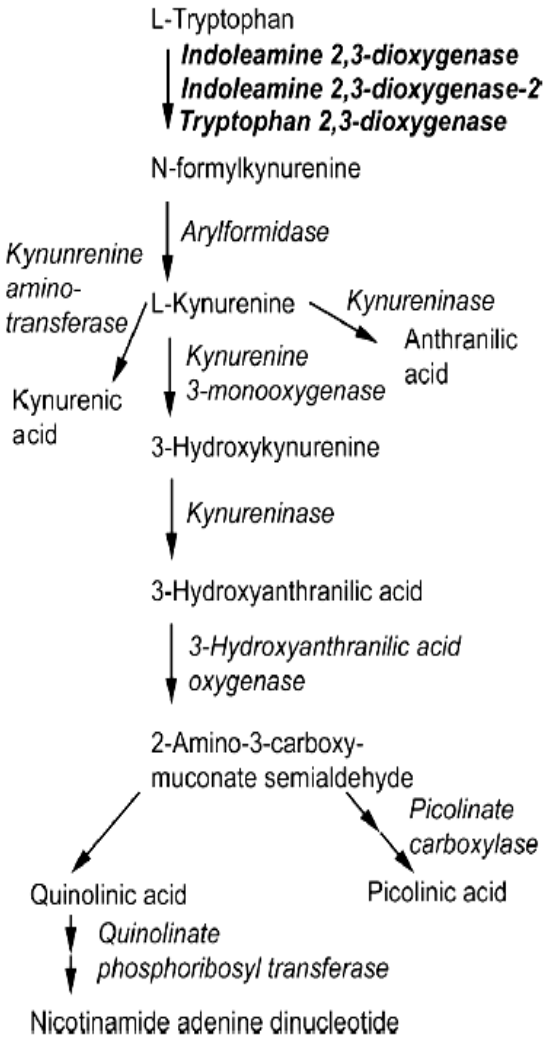

Figure 9: Kynurenine pathway of tryptophan metabolism [Ball *et al*., 2008].

The expression of IDO-1 also has an immunomodulatory role in inducing tolerance

by suppressing T-lymphocyte proliferation via tryptophan depletion with far implications in many fields of medicine, including fetal rejection and organ transplant survival [Munn *et al*., 1999]. The downstream metabolites of the kynurenine pathway can have physiological or patho-physiological activities, and it is not always clear whether the induction of this pathway exerts its effects through tryptophan depletion, by production of kynurenine and/or kynurenine derived metabolites or a combination of these two processes.

For example, the proliferation of T-lymphocytes is inhibited by downstream catabolites of the kynurenine pathway [Frumento *et al*., 2002]. Two of the major metabolites formed by the pathway are kynurenic acid (KA) and quinolinic acid (QA), both of which can bind to glutamate receptors activated by *N*-methyl-*D*-aspartate (NMDA). Kynurenic acid acts as an antagonist for NMDA receptors whereas QA is an agonist and may be neuroexcitotoxic at physiological concentrations [Perkins and Stone, 1982; Schwarcz *et al*., 1983].

Quinolinic acid acts through the excitatory amino acid acceptor site on the NMDA receptor [Schurr and Rigor, 1993; Stone *et al*., 2001], whereas kynurenic acid acts through the glycine binding site to inhibit the excitatory actions of glutamate, NMDA and kainic acid [Perkins and Stone, 1982; Stone *et al*., 2003]. Thus, the kynurenine pathway of tryptophan metabolism generates both a potential neuroexcitotoxin quinolinic acid and a neuroprotectant kynurenic acid and the balance between the levels of these molecules is critical in determining the consequences of activation of this pathway. The (neuroexcitotoxin : neuroprotectant) QA: KA ratio as well as IDO-1 activity have been found to be increased in experimental celebral malaria mouse implying that this imbalance contributes to the neurological symptoms and perhaps the morbidity of celebral malaria [Sanni *et al*., 1998].

The accumulation of QA within the brain has also been reported to occur in a broad spectrum of patients or experimental animals with inflammatory neurological diseases such as acquired immunodeficiency (AIDS) dementia complex caused by an infection of immunodeficiency virus type 1 (HIV-1) [Heyes *et al*., 1991], poliovirus brain infection, and isechemic brain injury [Saito *et al*., 1993]. The cerebrospinal fluid levels of QA correlated well with the severity of the neurological defects thus suggesting that QA plays a direct role in the pathogenesis of neurodegenerative disorders. The production of QA closely reflects the induction of the first and rate limiting enzyme IDO-1 in the kynurenine pathway within the central nervous system [Heyes *et al*., 1991]. Therefore the upregulation of IDO-1 in the brain leads to an accumulation of QA and results in neural degeneration.

Since the 1970s it has been believed that the first and rate limiting step in the kynurenine pathway is performed by either of two enzymes, tryptophan 2,3-dioxygenase (TDO) or indoleamine 2,3-dioxygenase (IDO-1), depending on the tissue and cell type. Although Shimizu *et al*., [1978] demonstrated in their work the existence of 3 various forms of IDO which differed in their isoelectric points; it was still believed that only IDO-1 and TDO were responsible for catalysing the first and rate-limiting step in the kynurenine pathway. This paradigm was overturned recently when a gene with homology to IDO was reported [Murray, 2007] and then subsequently demonstrated by three groups to encode an

enzyme with the ability to catabolise tryptophan [Ball *et al*., 2007; Metz *et al*., 2007; Yuasa *et al*., 2007]. The enzyme has been referred to as indoleamine 2,3-dioxygenase like protein, indoleamine 2,3-dioxygenase-2 or proto indoleamine 2,3-dioxygenase (INDOL1, IDO-2, IDO2, protoIDO) on the basis of its structural similarity to IDO-1 and its enzymatic activity. In mice, IDO-2 is predominantly expressed in the kidney followed by epididymis, testis and liver [Ball *et al*., 2007] as well as in the ovary and uterus. Although both IDO proteins are expressed in some tissues, e.g. epididymis, immunohistochemistry demonstrated that IDO-1 and IDO-2 are expressed in distinct cell types suggesting they are not functionally redundant. For example, IDO-1 was found in the principal and apical cells of the mouse caput epididymidis whilst IDO-2 is expressed in the tails of spermatozoa [Ball *et al*., 2007]. In addition, expression of the proteins in response to stimuli differs. For example, IDO-1 is induced systemically in endothelial cells during murine malaria infection, and this induction is dependent on the presence of interferon gamma [Hansen *et al*., 2004], whereas IDO-2 mRNA expression is unchanged or down-regulated [Ball *et al*., 2007]. The tryptophan catabolising activity of IDO-2 expressed in intact mammalian cells has been demonstrated [Ball *et al*., 2007; Metz *et al*., 2007]. The depletion of tryptophan by IDO-1 and IDO-2 activity also triggered signalling pathways such as phosphorylation of the translation initiation factor eIF-2α and translation of liver enriched inhibitory protein (LIP), an inhibitory isoform of CEPBβ transcription factor [Metz *et al*., 2007]. As the discovery of the IDO-2 enzyme is so recent, its biological role is still yet to be defined but its expression pattern in the kidney, reproductive system and a dendritic cell line suggest its involvement in kidney function, fertility and immunomodulation [Ball *et al.,* 2008].

1.2.3 Thioredoxin Networks: Glutaredoxin, Thioredoxin and Plasmoredoxin

Plasmodium parasites posses a number of proteins belonging to the thioredoxin superfamily which are characterised by a specific active site Cys-X-X-Cys motif [Rahlfs *et al*., 2003]. Despite the low degree of similarity between their primary sequences, the proteins are structurally related and they all posses the so called thioredoxin fold and have similar functions within the cell [Fernandes and Holmgreen, 2004]. They are considered to be redox messengers that interact with a variety of redox active proteins and metabolites such as ribonucleotide reductase, transcription factors, peroxidases, cyclophilins and low molecular weight thiols [Fernandes and Holmgreen, 2004].

Plasmodium falciparum possesses one classical glutaredoxin with the typical CPYC redox active site [Rahlfs *et al*., 2001]. This active site motif allows glutaredoxin to interact with proteins containing sulphydryl groups that need to be either oxidised or reduced, depending on their distribution, the redox state of the cell and their abundance. *Plasmodium* glutaredoxin has the ability to reduce ribonucleotide reductase and acts as an efficient reductant for plasmoredoxin, another member of the thioredoxin superfamily [Rahlfs *et al*., 2001; Becker *et al*., 2003].

Plasmoredoxin itself appears to be unique to *Plasmodium* parasites and contains a unique active site WCKYC motif [Rahlfs *et al*., 2001; Becker *et al*., 2003]. Its precise function in *Plasmodium* remains to be elucidated but it has been found to also reduce ribonucleotide reductase. In addition, *Plasmodium* possesses a genuine thioredoxin (Trx) [Kanzok *et al*., 2000; Rahlfs *et al*., 2002] which is reduced by thioredoxin reductase (PfTrxR) and confers reduction of the 2-Cys containing peroxiredoxin, ribonucleotide reductase and GSSG [Rahlfs *et al*., 2001; Rahlfs *et al*., 2003; Kanzok *et al*., 2000]. Thus all three members of the thioredoxin superfamily have overlapping functions in *Plasmodium*.

Plasmodium also possesses thioredoxin and glutaredoxin like proteins which are thought to be involved in the reduction of protein-GS-mixed disulphides that are inevitably formed during exposure to ROS and generally lead to a reversible inactivation of protein functions [Rahlfs *et al*., 2001; Rahlfs *et al*., 2003].

1.3 General Objective

Plasmodium parasites are developing unacceptable levels of resistance to one drug after another and science still has no magic bullet for malaria. Therefore there is need for identification of new drug targets and alternative antimalarial regimes. The study aimed at evaluating *Pf*GluPho as a new drug target, understanding tryptophan metabolism and unravelling more knowledge about the thioredoxin system networks.

1.3.1 Specific Objectives

1.3.1.1 Glucose-6-phosphate Dehydrogenase-6-Phosphogluconolactonase from *P. falciparum*

*Pf*GluPho is a unique bifunctional enzyme which is exclusively found in *Plasmodium species* and catalyses the first two steps of the PPP. In spite of the importance of the role this enzyme plays in the parasites PPP as well as in overcoming oxidative stress, studies using *Pf*GluPho have so far been restricted to the enzyme purified from parasite extract which is not only limiting in terms of the quantity of the enzyme required for inhibitor testing, crystal screening and biochemical characterisation of the enzyme, but also contains a high excess of the RBC G6PD. The desire and difficulties in cloning *Pf*GluPho have also been reported [O'Brien *et al*., 1994; Clark *et al*., 2001] thus making it impossible to heterologously overexpress *Pf*GluPho. This study aimed at cloning, heterologous overexpression and purification to homogeneity of *Pf*GluPho in order to obtain the purified enzyme in mg quantities. This would enable us to perform biochemical characterisation of the enzyme, screen for novel inhibitors and attempt to elucidate the three dimensional structure of the enzyme through crystallisation and x-ray diffraction analysis.

1.3.1.2 Tryptophan Metabolism

Indoleamine 2,3-dioxygenase, the first and rate-limiting enzyme in tryptophan metabolism, has been implicated in the pathogenesis of many diseases. The discovery of IDO-2 has not helped the situation but has demonstrated that the kynuenine pathway could be implicated in the pathogenesis of many other diseases than earlier thought. Inhibition of IDO has been targeted for the therapy of diseases such as cancer, neurological disorders and most notably cerebral malaria. Although IDO inhibitors exist, most of them exhibit their inhibitory activities at micromolar Ki values. As a result there is need for more potent IDO inhibitors. It would be highly advantageous to have access to large quantities of recombinant IDO-1 and IDO-2 to allow for development of more potent IDO inhibitors and allow for further studies on the enzymes. This study aims at heterologous overexpression and purification of mouse IDO-1 and IDO-2 to homogeneity. This would enable us to obtain sufficient amounts of the enzyme for biochemical characterisation (e.g. oligomerisation studies, kinetic characterisation), crystallisation trials and finally screen for more potent novel inhibitors for IDO. We also intend to test the antimalarial activity in *P. falciparum* cell culture for the IDO inhibitors that will be identified.

1.3.1.3 Thioredoxin Networks: Glutaredoxin, Thioredoxin and Plasmoredoxin

The *P. falciparum* parasite is endowed with a complex network of interacting enzymes which together form the redox metabolism network. Some of the members of this network have been demonstrated to have overlapping functions e.g. members of the thioredoxin superfamily. Their active site motifs allow them to interact with proteins containing sulphydryl groups that need to be either oxidised or reduced, depending on their distribution, their redox potential, the redox state of the cell and their abundance. More than 50 % of all the predicted parasite proteins functions are still unknown. Therefore the possibility that members of the thioredoxin super family could be interacting with novel proteins is rather high. This study aimed at identifying proteins which interact with and might be regulated by members of the thioredoxin superfamily namely glutaredoxin, plasmoredoxin and thioredoxin in *Plasmodium* parasites.

2 Materials

2.1 Chemicals

All chemicals used were of the highest available purity and were obtained from Roth (Karlsruhe, Germany), Merck (Frankfurt am Main, Germany) or Sigma-Aldrich (Steinheim, Germany).

Chemical	Source
Acetic acid	Roth, Karlsruhe
Acrylamide solution	BioRad, München
Ampicillin	Sigma, Steinheim
Ascorbic acid	Sigma, Steinheim
Bacto Agar	Roth, Karlsruhe
Boric acid	Roth, Karlsruhe
Bovine serum albumin	Roth, Karlsruhe
Bromophenol blue	Sigma, Steinheim
Carbenicillin	Roth, Karlsruhe
Chloramphenicol	Roth, Karlsruhe
Coomassie brilliant blue R250	Sigma, Steinheim
Cystatin	Roth, Karlsruhe
Ethidium Bromide	Sigma, Steinheim
Ethylenediaminetetraacetate (EDTA)	Roth, Karlsruhe
Gentamycin	Gibco, Karlsruhe
Glucose-6-phosphate Na-salt	Sigma, Steinheim
Glucoseamine-6-phosphate	Sigma, Steinheim
Deoxyglucose-6-phospate	Sigma, Steinheim
Glycerin	Roth, Karlsruhe
Hypoxanthin	Sigma, Steinheim
Imidazole	Roth, Karlsruhe
Isopropanol	Roth, Karlsruhe
Isopropylthiogalactoside (IPTG)	Roth, Karlsruhe
K_2HPO_4	Roth, Karlsruhe
Kanamycin	Roth, Karlsruhe
KH_2PO_4	Roth, Karlsruhe
Lipid rich bovine serum albumin (Albumax)	Gibco, Karlsruhe
Magnesium chloride	Roth, Karlsruhe
Mercaptoethanol	Sigma, Steinheim
Methyl tryptophan	Sigma, Steinheim
Methylene blue	Roth, Karlsruhe
Milk powder	BioRad, München
NADP	Biomol
NADPH	Biomol
Nickel-nitrilotriacetic acid (Ni-NTA)	Qiagen, Hilden

p-Dimethylaminobenzaldehyde (*p*-DMAB)	Sigma, Steinheim
Pepstatin	Sigma, Steinheim
Phenylmethylsulfonylfluoride (PMSF)	Sigma, Steinheim
Rhamnose	Promega. Mannheim
Sodium chloride	Roth, Karlsruhe
Sodium dodecyl sulphate (SDS)	Merck, Darmstadt
Sorbitol	Roth, Karlsruhe
TEMED	Sigma, Steinheim
Trichloroacetic acid	Sigma, Steinheim
Tris	Roth, Karlsruhe
Trypton	Roth, Karlsruhe
Tryptophan	Merck, Darmstadt
Tween 20	Merck, Darmstadt
Yeast Extract	Oxoid LTD, U.K
δ-Aminolevulinic acid hydrochloride (ALA)	Sigma, Steinheim

2.2 Antibodies

Antibody	**Source**
Mouse anti-histidine tag antibodies	Qiagen, Hilden
Anti-mouse antibody	Pearce
Anti-rabbit antibody	Pearce
Glucose-6-phosphate dehydrogenase peptide specific antibody	Eurogentech, Belgium
6-phosphogluconolactonase peptide specific antibody	Eurogentech, Belgium

2.3 Enzymes

Enzymes	**Source**
Catalase	Sigma, Steinheim
DNase 1	Roche, Mannheim
Pfu Polymerase	Promega, Mannheim
Quick DNA ligase	New England Biolabs, U.K
Red *Taq* polymerase	Sigma, Steinheim
Restriction enzymes	MBI, Fermentas
Yeast Glucose-6-phosphate dehydrogenase	Sigma, Steinheim
Yeast Phosphogluconate dehydrogenase	Sigma, Steinheim

2.4 Antibiotics Concentrations

Antibiotic	**Stock solution**	**Working concentration**
Carbenicillin	50 mg/ml in 50 % ethanol	100 µg/ml
Kanamycin	25 mg/ml in water	50 µg/ml
Chloroamphenicol	25 mg/ml in 100% ethanol	25 µg/ml

2.5 Kits

Kit	Source
Amine coupling kit and chip	Biacore AG, Sweden
Bradford kit	Biorad, München
Crystallisation kit (crystal screen 1& 2)	Hampton Research, Laguna Niguel, U.S.A
Primers	MWG-Biotech AG, Ebersberg
QIAprep spin mini prep kit	Qiagen, Hilden
QIAquick PCR purification kit	Qiagen, Hilden
Western lightning chemiluminescence reagent	Perkin Elmer, Boston, U.S.A

2.6 Biological Materials

2.6.1 Plasmids

Plasmids	Antibiotic Resistance	Source
pDest 17	Carbenicillin	Invitrogen
pRARE I & II	Chloroamphenicol	Novagen, Darmstadt
pET-28a	Kanamycin	Novagen, Darmstadt
pSK	Carbenicillin	Stratagen
pRIG	Chloroamphenicol, tRNAs for R, I and G	Wim Hol, (Baca & Hol, 2000)

2.6.2 *Escherichia coli* Cells

E. coli strain	Genotype	Source
KRX	[F', *tra*D36, Δ*omp*P, *pro*A^+B^+, *lac*I^q, Δ(*lac*Z)M15] Δ*omp*T, *end*A1, *rec*A1, *gyr*A96 (Nal^r), *thi*-1, *hsd*R17 (r_k^-, m_k^+), e14$^-$ ($McrA^-$), *rel*A1, *sup*E44, Δ(*lac-pro*AB), Δ(*rha*BAD): T7 RNA Polymerase	Promega, Mannheim
Rosetta	BL21 *lacYZ* deletion, Lacks *Ion* and *ompT* protease	Novagene
Novablue	*end*A1, *hsd*R17, (r_{k12}^- m_{k12}), *sup*E44, *thi*-1, *rec*A1, *gyr*A96, *rel*A1, *lac*F'[*pro*AB, *lac*I qZ*M*15, Tn10 (Tet^r)] (DE3-λcIst857, *ind*1, sam7, *nin*5, *lac*UV5-T7 gene1)	Novagene
C41	Miroux and Walker 1996	Avidis
PD2000 (G6PD mutant cells)	*garB10, fhuA22, ompF627(T^R_2), zwf-2, fadL701(T^R_2), relA1, pit-10, spoT1, rrnB-2, pgi-2, mcrB1, creC510*	Fraenkel, D Yale University

2.6.3 *Plasmodium falciparum* Strains

Strain	Origin	Source
K1 (Chloroquine-resistant strain)	South-East Asia	AG Prof. Lanzer, Heidelberg
Dd2 (Chloroquine-resistant strain)	Indochina	AG Prof. Lanzer, Heidelberg
HB3 (Chloroquine-sensitive strain)	Honduras	AG Prof. Lanzer, Heidelberg
3D7 (Chloroquine-sensitive strain)	Netherlands	AG Prof. Lanzer, Heidelberg

2.7 Buffers and Solutions

2.7.1 Buffers for Determination of Enzyme Activity

G6PD assay buffer	100 mM	Tris
	10 mM	$MgCl_2$
	0.5 mM	EDTA
	pH 8.0	
G6PD assay buffer for intact red blood cells	100 mM	Tris
	10 mM	$MgCl_2$
	0.5 mM	EDTA
	0.03 mM	Digitonin
	pH 8.0	
IDO assay buffer	100 mM	Potassium phosphate
	100 mM	KCl
	20 mM	Ascorbic acid
	200 µg/ml	Catalase
	10 µM	Methylene blue
	pH 6.5	

2.7.2 Buffers and Solutions for DNA Electrophoresis

10 × TBE	1 M	Tris
	1 M	Boric acid
	20 mM	EDTA
	pH 8.0 with acetic acid	
DNA sample buffer	0.1 %	Bromophenolblue
	1 mM	Tris
	60 %	Saccharose
	pH 8.3 with HCl	

2.7.3 Buffer for Extraction of *P. falciparum* Parasites from Red Blood Cells

Saponin lysis buffer	0.02 % (w/v)	Saponin
	7 mM	K_2HPO_4
	1 mM	NaH_2PO_4
	11 mM	$NaHCO_3$
	58 mM	KCl
	56 mM	NaCl
	1 mM	$MgCl_2$
	14 mM	Glucose
	pH 7.4 using HCl	

2.8 Protease Inhibitors

Inhibitor	Stock solution	Working concentration
PMSF	100 mM in ethanol	10 µl /10 ml US buffer
Pepstatin A	0.3 mM in DMSO	5 µl /10 ml US buffer
Cystatin	40 µM in US buffer	10 µl /10 ml US buffer

2.9 Medium for *E. coli* Culture

Luria-Bertani (LB)	5 g	Trypton
	10 g	Yeast extract
	5 g	NaCl
	ad 1000 ml bidistilled H_2O and autoclave	
Terrific Broth (TB)	12 g	Trypton
	24 g	Yeast extract
	9.4 g	K_2HPO_4
	2.2 g	KH_2PO_4
	4 ml	Glycerol
	ad 1000 ml bidistilled H_2O, autoclave and pH 7.0 ± 0.2	
2 x YT	16 g	Trypton
	10 g	Yeast extract
	5 g	NaCl
	ad 1000 ml bidistilled H_2O and autoclave	

2.10 Instruments

Instrument	Company
Analytical Balance	Scaltec Instruments, Göttingen
Beckmann Spectrophotometer DU® 650	Beckman, München
Biacore X	Biacore AG, Sweden
Biophotometer	Eppendorf, Hamburg
Infinite M200 multiplate reader	Tecan
ÄKTA/ Unicorn- FPLC system	Amershan Pharmacia Biotech
Hitachi Spectrophotometer U-2001	Hitachi Ltd, Tokyo
Incubator shaker	Thermo Life Sciences, Egelsbach
Microscope Axiostar	Zeiss, Jena
Mini-Spin Table Centrifuge	Eppendorf, Hamburg
OptimaTM TLX Ultracentrifuge	Beckman, München
PCR – Normal and – Gradient cyclers	Eppendorf, Hamburg
pH-Meter (Φ 350 pH/ Temp/ mV Meter)	Beckman, München
Quarz cuvettes	Hellma, Müllheim
Salvant, SpeedVac, Vacuum centrifuge	Thermo Life Sciences, Egelsbach
Sonicator	Bandelin Electronics, Berlin
Sorvall Centrifuge RC5C	Du Pont Company, Wilmington

3 Methods

3.1 General Methods

3.1.1 Preparation of Competent *E. coli* Cells

LB media (3 ml) containing the right antibiotic was inoculated with a small amount of *E. coli* cells glycerine storage culture and grown overnight in a shaking incubator at 37 ^{o}C. 100 ml of LB media containing the right antibiotic was then inoculated with the overnight culture and left to grow in a shaking incubator at 37 ^{o}C until an $O.D_{600}$ value of between 0.6-0.8 was achieved. The culture was then put into 4 Falcon tubes (25 ml into each) and placed on ice for 10 minutes. The culture was then centrifuged at 4000 rpm at 4 ^{o}C for 10 minutes to obtain a pellet, which was resuspended in 10 ml of ice cold 0.1 M $CaCl_2$ containing 10 % glycerine and left to stand on ice for 15 minutes. The resuspended pellet was again centrifuged at 4000 rpm at 4 ^{o}C for 10 minutes to obtain a pellet. The pellet was this time quickly resuspended in 1 ml of ice cold 0.1 M $CaCl_2$ containing 10 % glycerine. Into clearly labelled Eppendorf tubes, the resuspension was quickly aliquoted (50 µl into each), placed into liquid nitrogen for 2-5 minutes and then stored at -80 ^{o}C. The cells were competent and ready for use.

3.1.2 Preparation of Competent *E. coli* Cells Containing pRARE or pRIG Plasmid

Competent *E. coli* cells were transformed with the pRARE or pRIG plasmid as outlined under 3.1.3 transformation of competent *E. coli* cells. After colonies appeared on the LB agar plates containing the right antibiotic, one colony was picked and used to inoculate 3 ml of LB media containing antibiotic and grown in a shaking incubator overnight at 37 ^{o}C. 100 ml of LB media containing the right antibiotic was then inoculated with the overnight culture and the competent cells were then prepared as outlined in 3.1.1.

3.1.3 Transformation of Competent *E. coli* Cells

To 50 µl of competent *E. coli* cells 2 µl of the plasmid was added and mixed thoroughly by use of a pipette and left to stand on ice (4 ^{o}C) for 30 minutes. After 30 minutes heat shock was induced for 90 seconds at 42 ^{o}C and the cells were then placed on ice again for 2 minutes. Approximately 400 µl of LB media was added to the cells and stood for 1 hour at 37 ^{o}C, after which the cells were plated on LB agar plates containing the right selection marker or antibiotics. The plates were incubated overnight in an incubator at 37 ^{o}C and colonies were observed the next day.

3.1.4 SDS-Polyacrylamide Gel Electrophoresis

Sample buffer	62.5 mM	Tris-HCL
	25 %	Glycerol
	2 %	SDS
	0.01 %	Bromophenolblue
	5 %	Mercaptoethanol

Separating gel 7.5 % (15.1 ml)	3.75 ml	1.5 M Tris pH 8.8
	3.75 ml	Acrylamide (Rotiphorese® gel 30)*
	0.15 ml	SDS (10 % in water)
	7.35 ml	H_2O
	75 µl	APS (10 % in water)
	7.5 µl	TEMED
Sample gel 4 % (5 ml)	1.25 ml	0.5 M Tris pH 6.8
	0.65 ml	Acrylamide (Rotiphorese® gel 30)
	0.05 ml	SDS (10 % in water)
	3.05 ml	H_2O
	25 µl	APS (10 % in water)
	5 µl	TEMED
Electrophoresis buffer	25 mM	Tris
	192 mM	Glycine
	0.1 %	SDS
Coomassie staining solution	0.2 %	Coomassie Brillant Blue R250
	10 %	Acetic acid
	40 %	2-Propanol
Coomassie destaining solution	10 %	Acetic acid
	8 %	Ethanol

* various amounts of acrylamide (Rotiphorese® gel 30) 3.75, 4.95, 6, 7.5 ml for 7.5 %, 10 %, 12 %, and 15 % SDS-polyacrylamide gels respectively.

SDS-PAGE was performed according to Laemmli [1970]. In brief the proteins were mixed in a volume ratio of 1:1 with sample buffer and heated at 95 ^{o}C for 5 minutes to denature the proteins. The denatured proteins were then loaded on to pre-cast discontinuous polyacrylamide gels 10 % consisting of 2 parts namely; sample gel (Tris buffer pH 6.8, 4 % acrylamide, 1 % SDS) containing pockets on which the samples were loaded. The second part is the separating gel (Tris buffer pH 8.8, 7.5-15 % acrylamide, 10 % SDS) on which the proteins are separated according to their molecular weight. The gels were run at a voltage of 200 in an electrophoresis tank containing an electrophoresis buffer. Once the separation process was complete, the gel electrogram was stained with Coomassie stain and destained with Coomassie destaining solution until protein bands were clearly visible. Just in case the gel electrogram was required for Western blot, it was not stained with Coomassie rather it was immediately soaked into the cathode buffer.

3.1.5 Western Blot

Anode buffer I	300 mM	Tris
Anode buffer II	25 mM	Tris

Cathode buffer	40 mM	6 –Aminohexanoic acid
Blocking buffer	5 % Milk powder in TBS buffer	
TBS buffer	10 mM 155 mM pH 8.0 with HCl	Tris NaCl
TBST buffer	0.05 %	Tween 20 in 1000 ml TBS buffer
Ponceau staining solution	1 % 1 %	Ponceau S Acetic acid
Ponceau destaining solution	1 %	Acetic acid

Semi dry Western blot was performed according to Towbin *et al*., [1979]. A sample of the protein of interest was subjected to SDS-PAGE. The completed gel electrogram was blotted onto a sheet of PVDF (polyvinyl difluoride) membrane that had been activated by briefly soaking in methanol then quickly transferring it into anode buffer II solution. The transfer set up was made up of a cathode graphite plate onto which 5 filter papers and the gel electrogram pre-soaked in cathode buffer had been laid. The PVDF membrane was laid onto the gel electrogram followed by 2 filter papers pre-soaked in anode buffer II. Then 3 more filter papers pre-soaked in anode buffer I followed. Finally an anode graphite plate was laid on top of the set up to complete the transfer cassette. The transfer process was carried out at 0.8 mA / cm^2 of gel electrogram for 55 minutes.

To check for the efficiency of the transfer process, the PVDF membrane was stained for 30 seconds with Ponceau staining solution and immediately de-stained with 1 % acetic acid until clear protein bands were visible. The PVDF membrane bound proteins strongly and unspecifically. The excess adsorption sites on the PVDF were blocked using 5 % milk powder in TBS buffer so as to prevent non specific adsorption of antibodies. The membrane was rinsed 3 times for 10 minutes each with TBST and incubated with the primary antibody or the antibody for the protein of interest (e.g. anti-histidine IgG) for 1 hour. After washing away the unbound primary anti-body with TBST (3 times for 10 minutes each), the blot was incubated for 1 hour with a secondary antibody (e.g. anti-mouse in case anti-histidine is the primary antibody) directed against the primary antibody to which the protein of interest had been covalently linked. After washing away the unbound secondary antibody (3 times for 10 minutes each) with TBST, immunostaining of the membrane was performed by exposing the membrane to an enhanced chemiluminescence mixture for 1 minute. The membrane was then wrapped in a transparent foil paper and exposed to X-ray film for a period of between 30 seconds to 15 minutes. The final development of the X-ray film was performed using an X-ray film exposure machine.

3.1.6 Gel Filtration

The molecular mass of the recombinant protein was determined by native gel chromatography on a 16/60 superdex 200 prep grade column which was connected to an ÄKTA/ Unicorn- FPLC system (Amersham Pharmacia Biotech). Calibration of the column was performed using a gel filtration standard (Amersham Pharmacia Biotech) containing ferritin, aldolase, albumin, ovalalbumin and chymotrypsinogen as reference proteins. One millilitre of a 1 mg/ml protein solution was applied to the column that had previously been equilibrated with the appropriate buffer. Protein-containing fractions were detected spectrophotometrically at 280 nm and were collected at a flow rate of 1.0 ml/min. The peak areas and K_{AV} values were evaluated using the UNICORN 4.11 software. Protein-containing fractions were also analysed on SDS-PAGE. The pure protein fractions obtained after gel filtration (FPLC machine) were then concentrated using a 50 kDa viva spin column. Protein concentration was determined using the Bradford protein assay [Bradford, 1976] and a standard curve of bovine serum albumin, ranging in concentration from 0 to 1 mg/ml.

3.1.7 Protein Crystallisation

The hanging drop method was used for crystal screening. The principle of this method is basically the vaporisation between a micro drop of mother liquor and a much larger highly concentrated reservoir solution thereby causing a slow precipitation of the protein in a controlled manner. The protein molecule is normally initially dissolved in a buffered solution usually containing a mixture of solvents and salts. The sample solution is physically separated from a larger volume called a reservoir (Figure 10). The sample and reservoir are kept in a closed system, and as the solvent or salts vaporise from the drop (or sometimes are added to the drop) the precipitant concentration increases to a level optimal for crystallisation. Since the system is in equilibrium, these optimum conditions are maintained until the crystallisation is complete [Fairall *et al*., 1993, Shaw *et al*., 1993].

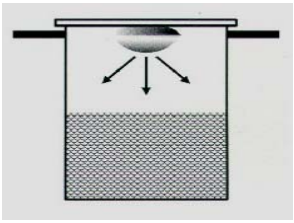

Figure 10: Hanging drop method of protein crystallisation.

In order to crystallise our protein of interest 2 µl drops of the protein were mixed with a similar volume of precipitant solution on a siliconised microscope glass slip. The glass slip was then placed over a small well (of a multiwell crystallisation plate) containing 800 µl of the precipitant solution. To make sure that the system was totally sealed silicon oil was added to the sides of the glass slip. Over 100 different solutions which varied in terms of pH, buffer, ionic strength, metallic content and precipitant were tested by use of Hampton research crystallisation kits (crystal screen I and II).

3.2 *Pf*GluPho Methods

3.2.1 Cloning of *Pf*GluPho

The gene of *Pf*GluPho was identified on chromosome 14. By polymerase chain reaction (PCR) on a *P. falciparum* 3D7 cDNA library, the whole *Pf*GluPho gene was amplified. The forward primer was designated to introduce a *Bam*HI restriction site (5′-CGC GGG ATC CGA TTA TGA GAA TTT TGT AAA AAG TGC AG-3′) and the reverse primer to introduce a *Hin*dIII restriction site (5′-GCG CAA GCT TTC AAT TAA TAT CTA ACA AAT CGT CTT C-3′). The PCR conditions as well as the PCR mix was as follows:

PCR mixture		The PCR programme used	
Volume in µL		Time in Seconds	Temperature in ^{o}C
5.0	Buffer	300	94
4.0	dNTP	30	94
1.0	Primer (100 pmol/µl)	30	55
1.0	Primer (100 pmol/µl)	180	60 (35 cycles)
1.0	Template	480	60
35.5	$H_2O_{dd\ autoclaved}$	∞	8
2.5	Red Taq Polymerase		
Total 50.0			

The amplified PCR product was cleaned using the QIAquick PCR purification kit, restricted with the corresponding restriction enzymes, purified again using the QIAquick PCR purification kit but could not directly be cloned into the pSK vector.

Since no native useful restriction site is present within *Pf*GluPho, we decided using a silent mutation to create a *Sac*I restriction site within the *Pf*GluPho gene. This would enable us to amplify the gene in two separate parts of 1000 and 1733 base pairs, which could later be combined by ligation to form the complete *Pf*GluPho gene. We emphasise the mutation was silent in that the amino acid sequence of the protein was not altered by our cloning strategy.

```
901 - AATACCACTGTTATATCTTGTGGTTATGAAAATTATACAAAATCTATTGAAGAAATTTAT - 960
      - N  T  T  V  I  S  C  G  Y  E  N  Y  T  K  S  I  E  E  I  Y- GAGCTC
961 - GATTCTAAATATGCTCTATCTCTTTATTCTAATAGTTTGAATAAAGAAGAATTATTAACT -1020
      - D  S  K  Y  A  L  S  L  Y  S  N  S  L  N  K  E  E  L  L  T   SacI
1021 - ATAATAATTTTTGGCTGTTCAGGTGATTTAGCCAAAAAAAAAATATATCCAGCTTTATTT - 1080
       - I  I  I  F  G  C  S  G  D  L  A  K  K  K  I  Y  P  A  L  F-
```

Figure 11: Silent mutation introduced in the *Pf*GluPho gene in order to creat a *Sac*I restriction site

The first part was amplified using the same *Bam*HI forward restriction site primer and a reverse primer containing a *Sac*I restriction site (5′-GCG CGA GCT CTT CTT TAT TCA AAC TAT TAG AAT AAA GAG-3′). The second part was amplified using a *Sac*I restriction site primer (5′-GCG CGA GCT CTT AAC TAT AAT AAT TTT TGG CTG TTC AG-3′) and the same reverse primer containg a *Hin*dIII restriction site. The PCR conditions and mixture was as follows:

PCR mixture		The PCR programme used	
Volume in µl		Time in Seconds	Temperature in ^{o}C
5.0	Buffer	300	94
4.0	dNTP	30	94
1.0	Primer (100 pmol/µl)	30	55
1.0	Primer (100 pmol/µl)	120	60 (35 cycles)
1.0	Template	240	60
35.5	$H_2O_{dd\ autoclaved}$	∞	8
2.5	Polymerase		
Total 50.0			

The amplified PCR products were restricted with the corresponding restriction enzymes, cleaned using the QIAquick PCR purification kit and ligated into a pSK vector which had also been restricted with the corresponding restriction enzymes. We chose to use the pSK vector which allows for the α-complementation test or blue and white screening in the presence of chromogenic X-gal (Davies and Jacob, 1968). The restriction enzyme reactions were performed overnight at room temperature and the reaction mixtures as well as the ligation reaction mixtures were as follows:

Restriction Enzyme Reactions Mixtures			
Volume in µl		Volume in µl	
25.0	PCR products	10.0	pSK plasmid
5.0	Buffer (yellow)	3.0	Buffer (yellow)
1.5	*Bam*HI or *Hin*dIII	1.0	*Bam*HI or *Hin*dIII
1.5	*Sac*I	1.0	*Sac*I
17.0	$H_2O_{dd\ autoclaved}$	15.0	$H_2O_{dd\ autoclaved}$
Total 50.0		Total 30.0	

Ligation Reaction Mixture	
Volume in µl	
8.0	Digested PCR product (*Bam*HI-*Sac*I or *Sac*I-*Hin*dIII)
2.0	pSK (*Bam*HI-*Sac*I or *Sac*I-*Hin*dIII)
10.0	Buffer
1.0	Quick ligase
Total 21.0	

The ligation mix was mixed thoroughly and incubated at room temperature for 6-7 minutes. 25 µl of competent *E. coli* Novablue (Novagene) cells were then transformed (as outlined under 3.1.3 transformation of *E.coli* cells) separately with 2 µl of the pSK / *Bam*HI-*Sac*I and pSK / *Sac*I-*Hin*dIII ligation mixture, plated onto X-gal LB (LAXI) plates and stood over night in an incubator at 37 ^{o}C. Blue (empty colonies) and white colonies (probably containing the insert of interest) were observed the next day. The white colonies were used to inoculate 3 ml of LB media tubes containing carbenicillin (100 µg/ml) and the culture was grown overnight. The next morning the culture was centrifuged at 10,000 x g to obtain a pellet. The supernatant was discarded and the pellet used for mini plasmid preparations using the QIAprep kit and spin columns. The prepared plasmids together with an empty pSK plasmid (control) were then

subjected to 1 hour of restriction cleavage at 37 ^{o}C using the respective restriction enzymes (*Bam*HI /*Sac*I or *Sac*I / *Hin*dIII). The restriction reaction mixture was as follows:

Restriction Enzyme Reactions Mixture	
Volume in µl	
25.0	Plasmid prep
5.0	Buffer (Yellow)
1.5	*Bam*HI or *Hin*dIII
1.5	*Sac*I
17.0	$H_2O_{dd\ autoclaved}$
Total 50.0	

The restricted plasmids were then analysed against the control plasmid using agarose gels stained with ethidium bromide. The plasmid containing the right size of insert and the right size of restricted plasmid in comparison to the marker and control were used for further verification of the insert by sequencing.

3.2.2 Mutagenesis PCR

Comparing our sequence results with the sequence present in the data bank (Gene Bank AAN37124, PlasmoDB PF14_0511) revealed the presence of the following mutations

pSK/ *Bam*HI-*Sac*I S^{315} changed to Y^{315}

pSK/ *Sac*I-*Hin*dIII N^{415} changed to S^{415}

Since we had different clones sequenced each with different mismatches to the database sequence we thought these were mutations derived from the *Taq*-Polymerase used. We therefore performed mutagenesis PCR in order to back mutate these mutations so that our gene sequence could conform to that present in the data bank. The PCR conditions and the mixture were as follows:

PCR mixture		The PCR programme used	
Volume in µl		Time in Seconds	Temperature in ^{o}C
5.0	10x *Pfu* Buffer	180	94
4.0	dNTP	30	94
1.0	Primer I	30	55
1.0	Primer II	510	60 (2 min/kb template)
1.0	Template (50 ng/µl)	510	60
2.5	DMSO	∞	8
34.5	$H_2O_{dd\ autoclaved}$		
1.0	*Pfu* Polymerase		
Total 50.0			

After the mutagenesis PCR, the products were cleaned using the Qiaquick PCR purification kit and restricted for 1 hour at 37 ^{o}C using *Dpn*I restriction enzyme. The reaction mixture was:

*Dpn*I Restriction Enzyme Reactions Mixtures	
Volume in µl	
42.0	PCR product
5.0	10x Buffer B
0.5	BSA (10 mg/ml)
2.5	*Dpn*I
Total 50.0	

The restricted PCR product was then transformed into Novablue competent cells, plated on LAXI plates and stood overnight in an incubator at 37 ^{o}C. The next day colonies probably containing the gene of interest were observed which were used to inoculate 3 ml of LB media tubes containing carbenicillin (100 µg/ml) and the culture was grown overnight in a shaking incubator at 37 ^{o}C. The next morning the culture was used for plasmid preparation using Qiaprep kit and spin columns. The plasmid inserts were verified by sequencing and by comparison of the sequences to those present in the data bank.

The *Dpn*I restriction reaction performed after the mutagenesis PCR is important because *Dpn*I is a restriction enzyme that targets methylated DNA. Since the template used in the mutagenesis PCR was a plasmid prep which had been prepared after transformation in *E. coli* cells, this meant it was methylated and therefore cleaved or destroyed leaving only the mutagenesis PCR product plasmid.

Once it was established that our 2 clones had the right sequence, we decided to cleave them out of the pSK plasmid and insert them into the expression vector pET-28a while combining them to form the bifunctional gene of *Pf*GluPho. This was performed in two steps: the first step was to insert the clone *Sac*/ *Hin*d then followed by the *Bam*/ *Sac* clone as the second step. The pSK plasmid containing the *Sac*/ *Hin*d clone and the pET-28a plasmid where the clone was to be inserted were subjected to restriction enzyme reaction under the following conditions:

Restriction Enzyme Reactions Mixtures			
pSK *Sac* / *Hin*d		pET-28a	
Volume in µl		Volume in µl	
4.0	Buffer	5.0	Buffer
2.0	*Hin*d III	2.0	*Hin*dIII
2.0	*Sac*I	2.0	*Sac*I
7.0	pSK *Sac*I-*Hin*dIII	25.0	pET-28a
5.0	$H_2O_{dd\ autoclaved}$	16.0	$H_2O_{dd\ autoclaved}$
Total 20.0		50.0	

The restriction cleavage reaction mixtures were mixed thoroughly and stood at 37 ^{o}C for 1 hour after which they were cleaned using the Qiagen PCR purification kit. Agarose gel electrophoresis was performed to check for the integrity of the restriction reaction. The next step was to try and insert the *Sac*/ *Hin*d clone into pET-28a. This was achieved by ligating the *Sac*/ *Hin*d clone into the pET-28a vector using the following ligation mixture:

Ligation Reaction Mixture	
Volume in µl	
6.0	pSK *Sac*/ *Hin*d
4.0	pET-28a *Sac*/ *Hin*d
10.0	Buffer
1.0	Quick Ligase
Total 21.0	

The reaction mixture was incubated for 6-7 minutes at room temperature, transformed into Novablue competent *E. coli* cells, plated on LB plates containing kanamycin (50 µg/ml) and stood overnight in an incubator at 37 ^{o}C. The next day colonies were observed which showed that the ligation reaction was successful, but to be sure we had the right clones, we inoculated 3 ml of LB medium containing kanamycin (50 µg/ml) using these colonies and grew them overnight. The next morning we performed plasmid preparations using the Qiaprep kit and spin columns. The prepared plasmids were then subjected to restriction cleavage using *Sac*I and *Hin*dIII restriction enzymes and the restriction products analysed using agarose gel stained with ethidium bromide. We were able to obtain the right band of interest and therefore we were sure we had the *Sac*I-*Hin*dIII clone within the pET-28a vector.

The next challenge was to insert the *Bam*HI-*Sac*I clone into the pET-28a vector containing the *Sac*I-*Hin*dIII clone. The *Bam*HI-*Sac*I clone was inserted into the pET-28/ *Sac*I-*Hin*dIII clone as follows; restriction reaction was performed on the pSK/ *Bam*HI-*Sac*I and pET-28a/ *Sac*I-*Hin*dIII plasmids in a reaction mixture of the following composition:

Restriction Enzyme Reactions Mixtures			
pSK/ *Bam*HI-*Sac*I		pET-28a/ *Sac*I-*Hin*dIII	
Volume in µl		Volume in µl	
5.0	Buffer	5.0	Buffer
1.0	*Bam*HI	1.0	*Bam*HI
2.0	*Sac*I	1.0	*Sac*I
20.0	pSK/ *Bam*HI-*Sac*I	20.0	pET-28a/ *Sac*I-*Hin*dIII
22.0	$H_2O_{dd\ autoclaved}$	22.0	$H_2O_{dd\ autoclaved}$
Total 50.0		50.0	

The restriction reaction was performed at 37 ^{o}C for 1 hour after which the plasmids were cleaned using the Qiagen PCR purification kit. An agarose gel electrophoresis was performed to check the integrity of the restriction reaction. The cleaned restriction reaction products were then ligated together in a reaction composition as follows:

Ligation Reaction Mixture	
Volume in µl	
6.0	pSK *Bam*HI-*Sac*I
3.0	pET-28a/ *Sac*I-*Hin*dIII
1.0	$H_2O_{dd\ autoclaved}$
10.0	Buffer
1.0	Quick Ligase
Total 21.0	

The ligated products were transformed using Novablue competent *E. coli* cells, plated on LB plates containing kanamycin (50 μg/ml) and stood in an incubator at 37 ^{o}C overnight. The next day colonies were observed which showed that the ligation reaction was successful, but to be sure we had the right clones, we inoculated 3 ml of LB medium containing Kanamycin (50 μg/ml) using these colonies and grew them overnight. The next morning we performed plasmid preparations using the Qiaprep kit and spin columns. The prepared plasmids were then subjected to restriction cleavage using *Bam*HI and *Hin*dIII restriction enzymes and the restriction products analysed using agarose gel stained with ethidium bromide. We were able to obtain the right band of interest and therefore we were sure we had the *Bam*HI-*Hin*dIII clone in the pET-28a vector and therefore we had the complete *Pf*GluPho clone.

Further confirmatory tests were performed to ascertain that we had the complete *Pf*GluPho clone. We performed a PCR using two sets of primers capable of amplifying the complete *Pf*GluPho gene; the *Bam*HI and *Hin*dIII primers which had been used earlier and another set of primers without the restriction site designated as N primer (5′-ATT ATG AGA ATT TTG TAA AAA GTG CAG-3′) and C primer (5′-TCA ATT AAT ATC TAA CAA ATC GTC TTC-3′). Once again when the PCR product was analysed on the agarose gel we were able to obtain the right band of interest. The inserts were further verified by sequencing and comparison of the sequences to those present in the data bank. The sequencing results revealed that we had the right clone and our cloning strategy was very successful. The pET28a vector would thus place a hexahistidyl tag at the N-terminus of the recombinant protein.

3.2.3 Heterologous Overexpression of *Pf*GluPho

E. coli KRX pRAREII cells were transformed with the pET-28a/ *Pf*GluPho plasmid. Cultures of transformed cells were grown in 1 Litre of Terrific Broth (TB) medium [containing kanamycin (50 μg/ml) and chloramphenicol (25 μg/ml) antibiotics] until an OD_{600} of between 0.3 and 0.4 was achieved. The cultures were then transferred to room temperature and grown further to an OD_{600} of between 1.0 and 1.5. Rhamnose (20% stock solution) was then added to a final concentration of 0.1% and the culture was further grown overnight. Cells were collected as a pellet by centrifugation at 8,000 g for 15 minutes at 4 ^{o}C and resuspended in 100 mM Tris buffer pH 7.8, 500 mM NaCl. After addition of protease inhibitor cocktail consisting of pepstantin, cystantin and PMSF, the pellet was stored at -20 ^{o}C.

3.2.4 Optimisation of the Heterologous Overexpression of *Pf*GluPho

The optimisation of the heterologous overexpression of *Pf*GluPho was performed using different *E. coli* cell lines (G6PD deficient cells PD2000 and other non deficient cells) as well as varying the different expression parameters as summarised in Table 3.

3.2.5 Purification of *Pf*GluPho

A small amount of DNase as well as lysozyme (4 mg/g pellet) was added to the thawed pellet and stirred over ice for 1 hour. The cells were sonicated 3 times for 30 seconds each at maximum power and centrifuged at 16,000 g for 30 minutes. The clear supernatant was then applied to a 1 ml Ni-NTA column, washed with 5 ml of 100 mM Tris buffer, pH 7.8, 500 mM NaCl and eluted using a stepwise imidazole concentration gradient. The pure fractions as observed on the SDS gel were pooled together, concentrated using a 50 kDa viva spin column and further purified by gel filtration using an ÄKATA/ Unicorn FPLC system as outlined in 3.2.7.

3.2.6 Optimisation of the Purification of *Pf*GluPho

The purification process was optimised using two column materials namely: the Ni-NTA and the 2' 5' ADP Sepharose 4B in combination with gel filtration using an FPLC machine (Table 2). Different buffers, pH and salt concentrations were also optimised for the purification process (Table 3).

3.2.7 Gel Filtration of *Pf*GluPho

Gel filtration was performed as outlined in Section 3.1.6 with a minor modification. The buffer used for gel filtration was 100 mM Tris buffer, pH 7.8, 500 mM NaCl. The protein containing fractions obtained after gel filtration (FPLC machine) were analysed on SDS-PAGE and then concentrated using a 50 kDa viva spin column. Protein concentration was determined using the Bradford protein assay [Bradford, 1976] and a standard curve of bovine serum albumin, ranging in concentrations from 0 to 1 mg/ml.

3.2.8 Western Blot Using *Pf*GluPho Specific Antibody and *P. falciparum* Proteins

The Western blot using peptide specific antibodies for *Pf*GluPho produced from rabbits which had been immunized with synthetic peptides of *Pf*GluPho (N-teminal peptide composed of aa 118-133: KEQLYKPDTTKSIVDC and C-terminal peptide composed of aa 896-910: CVRKSSFYEDDLLDIN) (Eurogentec, Seraing, Belgium) was performed as outlined in 3.1.5 but with a few modifications. The primary antibody was *Pf*GluPho specific antibody diluted using 5 % milk powder in TBST (1:5,000). The secondary antibody was anti-rabbit diluted in TBST. The SDS-PAGE (7.5 %) was performed using *P. falciparum* proteins (concentrations loaded on the gel 45, 70, 105 µg) as well as recombinant *Pf*GluPho. The *P. falciparum* proteins were prepared as outlined in 3.6.4.

3.2.9 *Pf*GluPho's G6PD Assays

3.2.9.1 Determination of K_m Values for G6P, $NADP^+$ and Steady State Kinetics

The standard two substrate G6PD assay which measures the reduction of $NADP^+$ to NADPH at 340 nm was performed at 25 ^oC according to Beutler, [1984]. In brief the standard reaction mixture for measurement of the K_m for G6P on *Pf*GluPho's G6PD was composed of

100 µM $NADP^+$, the standard G6PD assay buffer (100 mM Tris, 0.5 mM EDTA, 10 mM $MgCl_2$, pH 8.0), *Pf*GluPho enzyme and varying amounts of G6P (200-5 µM) which was added to start the reaction. The total reaction volume was 500 µl. Measurement of the K_m for $NADP^+$ on *Pf*GluPho's G6PD on the other hand was performed by varying the concentrations of $NADP^+$ (200-2 µM) and fixing the concentration of G6P at 100 µM. The same method was also used for the determination of the kinetic parameters (K_m for G6P and K_m for $NADP^+$) for yeast G6PD as an internal control. The steady state kinetics of *Pf*GluPho's G6PD for G6P were performed by holding the concentration of $NADP^+$ at the K_m value while varying the concentration of G6P (100-5 µM). Likewise the steady state kinetics for $NADP^+$ were performed by holding the concentration of G6P at K_m value while varying the concentration of $NADP^+$ (50-2 µM).

$$G6P + NADP^+ \xrightarrow{G6PD} 6PGL + NADPH + H^+$$

G6PD assay (340 nm):

G6PD assay buffer : 480 - x µl
(100 mM Tris, 0.5 mM EDTA, 10 mM $MgCl_2$, pH 8.0)
$NADP^+$ (10 mM) : 10.0 µl (ad 200 µM)
G6PD : x µl
——————— Baseline ———————
G6P (4 mM) : 25 µl (ad 200 µM)

$\varepsilon_{NADPH} = 6.22\ mM^{-1}*cm^{-1}$

$$VA = \frac{\Delta A/\min * Vo}{6.22 * Vi}\ [U/ml]$$

where V_o is the total volume of assay and V_i is volume of enzyme used.

The stability of the baseline was determined before the assays were carried out in order to check for background reactions that could affect the integrity of our assays. Such background reactions could be from *E. coli* proteins that could be co-purified with *Pf*GluPho. A standard reaction mixture for the G6PD assay was prepared as outlined above in the presence of *Pf*GluPho but the reaction was not started by adding G6P. Instead the stability of the baseline was checked by measuring the absorbance at 340 nm. In a similar set up an expression was performed using KRX pRAREII cells without *Pf*GluPho and purified as outlined for *Pf*GluPho. The fractions that normally contain positive bands for *Pf*GluPho were then used to check for the stability of the baseline as outlined.

3.2.9.2 *Pf*GluPho's G6PD Assays with the Substrate Analogue 2-Deoxyglucose-6-Phosphate

The steady state kinetics of *Pf*GluPho's G6PD using the substrate analogue 2-deoxyG6P were performed by holding the concentration of $NADP^+$ at the K_m value while varying the concentration of 2-deoxyG6P (100-0.1 mM). Likewise the steady state kinetics for $NADP^+$ was performed by holding the concentration of 2-deoxyG6P at K_m value while varying the concentration of $NADP^+$ (50-2 μM).

3.2.9.3 *Pf*GluPho's G6PD Inhibition with NADPH, Glucoseamine-6-Phosphate and ATP-Ribose

In product inhibition studies, the initial rates were measured for a series of NADPH concentrations (0-20 μM) by holding the concentration of G6P at the K_m value while varying the concentration of $NADP^+$ (2-50 μM). A similar experiment was carried out by use of the same series of NADPH concentration (0-20 μM) by holding the concentration of $NADP^+$ at the K_m value while varying the concentration of G6P (5-100 μM). In analogous fashion, glucoseamine-6-phophate and ATP-ribose were used as inhibitors covering the same combination and ranges of substrate concentrations as used in the experiments with NADPH.

3.2.9.4 *Pf*GluPho's G6PD Assays with GSSG, GSH and *Pf*GR

To check if *Pf*GluPho activity is regulated through the interaction with *Pf*GR or undergoes allosteric regulation in the presence of GSH or GSSG, the G6PD assay was performed in the presence of either; 2 mM GSH, 1 mM GSSG, *Pf*GR 10 mU/ml or in the presence of both 10 mU/ml *Pf*GR and 2 mM GSH.

3.2.9.5 *Pf*GluPho's G6PD pH, Buffers and Salt Profile

Several buffers as outlined below were tested in order to determine the best buffer, pH and salt conditions optimum for *Pf*GluPho activity:

Buffer	pH range	Salts
Na-phosphate buffer 25 mM	6.2 - 8.8	NaCl 0 - 300 mM
Tris buffer 100 mM	6.6 - 8.8	NaCl 0 - 500 mM, $MgCl_2$ 0 - 500 mM
Hepes buffer	6.6 - 8.2	$MgCl_2$ 0 - 100 mM

3.2.9.6 Test for G6PD Activity in Full Blood

G6PD activity in fresh full blood samples obtained from three donors from our labs was determined according to the standard G6PD assay (as outlined in 3.2.10.1) but with a few modifications. The standard G6PD assay for measuring K_m values for G6P and $NADP^+$ was set up as earlier outlined but the standard assay buffer contained in addition 0.03 mM Digitonin for red blood cell lysis.

3.2.10 *Pf*GluPho's 6-PGL Assays

3.2.10.1 Determination of the K_m for 6-PGL

The analysis of *Pf*GluPho's 6-PGL activity was performed using a time course study. The assay system consisted of a 500 µl solution composed of 200 µM $NADP^+$, the standard G6PD assay buffer (100 mM Tris, 0.5 mM EDTA, 10 mM $MgCl_2$, pH 8.0), *Pf*GluPho enzyme and 150 µM of G6P which was added to start the reaction. After a given period of time (1, 2, 4, 6, 8, 10, 12, 15 and 20 minutes) 6-phosphogluconate dehydrogenase (6-PGD) (yeast, Sigma) was added to the reaction mixture and the reaction allowed to continue for a further 3 minutes. The reaction was performed at 25 ^oC and absorbance readings taken at 340 nm. The absolute and linear changes in absorbance indicating the consumption of G6P and therefore production of 6-phosphoglucono-δ-lactone (6-PG-δ-L) were determined at each time point before and after addition of 6-PGD. The difference between these values were used for the calculation of 6-PGL activity.

Hydrolysis of 6-PG-δ-L by the enzyme 6-PGL leads to the formation of 6-phosphogluconate (6-PGn) which is converted by the action of the enzyme 6-PGD to ribose-5-phosphate. In order to estimate the amount of 6-PGn available to 6-PGD after 6-PG-δ-L hydrolysis by *Pf*GluPho's 6-PGL, 6-PGD assays in the absence of *Pf*GluPho were performed and used as a calibration curve. The assay consisted of 200 µM $NADP^+$, assay buffer (100 mM Tris buffer, 0.5 mM EDTA, 10 mM $MgCl_2$, pH 8.0), 6-PGD (Yeast, Sigma) (0.08 U/ml) and varying amounts of 6-PGn (100-5 µM). The total volume of the assay was 500 µl and the reaction was performed at 25 ^oC with absorbance readings being taken at 340 nm. Prior to experiments involving yeast 6-PGD, the approximate K_m values for both substrates ($NADP^+$ and 6-PGn) were determined. The standard two substrate 6-PGD assay which measures the reduction of $NADP^+$ to NADPH at 340 nm was performed at 25 ^oC. In brief the standard reaction mixture for measurement of the K_m for 6-PGn on 6-PGD was composed of 200 µM $NADP^+$, the standard G6PD assay buffer (100 mM Tris, 0.5 mM EDTA, 10 mM $MgCl_2$, pH 8.0), yeast 6-PGD enzyme (0.08 U/ml) and varying amounts of 6-PGn (200-5 µM) which was added to start the reaction. The total reaction volume was 500 µl. Measurement of the K_m for $NADP^+$ on 6- PGD on the other hand was performed by varying the concentrations of $NADP^+$ (200-2 µM) and fixing the concentration of 6-PGn at 100 µM.

3.2.10.2 *Pf*GluPho's 6-PGL Assays in the Presence of GSSG and GSH

The standardised *Pf*GluPho's 6-PGL assay was performed in the presence of either 5 mM GSSG, 5 mM GSH, 5 mM GSSG plus 10 µM Glutathione reductase (GR), 5 mM GSH and 5 mM GSSG plus 10 µM GR. The reaction was performed for 10 minutes before the addition of 6-phosphogluconate dehydrogenase and then allowed to continue further for 3 minutes. Data collection was performed as outlined in 3.2.10.1.

3.2.11 *Pf*GluPho Crystal Screening

Crystal screening was performed as outlined in 3.1.7. In order to crystallise *Pf*GluPho 2 µl drops of the protein were mixed with a similar volume of precipitant solution on a siliconised microscope glass slips. The glass slip was then placed over a small well (of a multiwell crystallisation plate) containing 800 µl of the precipitant solution. To make sure that the system was totally sealed silicon oil was added to the sides of the glass slip. Over 100 different solutions which varied in terms of pH, buffer, ionic strength, metallic content and precipitant were tested by use of Hampton research crystallisation kits (crystal screen I and II). We also tested various solutions from the published G6PD structures [Cosgrove *et al*., 1998; Cosgrove *et al*., 2000; Au *et al*., 2000; Delarue *et al*., 2007]. *Pf*GluPho obtained after gel filtration (FPLC purification) was used for the crystallisation trials. The concentration of the protein was 15 mg/ml from a total of 25 litres of culture.

3.2.13 *Pf*GluPho Inhibitor Screening

The standard G6PD assay method was optimised for the first time for screening of *Pf*GluPho G6PD inhibitors using an Infinite M200 (Tecan) multiwell plate reader with monochromator. In brief the method involved a 20 ml master mix composed of standard G6PD buffer, $NADP^+$ (200 µM) and *Pf*GluPho (32 µg/ml). The assay was performed by mixing together G6PD buffer (79 µl), inhibitor 5 µg/ml (1 µl of 1 mg/ml) and 100 µl of the master mix (final concentration $NADP^+$ 100 µM, *Pf*GluPho 16 µg/ml). The assay was started by adding G6P (20 µl) 100 µM and the absorbance measured at 340 nm. Total volume for the assay was 200 µl. A total of 2,000 compounds were screened and IC_{50} values determined. The best compounds were further tested to determine the inhibition mechanism.

Buffer:	100 mM Tris, 0.5 mM EDTA, 10 mM $MgCl_2$, pH 8.0	
*Pf*GluPho:	0.91 mg/ml	
$NADP^+$:	10 mM (8.37 mg/ml)	
G6P:	1 mM (0.282 mg/ml)	
Master Mix:	Buffer	18.424 ml
	$NADP^+$ (200 µM)	0.390 ml (add 100 µM)
	*Pf*GluPho	0.686 µl (add 16 µg)
Assay mix:	Buffer	79 µl
	Inhibitor (1 mg/ml)	1 µl (add 5 µg/ml)
	Master mix	100 µl
	Mix thoroughly	
	G6P (1 mM)	20 µl (add 100 µM)

Measure absorbance at 340 nm

3.3 Human 6-PGL Methods

3.3.1 Heterologous Overexpression of Human 6-PGL

Expression of human 6-PGL was performed using *E. coli* KRX pRAREII cells transformed with pET-28a human 6-PGL plasmid. The expression was performed as outlined in 3.2.3 with minor modifications. The expression was performed for a total time period of 4 hours from onset of induction with rhamnose. The temperature on the other hand was maintained at 37 °C throughout the expression.

3.3.2 Purification of Heterologously Overexpressed Human 6-PGL

Purification of human 6-PGL was performed as outlined in 3.2.5 in a method incorporating both the Ni-NTA column material and gel filtration using an ÄKATA/Unicorn FPLC system (3.2.7).

3.3.3 Human 6-PGL Assay

The human 6-PGL activity was performed using a time course study as described for *Pf*GluPho's 6-PGL (3.2.10.1) with a few modifications. As opposed to assays involving the bifunctional *Pf*GluPho which contains G6PD activity, in this assay yeast G6PD was used for the enzymatic generation of 6-PG-δ-L which is the substrate for 6-PGL. The assay system consisted of a 500 µl solution composed of 200 µM $NADP^+$, the standard G6PD assay buffer (100 mM Tris, 0.5 mM EDTA, 10 mM MgCl2, pH 8.0), G6PD (Yeast Sigma) human 6-PGL and 150 µM of G6P which was added to start the reaction. Data collection was performed as outlined in 3.2.10.1.

3.4 MouseIDO-1 and MouseIDO-2 Methods

3.4.1 Heterologous Overexpression of Recombinant Mouse IDO-2 (mIDO-2)

E. coli KRX cells were transformed with the pDEST 17/ mIDO-2 plasmid. Cultures of transformed cells were grown in 1 litre of Terrific Broth (TB) medium containing carbenicillin (50 µg/ ml) at 37 ^oC until an OD_{600} of 0.8. The cultures were then transferred to room temperature and grown further to an OD_{600} between 1.0 and 1.5. rhamnose (20 %) and δ-aminolevulinic acid (ALA) hydrochloride (250 mM) were then added to final concentrations of 0.1 % and 0.5 mM, respectively and the cultures were further grown overnight. Cells were collected as a pellet by centrifugation at 8,000g for 15 minutes and resuspended in 25 mM Tris (hydroxymethyl) methylamine buffer pH 7.4, 150 mM NaCl.

3.4.2 Optimisation of Rhamnose for Heterologous Overexpression of Mouse IDO-2

The KRX/ pDEST 17-IDO-2 cells were grown according to the general method outlined. Concentrations of rhamnose were varied at the time of induction stage using final concentrations of between 0.05 % and 0.1 % (recommended maximum). The growth trials were performed in 500 ml TB medium and LB medium.

3.4.3 Purification of Heterologously Overexpressed Mouse IDO-2

After resuspension the pellet was sonicated 3 times for 20 seconds each at maximum power and centrifuged at 16,000g for 30 minutes. The clear supernatant was then applied to a 1 ml Ni-NTA column, washed with 5 ml of 25 mM Tris buffer, pH 7.4, 150 mM NaCl and eluted using a stepwise imidazole concentration gradient. 20 % glycerol was immediately added to the eluted fractions.

3.4.4 Heterologous Overexpression of Recombinant Mouse IDO-1 (mIDO-1)

E. coli Rosetta cells were transformed with the pDEST 17/ mIDO-1 plasmid. Cultures of transformed cells were grown in 1 litre of LB medium containing carbenicillin (50 µg/ml) and chloroamphenicol (35 µg/ml) at room temperature until an OD_{600} between 0.3 and 0.4. Isopropyl-β-D-thiogalactopyranoside (IPTG) (1 M) and δ-Aminolevulinic acid (ALA) hydrochloride (250 mM) were then added to final concentrations of 0.025 mM and 0.5 mM, respectively and the cultures were further grown overnight. Cells were collected as a pellet by centrifugation at 8,000g for 15 minutes, resuspended in 25 mM Tris buffer pH 7.4, 150 mM NaCl. Purification of IDO-1 was as outlined for IDO-2 in 3.3.3.

3.4.5 IDO Assay Methylene Blue/ Ascorbic Acid Method

Unless otherwise stated the assays were performed using freshly prepared samples. IDO-2 activity was determined as described by Takikawa *et al.* [1988] with minor modifications. In brief, the standard reaction mixture (200 µl) contained 100 mM potassium phosphate buffer pH 6.5, 100 mM KCl, 20 mM ascorbic acid (neutralised with NaOH), 200 µg/ml catalase, 10 µM methylene blue, 30 mM L-tryptophan, and purified IDO-2. The reaction was carried out at 37 ^{o}C for 60 min and stopped by the addition of 40 µl of 30 % (w/v) trichloroacetic acid. After heating at 65 ^{o}C for 15 min, the reaction mixtures were centrifuged at 11,500 g for 7 minutes. The supernatant (125 µl) was transferred into a well of a 96-well microtitre plate and mixed with 125 µl of 2 % (w/v) *p*-dimethylaminobenzaldehyde (*p*-DMAB) in acetic acid. The yellow pigment derived from kynurenine was measured at 480 nm using a microtitre plate reader. A standard curve of L-kynurenine was used, ranging in concentration from 0 to 500 µM. The kinetic parameters (K_m, V_{max}) were determined using the same method by varying the substrate (L-tryptophan concentration between 0 and 60 mM). The assays involving IDO-1 were performed as outlined with the substrate L-tryptophan concentration being maintained at 400 µM and varied between 0 to 200 µM for the determination of kinetic parameters (K_m, V_{max}). Protein concentration was determined using the Bradford protein assay [Bradford, 1976] and a standard curve of bovine serum albumin, ranging in concentration from 0 to 1 mg/ml.

3.4.6 IDO Assay Cytochrome b_5/ Cytochrome P450 Method

The reduction of mouse IDO by cytochrome b5 was performed as outlined by Maghzal *et al*. [2008]. In brief the reaction involved the addition of mouse IDO to a reaction

mixture purged with argon gas and containing 0.2 µM human recombinant cytochrome b_5, 2 µM of human NADPH: cytochrome P450 reductase, 56 units of G6PD, 375 units of bovine catalase, 20 mM G6P, 4 mM $NADP^+$, and 200 µM diethylene triamine pentaacetic acid in 100 mM phosphate buffer, pH 7.4. The reaction was carried out at 25 °C in a septum sealed cuvette thoroughly purged with argon gas. Difference spectra were recorded every 30 s from 380 to 680 nm against a reference sample containing the reaction mixture without mouse IDO, using a spectrophotometer. Experiments were performed in the absence and presence of CO (approximately 1 mM), by thoroughly purging the reaction mixture and the cuvette with CO gas.

3.4.7 Determination of pH and Salt Profiles

The pH stability test was carried out in a standard reaction mixture containing 100 mM potassium phosphate buffer, 100 mM KCl. The pH was varied by increments of pH 0.2 within a range of pH 6-9. For salt stability tests the standard reaction mixture contained 100 mM potassium phosphate buffer, pH 7.4 with salt concentrations being varied within a range of 0-300 mM.

3.4.8 Gel Filtration of Heterologously Overexpressed Mouse IDO-1 and Mouse IDO-2

Gel filtration was performed as outlined in 3.1.6 with minor a modification. The buffer used for gel filtration was 50 mM Tris pH 7.6, 300 mM NaCl. The protein containing fractions obtained after gel filtration (FPLC machine) were analysed on SDS-PAGE and then concentrated using a 50 kDa viva spin column. Protein concentration was determined using the Bradford protein assay [Bradford, 1976] and a standard curve of bovine serum albumin, ranging in concentrations from 0 to 1 mg/ml.

3.4.9 Protein Modelling of Mouse IDO-2

The structural model for mouse IDO-2 was predicted using “Swiss-Model” [Peitsch, 1995]. The preparation of the homology project was carried out in the web-interface of the programm SWISS-PDB VIEWER. At the beginning the FASTA amino acid sequence of mouse IDO-2 was loaded into the interface. Then suitable template structures based on their sequence similarity to IDO-2 were identified. With Swiss-Model this is achieved by comparing the target sequence with all entries of the ExPDB sequence database using blastp. Suitable templates were sorted by statistical significance and could be downloaded readily. For the sequence of mouse IDO-2 only two templates were listed: i) the cyanide bound form of the 4-phenylimidazole and ii) the cyanide bound form of the human IDO-1. A comparison of the amino acid sequences of the human IDO-1 and the IDO-2 of mouse revealed an indentity of 43 %. So the structural model was built in homology to the homodimeric crystal structure of human IDO-1 (PDB-ID: 2D0T). With the “Magic fit” tool of the program, an initial alignment of both sequences was made and then improved by manual alterations. In parallel the backbone of the target protein was built up based on the localisation of accordant

atoms in the template structure. The entire project was submitted to SWISS-MODEL, where extensive optimisation and minimisation steps were carried out by the GROMOS 96 forcefield [Fraternali and Van Gunsteren, 1996]. The model's coordinates and all intermediate analysis results are then returned to the user by e-mail.

3.4.10 Inhibitor Screening for Mouse IDO-1

The inhibitor assays were performed in a 96 well microtitre plate as described by Takikawa *et al*. [1988] with minor modifications. In brief, the standard reaction mixture (200 µl) contained 100 mM potassium phosphate buffer pH 6.5, 100 mM KCl, 20 mM ascorbic acid (neutralised with NaOH), 200 µg/ml catalase, 10 µM methylene blue and purified IDO-1 optimised based on its activity. The reaction mixture was added to the substrate L-tryptophan and the inhibitor. The L-tryptophan was serially diluted from 200 to 25 µM and the inhibitor was tested at concentrations between 0.01-0.08 µg/ml.The reaction was carried out at 37 ^{o}C for 60 min and stopped by the addition of 40 µl of 30 % (w/v) trichloroacetic acid. After heating at 65 ^{o}C for 15 min, the reaction mixtures were centrifuged at 11,500 g for 7 min. The supernatant (125 µl) was transferred into a well of a 96 well microtitre plate and mixed with 125 µl of 2 % (w/v) *p*-dimethylaminobenzaldehyde (*p*-DMAB) in acetic acid. The yellow pigment derived from kynurenine was measured at 480 nm using a microtitre plate reader. A standard curve of L-kynurenine was used, ranging in concentration from 0 to 500 µM.

Pipetting scheme:

50 mM potassium phosphate buffer, pH 6.5		166.5 – x µl
Master Mix		22.5 µl
{Ascorbic acid (neutralised with NaOH) 400 mM	10 µl	
Catalase 4 mg/ml	10 µl	
Methylene blue 800 µM	2.5 µl}	
L-Kynurenine or IDO1		x µl
Inhibitor		1 µl

Cover the plate with a foil paper

stand at room temperature 10 min

Add tryptophan 8 mM 10 µl

37 °C, 60 min

Add trichloroacetic acid 30% 40 µl

65 °C, 15 min

Centrifuge at 11500 x g (2800 rpm), for 7 min

To 100 µl of the supernatant add 100 µl 2 % *p*-DMAB in acetic acid

Measure absorbance at 480 nm (or 450 nm) using a multiwell plate reader

Master Mix per Plate

Buffer	17.215 ml	
Ascorbic acid	1.1 ml	
Catalase	1.1 ml	
Methylene blue	0.275 ml	
	19.69 ml	then use 179 µl/well

3.5 Thioredoxin Networks Methods

3.5.1 Site Directed Mutagenesis of *Pf*Plasmoredoxin

The reduced form of *Pf*Plasmoredoxin (*Pf*Plrx) and target proteins form mixed disulfide intermediates during the reduction pathway. Then *Pf*Plrx itself forms an internal disulfide bridge thus releasing the reduced target protein. This intermediate step should be stabilised when *Pf*Plrx lacks the second cysteine residue and the intermediate should only dissociate in the presence of DTT. Site directed mutagenesis PCR was performed as outlined in 3.2.2. in order to mutate cysteine 63 to serine and generate the mutated *Pf*Plrx^{C63S} using *Pfu* polymerase (Promega) and mutation primers (Sense: 5'-GGTGTAAATAC*AGT*GTAACCTTT ATAG-3'; Antisense: 5'-CTATAAAGGTTAC*ACT*GTATTTACACC-3'). The *DpnI* restriction of methylated nonmutated template was performed as outlined in 3.2.2 and the mutations verified by sequencing. Competent *E. coli* XL1-Blue cells were then transformed using pQE/ *Pf*Plrx^{C63S} plasmid as outlined in 3.1.3.

3.5.2 Heterologous Overexpression and Purification of *Pf*Plasmoredoxin

The expression of *Pf*Plasmoredoxin (mutant and wild type) was performed using the *E. coli* M15 strain transformed with the pQE/ *Pf*Plrx plasmid. Cultures of transformed cells were grown in 0.5 litre LB media [containing carbenicillin (100 µg/ml) and kanamycin (50 µg/ml)] until an OD_{600} 0.5 to 0.6. The culture was then induced with 1 mM isopropyl-β-D-1-thiogalactopyranoside and grown for further 4 hours. Cells were collected as a pellet by centrifugation at 8,000 g for 15 minutes at 4 °C and resuspended in 50 mM sodium phosphate buffer, 300 mM NaCl, pH 8.0. After addition of protease inhibitor cocktail consisting of pepstantin, cystantin and PMSF, the pellet could be stored at -20 ^{o}C for future use or purified immediately. A small amount of DNase as well as lysozyme (4 mg/g pellet) was added to the pellet and stirred over ice for 30 minutes. The cells were sonicated 3 times for 30 seconds each at maximum power and centrifuged at 16,000g for 30 minutes. The clear supernatant was then applied to a 1 ml Ni-NTA column, washed with 5 ml of 50 mM sodium phosphate buffer, 300 mM NaCl, pH 8.0 and eluted using a stepwise imidazole concentration gradient. The pure fractions as observed on the SDS gel were pooled together, concentrated and the concentration determined using the Bradford protein assay [Bradford, 1976] and a standard curve of bovine serum albumin, ranging in concentrations from 0 to 1 mg/ml. In order to couple *Pf*Plrx to the activated CNBr-Sepharose 4B resin for the pull down assays, the protein was dialysed using 100 mM $NaHCO_3$, 500 mM NaCl, pH 8.3.

3.5.3 Preparation of *Pf*Plasmoredoxin-Immobilised Resin

*Pf*Plasmoredoxin mutant (*Pf*Plrx^{C63S}) (2-5 mg) in 100 mM sodium carbonate pH 8.3 containing 500 mM NaCl (coupling buffer) was incubated for 1 h at room temperature under gentle agitation with (2 ml) CNBr-activated Sepharose 4B resin, which had been swelled in 1 mM HCl according to the manufacturer's instructions. The coupling reaction was terminated by centrifugation and after washing the resin with the coupling buffer, the unreacted side

chains of the resin were blocked by incubation with 100 mM Tris buffer, pH 8.0 for 2 hours at room temperature.

3.5.4 Collection of Target Proteins by Immobilised *Pf*Plrx^{C63S} Mutant

Plasmodium falciparum cell lysate (prepared as outlined in 3.6.4) containing 7-10 mg protein was incubated with 2 ml of *Pf*Plrx^{C63S} immobilized resin at room temperature for at least 2 h under gentle stirring. Non specifically bound proteins were then removed by washing the resin severally with 100 mM Tris buffer, pH 8.0, 500 mM NaCl until the absorbance of the wash solution at 280nm was zero. The resin was then suspended in 100 mM Tris buffer, pH 8.0, 500 mM NaCl, and 10 mM DTT and incubated for 30 minutes at room temperature under gentle agitation. The eluted proteins were separated from the resin and collected by centrifugation. SDS-PAGE was performed with 15 % acrylamide gels and the separated protein bands visualized by Coomassie Brilliant Blue.

3.5.5 Protein Bands Excision, Digestion and Identification

Coomassie stained protein bands were excised manually and destained by washing them three times while vortexing for 10 min each using 25 mM NH_4HCO_3 in 50 % acetonitrile solution. The gel pieces were then dried using a vacuum centrifuge and rehydrated using 25 mM NH_4HCO_3 and procine trypsin (Promega). The trypsin digestion was performed overnight at 37 °C. The digest solution was then removed followed by the addition of 30 µl (enough to cover the gel pieces) of 5 % trifluoroacetic acid in 50 % acetonitrile and incubated for 20 min to extract the peptides. The peptide extraction was repeated 3 times. The peptide extraction solution was then removed, combined with the trypsin digestion solution and concentrated. The concentrated solutions were then loaded onto the MALDI target plate by mixing 0.3 µl of each solution with the same volume of matrix solution (10 mg/ml α-cyanohydroxycinnaminic acid in acetonitrile/H_2O (1:1, v/v) and allowed to dry. Measurements were performed using a Voyager 4182 matrix assisted laser desorption ionization time of flight (MALDI-TOF) instrument (Applied Biosystems, Darmstadt, Germany), operating in the positive ion reflector mode with an accelerating voltage of 25 kV. The laser wavelength was 337 nm and the laser repetition rate was 20 Hz. The final mass spectra were produced by using an average of 60 laser shots. Each spectrum was internally calibrated with the masses of two trypsin autolysis products. Peptide mass fingerprinting identification was performed by comparing the tryptic peptide mass maps against Swiss-Prot (http://www.expasy.uniprot.org) and PlasmoDB (http://www.plasmodb.org) databases using the search engine Protein Prospector MS-Fit. Standard search parameters were set to allow a mass accuracy of 15 ppm and two missed tryptic cleavages.

3.5.6 Biomolecular Interaction Analysis using Biacore ® X System

Biacore X from Biacore AB is a system for real time biomolecular interaction analysis (BIA) using surface plasmon resonance technology. Real time BIA monitors the formation and dissociation of molecular complexes on a sensor surface as the interaction occurs by attaching one molecule (referred to as the ligand) to the surface, the interaction of another molecule in free solution (analyte) with the ligand is followed. Measurements are made under conditions of continous flow, where the sensor surface forms one wall of the flow cell. For majority of applications, the biospecific surfaces can be regenerated and reused for an extended series of analyses.

The detection principle in BIA is based on surface plasmon resonance (SPR). This is a non invasive optical measuring technique which measures the mass concentration of biomolecules on the sensor surface. The technique does not require any labelling of the interacting components. The response is essentially independent of the nature of the biomolecule, so that all steps in an interacxtion analysis are followed with the same criterion.

3.5.6.1 Biacore ® X System

Protein-protein interaction was studied using a Biacore ® X Biosensor System (Biacore AB; Uppsala). Immobilisation of S-adenosyl-L-homocysteine hydrolase (SAHH) to the sensor chip CM5 via primary amine groups was performed in the instrument as follows: The carboxymethylated surface of the sensor chip CM5 was activated with a 1:1 mixture of 0.1 M N-hydroxysuccinimide (NHS) and 0.4 M 1-ethyl-3-(3-dimethylaminopropyl) carbodiimide hydrochloride (EDC) (provided in the amine coupling kit; Biacore AB). 35 µl (60 µg/ml) of SAHH in 10 mM sodium acetate, pH 4.5 were injected to flow cell 2 (FC2) to be immobilized on the sensor surface via primary amine groups. Residual unreacted active ester groups were blocked with 1 M ethanolamine-HCl, pH 8.5 (amine coupling kit). Studies were performed using HBS buffer (10 mM HEPES, 150 mM NaCl, 3.4 mM EDTA, 0.005% Nonidet P-40, pH 7.4) at a flow rate of 10 µl/min. Protein-protein interaction studies between SAHH and *Pf*Plrx^{C63S} were performed as follows: SAHH which was bound on the sensor chip surface was oxidized using 30 µl of 0.5 mM 5,5'-dithiobis (2-nitrobenzoate) (DTNB) before 30 µl of *Pf*Plrx^{C63S} (10 µM in HBS buffer or the running buffer) were injected, followed by buffer flow over the chip and an elution step with 2 mM DTT in a volume of 30 µl. Difference in resonance spectra (FC2–FC1) were recorded and evaluated using the software BIAevaluation 3.0 (Biacore AB). The sensor chip CM5 surface was equilibrated using HBS buffer and was ready for the next cycle.

3.6 *P. falciparum* Cell Culture Methods

3.6.1 Maintainance of *P. falciparum* Parasites in Cell Culture

Intraerythrocytic stages of *P. falciparum* strains were cultured according to Trager and Jensen [1976] with slight modifications. The parasites were propagated in leukocyte free erythrocytes (A^+) at 33 % haematocrit at 37 ^oC under reduced oxygen (3 % O_2, 3 % CO_2, and 95 % N_2) in tissue culture (RPMI 1640-Gibco) medium containing 4 % human serum (A^+) and 0.2 % Albumax (lipid rich bovine serum albumin). Albumax is needed to reduce the rate at which erythrocytes deteriorate *in vitro* and regulates the pH drift when cultures are exposed to ambient air. The media was further supplemented with 9 mM (0.16 %) glucose, 0.2 mM hypoxanthine, 2.1 mM L-glutamine and 22 µg/ml gentamycin. Chloroquine sensitive strains (3D7 and HB3) and resistant strains (K1 and Dd2) of *P. falciparum* [Su *et al*., 1997] were grown in continuous culture in the laboratory. Day to day monitoring of parasite growth was done by observing the parasitemia on Giemsa stained thin blood films. Depending on the strain, parasites typically propagate 3-8 fold every 48 hours, care was taken therefore to avoid parasite cultures attaining very high parasitemia beyond that adequate (3-10 %) for growth. Normally the percentage parasitemia used varied according to the need or experiment.

Strain	Clone	Drug resistance	Multiplication rate	CQ IC_{50} in nM
3D7	Yes from NF54	None	4-5	8.6 ± 0.4
HB3	Yes	PYR	6	16.8 ± 0.5
Dd2	Yes from WR82	CQ,QN,PYR,SDX	5-6	90.2 ± 10.6
K1	No	CQ,PYR	4-5	155.0 ± 11.4

Table 1: Characteristics of *P. falciparum* strains used (Fidock *et al*., 2004; Su *et al*., 1997) CQ: chloroquine, QN: quinine, PYR: pyrimethamine, SDX: sulfadoxine.

3.6.2 Synchronisation

Synchronisation of the parasites in culture to ring stages was carried out by treatment with 5 % (w/v) sorbitol [Lambros and Vanderberg, 1979] which leads to about 10 % parasitemia of predominantly ring stage phase of the culture. Five millilitres of 5 % sterile sorbitol preheated to 37 ^oC was added to 0.5 ml parasitised erythrocyte pellet from culture and left for 5 minutes at 37 ^oC. The sorbitol mixture was centrifuged at 1900 rpm for 3 minutes at room temperature to spin down the erythrocytes. The sorbitol was then off aspirated and the pellet quickly resuspended in complete medium for a quick wash after which the pellet was resuspended and returned to culture. In case the culture was not sufficiently synchronised, the procedure was repeated after 48 hours when the culture was at the ring stage again.

3.6.3 Drug Sensitivity Assays

Isotopic drug sensitivity assays using the semi-automated microdilution technique first described by Desjardins *et al*. [1979], was employed to investigate the susceptibility of the malaria parasite *P. falciparum* to inhibitors which had shown enzyme activity inhibition (at nanomolar range) towards IDO. The method involves the incorporation of radioactive H^3-

hypoxanthine which is taken up by the parasite as a precursor of purine deoxynucleotides for DNA synthesis.

The assay was performed according to Fivelman *et al*. [2004]. In brief a two fold serial dilution of the starting concentration of each drug to be tested (B1-B12) (Figure 12) was performed in 96 well microtitre plates (Nunc^R) so that each well contained 100 µl of half the concentration of the drug in the preceding well above. The starting concentration of each drug was chosen such that the IC_{50} value (concentration that produces 50 % reduction in the uptake of H^3-hypoxanthine) falls in the middle of the microtitre plate. Using parasites present in hypoxanthine free medium, 100 µl of a 2 times stock of previously diluted parasites (parasitemia of 0.5 % and a haemocrit of 2.5 %) were added into each well so that the parasites were at a final parasitemia of 0.5 %, 1.25 % haematocrit and with over 70 % of the parasites being in the ring stage. Parasitised red blood cells were used as the positive control whereas non-parasitised red blood cells served as the negative control. The plates were then incubated as normal culture for 48 hours after which 50 µl (final concentration 0.5 µCi /well) of H^3-hypoxanthine was added per well.

<table>
<tr><td></td><td>1</td><td>2</td><td>3</td><td>4</td><td>5</td><td>6</td><td>7</td><td>8</td><td>9</td><td>10</td><td>11</td><td>12</td></tr>
<tr><td>A</td><td colspan="8">Positive control</td><td colspan="4">Negative control</td></tr>
<tr><td>B</td><td colspan="2" rowspan="7">Drug 1</td><td colspan="2" rowspan="7">Drug 2</td><td colspan="2" rowspan="7">Drug 3</td><td colspan="2" rowspan="7">Drug 4</td><td colspan="2" rowspan="7">Drug 5</td><td colspan="2" rowspan="7">Drug 6</td></tr>
<tr><td>C</td></tr>
<tr><td>D</td></tr>
<tr><td>E</td></tr>
<tr><td>F</td></tr>
<tr><td>G</td></tr>
<tr><td>H</td></tr>
</table>

Figure 12: Semi-automated microdilution method of drug sensitivity assays: Arrangement of drugs on a 96 well microtitre plate. A1-A8: Positive control, red blood cells and parasites, A9-A12: Negative control, red blood cells only (without parasites), B1-H12: Serial drug dilutions for 6 different compounds in duplicates.

The plates were further incubated for 24 hours after which they were frozen at -80 ^oC for at least 1 hour to freeze the cells. The plates were then thawed and using a glass filter (Perkin-Elmer, Rodgau-Jügesheim, Germany) harvested and dried. Radioactivity in counts per minute (cpm) from each well was measured in a β-counter and considered to be proportional to the respective growth of *P. falciparum* in the well. The IC_{50} values were determined by linear regression analysis on the linear segments of the curve. Percent reductions in growth were used to plot percent inhibition of growth as a function of drug concentration. Assays were typically repeated twice or three times on different occasions.

3.6.4 Preparation of *P. falciparum* Proteins from Cell Culture

The *P. falciparum* proteins were prepared from 10 large Petri-dishes of *P. falciparum* cell culture with 15 % parasitemia and 3.3 % haematocrit. The parasites were isolated by suspending the erythrocytes in a 20 fold volume of saponin buffer containing 7 mM K_2HPO_4, 1 mM NaH_2PO_4, 11 mM $NaHCO_3$, 58 mM KCl, 56 mM NaCl, 1 mM $MgCl_2$, 14 mM glucose and 0.02 % saponin pH 7.5 for 10 minutes at 37 ^oC. After centrifugation (2,700 rpm, 3 minutes, 25 ^oC) the pellet was washed 3 times with 20 fold volume of buffer centrifuged to form a pellet which was stored at -80 ^oC after addition of protease inhibitor.

The pellet which had been stored at -80 ^oC prepared from 10 Petri-dishes of *P. falciparum* cell culture was thawed. The Eppendorf tube cover was then sealed completely using parafilm. The pellet was then frozen and thawed 3 times using liquid nitrogen. In between each freezing and thawing procedure, the pellet was vigourously mixed (shaken) using a table shaker and briefly centrifuged before being immersed again into the liquid nitrogen tank. In case the pellet was too thick or viscous, 200-400 µl of buffer was added. The pellet was then sonicated 5 x 20 seconds and the pellet centrifuged at 50,000 rpm for 30 min. The concentration of the *P. falciparum* proteins present in the supernatant was then determined using the Bradford [1976] method and a standard curve of bovine serum albumin, ranging in concentration from 0 to 1 mg/ml.

4 Results

4.1 *Pf*GluPho

4.1.1 Heterologous Overexpression and Purification of Recombinant *Pf*GluPho

Studies using *Pf*GluPho have so far been restricted to the enzyme purified from parasite extract which is not only limiting in terms of the quantity of the enzyme required for inhibitor testing, crystal screening and biochemical characterisation of the enzyme, but also contains a high excess of the RBC G6PD. The desire and difficulties in cloning *Pf*GluPho have also been reported [O'Brien *et al*., 1994; Clark *et al*., 2001] making it impossible to heterologously overexpress *Pf*GluPho so far.

Our cloning strategy, heterologous overexpression and purification method was successful and enabled us to clone, heterogously overexpress and purify *Pf*GluPho to homogeneity. The heterologous overexpression and purification of recombinant *Pf*GluPho was optimised as summarised in Tables 2, 3 and 4.

Buffer	Comments
US buffer	Was found not to be the best buffer for resuspension as well as purification
100 mM Tris, 150 mM NaCl pH 7.4	Was not the optimum buffer for resuspension and purification
100 mM Tris, 150 mM NaCl pH 7.8	Was found to be a good buffer but probably by increasing the salt concentration it would be better
100 mM Tris, 500 mM NaCl pH 7.8	Was found to be the best buffer and therefore used for further resuspension of the pellet as well for the purification process

Table 2: Optimisation of the buffers used for purification of *Pf*GluPho

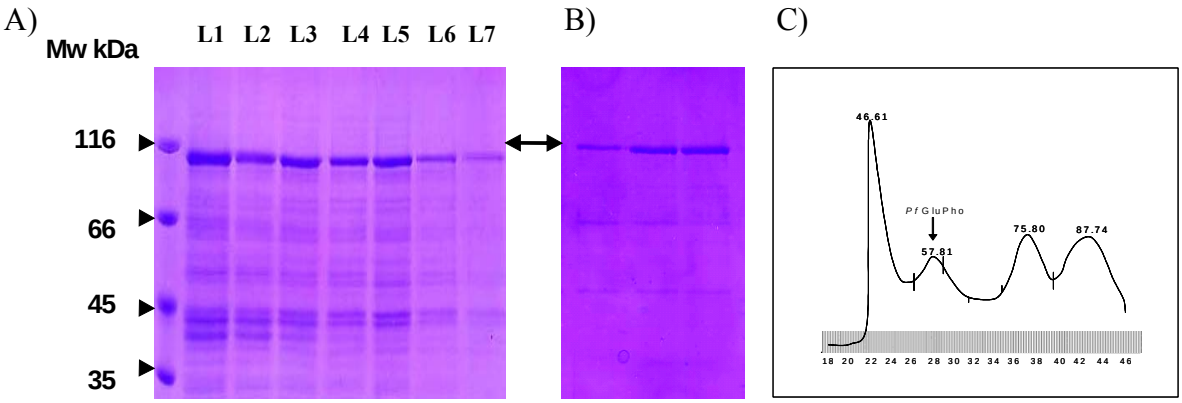

Figure 13: SDS gel 10 % after Ni-NTA and gel filtration of *Pf*GluPho. A) 10 % SDS gel of elution fractions after Ni-NTA column purification where L1 corresponds to: 60 mM imidazole, L2 and L3: 80 mM imidazole L4 and L5: 250 mM imidazole, L6 and L7: 500 mM imidazole. B) 10 % SDS gel of *Pf*GluPho containing fractions after gel filtration. C) Gel filtration chromatogram after Ni-NTA, an elution time of 57.81 corresponds to 636 kDa.

Western blot analysis using anti-histidine antibodies yielded a positive signal for the recombinant *Pf*GluPho. When the Western blot was repeated using *Pf*GluPho peptide specific antibodies a positive signal was also present for the recombinant protein as well as for *P. falciparum* proteins obtained from cell culture.

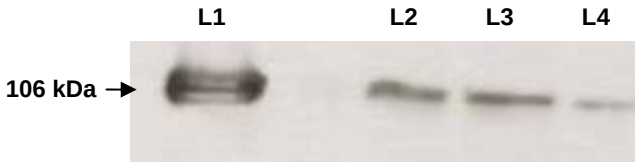

Figure 14: Western blot analysis using *Pf*GluPho peptide specific antibody. On the blot photo L1 represents recombinant *Pf*GluPho whereas L2 (105 µg), L3 (70 µg), L4 (45 µg) represent *P. falciparum* proteins obtained from cell culture lysate.

4.1.2 *Pf*GluPho Oligomerisation Studies

The oligomeric structure of *Pf*GluPho is obscure and comparable data from other protozoan G6PDs is not yet available. Whether GluPho exists as a dimer as it is in most G6PD enzymes or as a tetramer as it is reported in doves [Cooper and Irwin, 1968] or if it exists in transition between dimer and tetramer as in humans [Birke *et al*., 1989] is not known. *Pf*GluPho was found to be a hexamer with a subunit molecular weight of 106 ± 3.3 kDa. Oligomerisation studies performed in the presence of G6P (1 mM) and $NADP^+$ (200 µM) using a native gel filtration chromatography revealed that *Pf*GluPho maintains its hexameric structure both in the presence and absence of its substrate and coenzyme (Figure 15). Addition of DTT (5 mM) to the running buffer (50 mM sodium acetate buffer, 150 mM NaCl, 50 mM EDTA pH 7.0) in the presence or absence of the substrate or coenzyme did not lead to any observable change in the hexameric structure of *Pf*GluPho implying that the hexameric structure is not due to or influenced by intermolecular disulphide bridges. This clearly distinguishes *Pf*GluPho from other G6PDs, e.g. from the human and yeast enzymes which have been shown to change their conformation upon binding of substrates [Birke *et al*., 1989, Kuby *et al*., 1974].

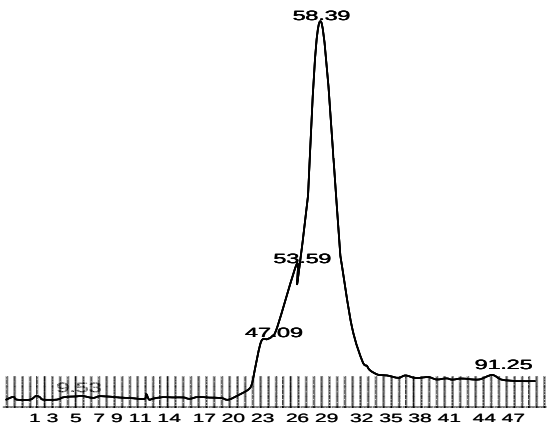

Figure 15: *Pf*GluPho hexameric structure in the presence of G6P and $NADP^+$. In this gel filtration chromatogram the elution time of 58.39 corresponds to a molecular weight of 636 kDa.

***E. coli* cell line**	**Medium**	**Temperature ^{o}C**	**Time**	**Inductor and Concentration**	**Western blot**	**Inference**
Rosetta	LB, TB	23, 27, 37	3hrs, overnight	IPTG (0.025, 0.05, 0.075, 0.1, 0.5, 1.0 mM)	Tested Positive	Medium: no significant difference Temperature: between 23-27 ^{o}C was the best IPTG: 0.1 mM was the best, Final yield very low
C41 pRIG	LB, TB, 2xYT	23, 27, 37	3hrs, overnight	IPTG (0.025, 0.05, 0.075, 0.1, 0.5, 1.0 mM)	Tested Positive	Medium: very low expression with 2xYT Temperature: between 23-27 ^{o}C was the best IPTG: 0.1 mM was the best, Final yield very low
C41 pRARE	LB, TB, 2xYT	25, 37	3hrs, overnight	IPTG (0.1, 0.5, 1.0, 2.0 mM)	Tested Positive	Medium: very low expression with 2xYT 25 ^{o}C was the best Overnight expression was the best IPTG: 0.1 mM was the best, Final yield very low
PD2000	LB, TB	25, 37	3hrs, overnight	IPTG (0.1, 0.5, 1.0, 2.0 mM)	Tested Positive	Medium: no significant difference 25 ^{o}C was the best Overnight expression was the best Final yield very low
PD2000 pRAREII	LB, TB	25, 37	3hrs, overnight	IPTG 1.0 and 2.0 mM	Tested Positive	Medium: no significant difference 25 ^{o}C was the best Overnight expression was the best Final yield very low although expression better in the presence of pRAREII
KRX	LB, TB	37 ^{o}C to O.D$_{600}$ of 0.4 then room temperature until O.D$_{600}$ of 1.2 induce	3hrs, overnight	Rhamnose: 0.05 and 0.1 %	Tested Positive	Medium: TB was the best Overnight expression was the best Rhamnose: 0.1 % was the best Final yield improved
KRX pRAREII	LB, TB	37 ^{o}C to O.D$_{600}$ of 0.4 then room temperature until O.D$_{600}$ of 1.2 induce	3hrs, overnight	Rhamnose 0.05 and 0.1 %	Tested Positive	Medium: TB was the best Overnight expression was the best Rhamnose: 0.1 % was the best Expression better in the presence of pRAREII Final yield the best therefore adopted as the standard method for expression of *Pf*GluPho.

Table 3: Optimisation of the heterologous overexpression of *Pf*GluPho. Western blot was performed using anti-histidine antibody and all samples tested positive for *Pf*GluPho.

Material	Condition used	Inference
Ni-NTA (one column system)	Equilibrated the column material with buffer containing 10 mM imidazole then loaded the lysate containing protein and eluted with an imidazole concentration gradient.	When the column material is pre-equilibrated with 10 mM imidazole the protein binds very weakly.
2' 5' ADP Sepharose 4B (one column system)	Loaded the lysate containing protein and eluted with an $NADP^+$ concentration gradient.	When examining the SDS gels of the eluted fractions very weak bands are observed.
Ni-NTA (one column system)	Equilibrated the column material with buffer without 10 mM imidazole then loaded the lysate containing protein and eluted with an imidazole concentration gradient.	Protein binds well. 20 % pure protein obtained as observed on SDS gels.
Ni-NTA then 2' 5' ADP Sepharose 4B (two column system)	Equilibrated the column material with buffer, loaded the lysate containing protein on Ni-NTA material and eluted with an imidazole concentration gradient then loaded the pure fraction as seen on SDS gel on a 2' 5' ADP Sepharose 4B column.	20 % pure protein obtained after Ni-NTA column but the protein seems to be binding weakly to the 2' 5' ADP Sepharose 4B column material upon comparison of SDS gels of the pure fractions after the 2 columns.
2' 5' ADP Sepharose 4B then Ni-NTA (two column system)	Loaded the lysate containing protein on a 2' 5' ADP Sepharose 4B, eluted with an $NADP^+$ concentration gradient then loaded the pure fractions as observed on SDS on Ni-NTA column.	Reversing the conditions by using 2' 5' ADP Sepharose 4B column then Ni-NTA column leads to very weak bands on SDS gel. The band of a 20% pure protein obtained when Ni-NTA is the first column is not present in this case.
2' 5' ADP Sepharose 4B (two column system)	Eluted the protein from the first column, dialysed them to remove $NADP^+$ then loaded the pure fraction as seen on SDS gel on a second column.	We can conclude from this experiment that generally the protein binds very weakly to the 2' 5' ADP Sepharose 4B column material.
Ni-NTA (two column system)	Ran the first column then dialysed to remove imidazole then loaded the pure fraction as seen on SDS gel on a second Ni-NTA column material.	The protein binds very well. The protein binds even better on the second column even though it had been equilibrated with 10 mM imidazole. The two column system using Ni-NTA does not improve purity.
Ni-NTA then gel filtration using 16/60 superdex 200 prep grade column	Equilibrated the column material with buffer, loaded the lysate-containing protein on Ni-NTA material and eluted with an imidazole concentration gradient then loaded the pure fraction as seen on SDS gel on a FPLC machine for gel filtration.	Protein binds well to Ni-NTA column. 20 % pure protein obtained as observed on SDS gels after Ni-NTA column. Homogenous pure protein is obtained after gel filtration. Best method and adopted for further purifications.

Table 4: Optimisation of the purification of heterologously overexpressed *Pf*GluPho.

4.1.3 *Pf*GluPho's G6PD Kinetic Studies

It is appropriate to determine the approximate K_m values for each substrate prior to an initial velocity experiment. This allowed experiments to be conducted by varying the substrate concentration over a specific range relative to each K_m value. *Pf*GluPho was found to be exhibiting very high affinities and therefore low K_m values for both G6P and $NADP^+$ (Table 5) but exhibited low affinity and therefore high K_m values for the G6P analogue 2-deoxyglucose-6-phosphate. Measuring the G6PD activity in full blood samples showed that the human G6PD has a comparatively lower affinity and therefore a higher K_m for G6P and $NADP^+$ (Table 5). Control G6PD assay experiments were performed using commercial yeast G6PD.

*Pf*GluPho's G6PD initial rate studies using different combinations of G6P and $NADP^+$ yielded linear converging double reciprocal plots (Figure 16). An intersecting pattern was also obtained when the results were replotted with G6P as the independent variable (Figure 16). The secondary plots of the slopes and intercepts against the reciprocal of the substrate or coenzyme also yielded straight linear plots (Figure 17 and 18). In theory for scattered data, a simple linear fit may introduce a false weighting. Here however, an internal check was applied by using both possible plotting sequences to extract kinetic parameters, i.e. using both $1/[NADP^+]$ and 1/[G6P] as alternative variables for the primary plots.
The initial rate equation for the two substrate reaction catalysed by G6PD in the nomenclature of Dalziel [1957] is of the form

$$e/v = \Phi_0 + \Phi_X/[X] + \Phi_Y/[Y] + \Phi_{XY}/[X][Y]$$

where X and Y are sugar phosphate and coenzyme respectively.

The Φ ($\Phi = 1/k_{cat}$) parameters are obtained from initial rate measurements at varying concentrations of X for a series of fixed concentrations of Y. Rearrangement of the equation shows that the intercepts of primary double reciprocal plots with 1/[X] as the variable are given by $\Phi_0 + \Phi_Y/[Y]$ and the slopes by $\Phi_X + \Phi_{XY}/[Y]$. The secondary plots of these slopes and intercepts against 1/[Y] provide estimates for the individual initial rate parameters. [Dalziel, 1957]. The Dalziel parameters for the initial rate measurements for *Pf*GluPho are as shown in Table 6. The initial rate behaviour gives no indication of any complexities in $NADP^+$ binding.

4.1.4 *Pf*GluPho's G6PD Alternative Substrate Studies

An alternative substrate, when available can be a useful tool for differentiating kinetic models as first reported by Wong and Hanes [1962]. The alternative substrate used here is 2-deoxyG6P. The corresponding kinetic parameters are given in Table 5 and Table 6. A comparison of the kinetic parameters shows that the enzyme has a higher affinity for its natural substrate G6P than for the substrate analogue 2-deoxyG6P (K_m G6P 18.1 μM vs K_m 2-deoxyG6P 2.5 mM).

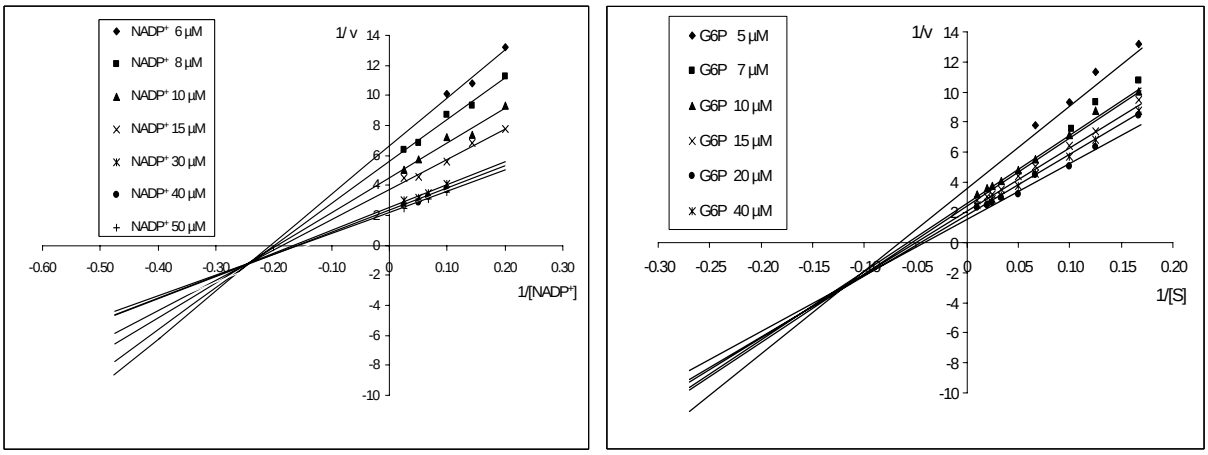

Figure 16: *Pf*GluPho's G6PD double reciprocal plots of $NADP^+$ and G6P

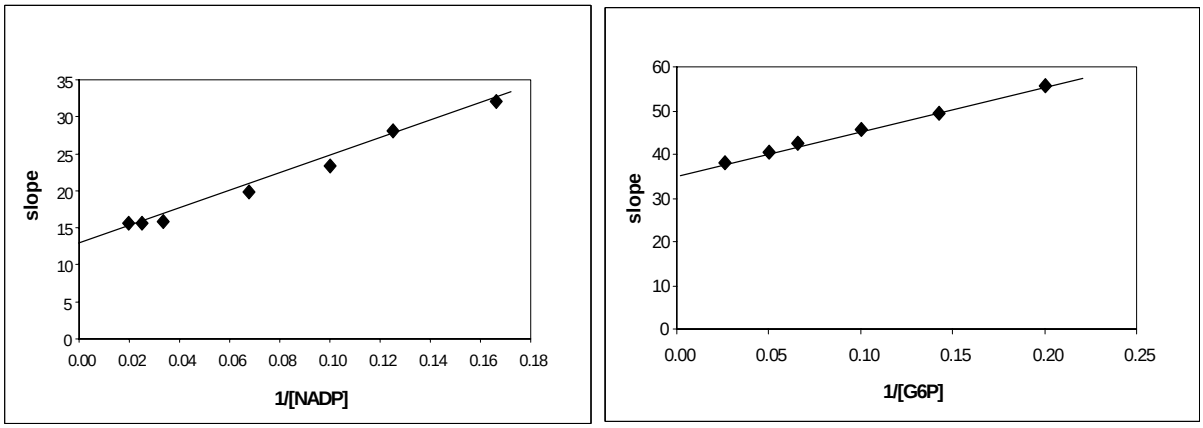

Figure 17: Secondary plots of slopes of *Pf*GluPho's G6PD primary plots against 1/ [substrate]

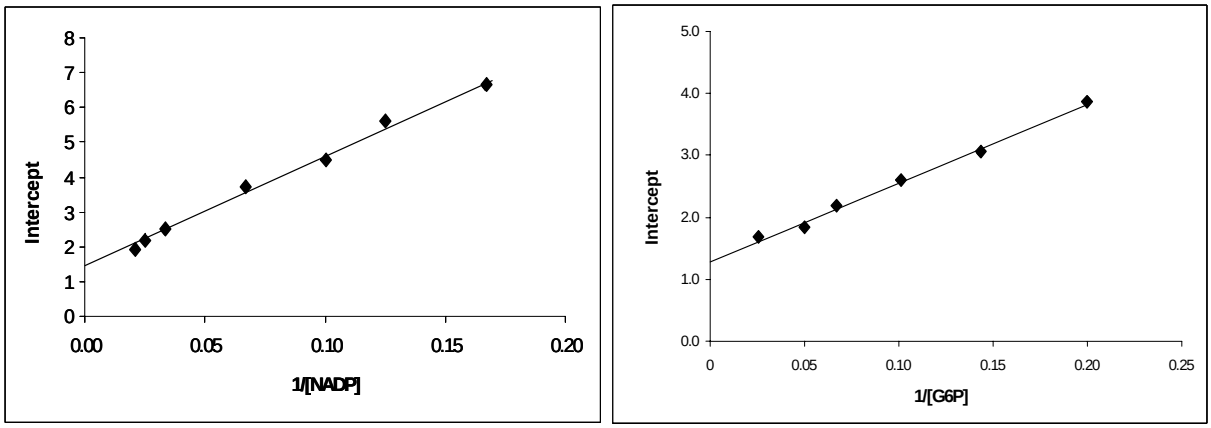

Figure 18: Secondary plots of intercepts of *Pf*GluPho's G6PD primary plots against 1/ [substrate]

4.1.5 *Pf*GluPho's G6PD Glucoseamine 6-Phosphate Inhibition

Glucoseamine-6-phosphate which is an analogue of G6P was chosen as a dead end inhibitor for our study and was found to be a mixed inhibitor with respect to both G6P and $NADP^+$ (Figure 19).

4.1.6 *Pf*GluPho's G6PD ATP-Ribose Inhibition

The $NADP^+$ fragment ATP-ribose which is an analogue of $NADP^+$ was found to be a mixed inhibitor with respect to both substrates G6P and $NADP^+$ (Figure 20).

A)

	G6PD Enzymes				
Substrate	***Pf*GluPho's G6PD (Recombinant)**				**Literature Values**
	K_m (µM)	**V_{max} (U/mg)**	**k_{cat} s^{-1}**	**k_{cat}/K_m (M^{-1} s^{-1})**	**K_m (µM)**
G6P	18.1 ± 0.5	116 ± 5	206 ± 9	11.4 x 10^7	11[a], 27[b]
$NADP^+$	5.1 ± 0.4	114 ± 9	203 ± 12	3.98 x 10^7	0.8[a], 4.5[b]
2-DG6P	2600 ± 141	105 ± 7	186 ± 12	7.1 x 10^4	10000[a]

	Human G6PD (Recombinant)				Literature Values	
	K_m (µM)	**V_{max} (U/mg)**	**k_{cat} s^{-1}**	**k_{cat}/K_m (M^{-1} s^{-1})**	**K_m (µM)**	**k_{cat}/K_m (M^{-1} s^{-1})**
G6P	ND	-	-	-	54.8[c], 43.4[d]	[c]2.9 x 10^6
$NADP^+$	ND	-	-	-	6.76[c], 11[d]	[c]2.3 x 10^7
2-DG6P	ND	-	-	-	1674[c]	[c]1.9 x 10^4

	Human G6PD (Full Blood)	Literature Values
	K_m (µM)	**K_m (µM)**
G6P	24 ± 1.3	27[a]
$NADP^+$	8.1 ± 2.4	9[a]

	Yeast G6PD (Sigma)		
	K_m (µM)	**V_{max} (U/mg)**	**K_m (µM)**
G6P	53 ± 1	323 ± 7	51[e]
$NADP^+$	24 ± 0.9	415 ± 14	19[e]

B)

	6-PGL Enzymes				
	***Pf*GluPho's 6-PGL (Recombinant)**				**Literature Values**
Substrate	**K_m (µM)**	**V_{max} (U/mg)**	**k_{cat} s^{-1}**	**k_{cat}/K_m (M^{-1} s^{-1})**	**K_m (µM)**
6-PG-δ-L	26.2 ± 4.9	74.9 ± 1.8	133 ± 3	5.08 x 10^6	-

	Human 6-PGL (Recombinant)				
Substrate	**K_m (µM)**	**V_{max} (U/mg)**	**k_{cat} s^{-1}**	**k_{cat}/K_m (M^{-1} s^{-1})**	**K_m (µM)**
6-PG-δ-L	32.5 ± 4.9	712 ± 11	344 ± 3	1.0 x 10^7	-

C)

	6-PGD Enzyme		
	Yeast 6-PGD (Sigma)		**Literature Values**
Substrate	**K_m (µM)**	**V_{max} (U/mg)**	**K_m (µM)**
6-PGn	48.9 ± 2.4	330 ± 43	55[f]
$NADP^+$	9.9 ± 1.5	325 ± 5	

Table 5: Kinetic parameters of G6PD and 6-PGL enzymes. A) Kinetic parameters of G6PD enzymes determined in the study as well as the existing literature values. B) 6-PGL kinetic parameters of the recombinant *Pf*GluPho's 6-PGL enzyme in comparison to the recombinant human homologue. C) Yeast 6-PGD kinetic paparameters. **2-DG6P** means 2-deoxyG6P, **ND** means not determined, **6-PG-δ-L** means 6-phosphoglucono- δ-lactone, **6-PGn** means 6-phosphogluconate. **a**: Yoshida and Roth, 1987, **b**: Kurdi-Haidar and Luzzatto, 1990, **c**: Wang *et al*., 2002, **d**: Birke *et al*., 1989, **e**: Gould and Goheer, 1976, **f**: Weiwei *et al*., 2007.

A) G6P and NADP

Row no.	Φ_0 (s)	Φ_{G6P} (µM.s)	Φ_{NADP} (µM.s)	$\Phi_{NADP\ G6P}$ ($\mu M^2.s$)	$\Phi_{NADP}\Phi_{G6P}$ ($\mu M^2.s^2$)	$\Phi_{NADP\ G6P}$ / Φ_{G6P} (µM)	$\Phi_{NADP\ G6P}$ / Φ_{NADP} (µM)	$\Phi_{NADP\ G6P}$ / $\Phi_{G6P}\Phi_{NADP}$ (s^{-1})	k_{cat} (s^{-1})
1	0.005	0.088 ± 0.003	0.025	0.449 ± 0.4	0.002	5.1	18.13 ± 0.54	206	206
2	0.005	0.089 ± 0.01	0.025	0.455 ± 0.4	0.002	5.1 ± 0.35	18.13	203	203
3	0.005	0.089 ± 0.001	0.025 ± 0.0003	0.45 ± 0.005	0.002 ± 0.001	5.1	18.13	204.5 ± 2.1	205

B) 2-DeoxyG6P and NADP

Row no.	Φ_0 (S)	$\Phi_{2\text{-}DG6P}$ (µM.s)	Φ_{NADP} (µM.s)	$\Phi_{NADP\ 2\text{-}DG6P}$ ($\mu M^2.s$)	$\Phi_{NADP}\Phi_{2\text{-}DG6P}$ ($\mu M^2.s^2$)	$\Phi_{NADP\ 2\text{-}DG6P}$/ $\Phi_{2\text{-}DG6P}$ (µM)	$\Phi_{NADP\ 2\text{-}DG6P}$/ Φ_{NADP} (µM)	$\Phi_{NADP\ 2\text{-}DG6P}$ / $\Phi_{2\text{-}DG6P}\Phi_{NADP}$ (s^{-1})	k_{cat} (s^{-1})
1	0.005	13.98	0.027	71.4	0.383	5.1	2600	186	186
2	0.005	13.4	0.026	68.4	0.352	5.1	2600	194	194
3	0.005	13.69 ± 0.41	0.027 ± 0.0008	69.8 ± 2.1	0.368 ± 0.022	5.1	2600	190 ± 5.5	190

C) Human G6PD Literature Values [Wang *et al*., 2002].

Row	Φ_0 (S)	Φ_{G6P} (µM.s)	Φ_{NADP} (µM.s)	$\Phi_{NADP\ G6P}$ ($\mu M^2.s$)	$\Phi_{NADP}\Phi_{G6P}$ ($\mu M^2.s^2$)	$\Phi_{NADP\ G6P}$ /Φ_{G6P} (µM)	$\Phi_{NADP\ G6P}$ / Φ_{NADP} (µM)	$\Phi_{NADP\ G6P}$ / $\Phi_{G6P}\Phi_{NADP}$ (s^{-1})	k_{cat} (s^{-1})
A	0.0062	0.34	0.042	2.3	0.014	6.76	54.8	161	161
	Φ_0 (S)	$\Phi_{2\text{-}DG6P}$ (µM.s)	Φ_{NADP} (µM.s)	$\Phi_{NADP\ 2\text{-}DG6P}$ ($\mu M^2.s$)	$\Phi_{NADP}\Phi_{2\text{-}DG6P}$ ($\mu M^2.s^2$)	$\Phi_{NADP\ 2\text{-}DG6P}$/ $\Phi_{2\text{-}DG6P}$ (µM)	$\Phi_{NADP\ 2\text{-}DG6P}$/ Φ_{NADP} (µM)	$\Phi_{NADP\ 2\text{-}DG6P}$ / $\Phi_{2\text{-}DG6P}\Phi_{NADP}$ (s^{-1})	K_{cat} (s^{-1})
B	0.031	68	0.28	451	19.04	6.64	1643	25	32.3

Table 6: *Pf*GluPho Dalziel parameters calculated using the initial velocity data. A) Kinetic data determined using primary plots against both reciprocal of G6P (row 1) and reciprocal of $NADP^+$ (row 2). The mean value for G6P and $NADP^+$ is presented (row 3). B) Kinetic data determined using primary plots against both reciprocal of 2-DeoxyG6P (row 1) and reciprocal of $NADP^+$ (row 2). The mean value for $NADP^+$ and 2-DeoxyG6P is presented (row 3). C) Human G6PD literature values [Wang *et al*., 2002]; Row a: The mean value for G6P and $NADP^+$, Row b: mean value for $NADP^+$ and 2-DeoxyG6P.

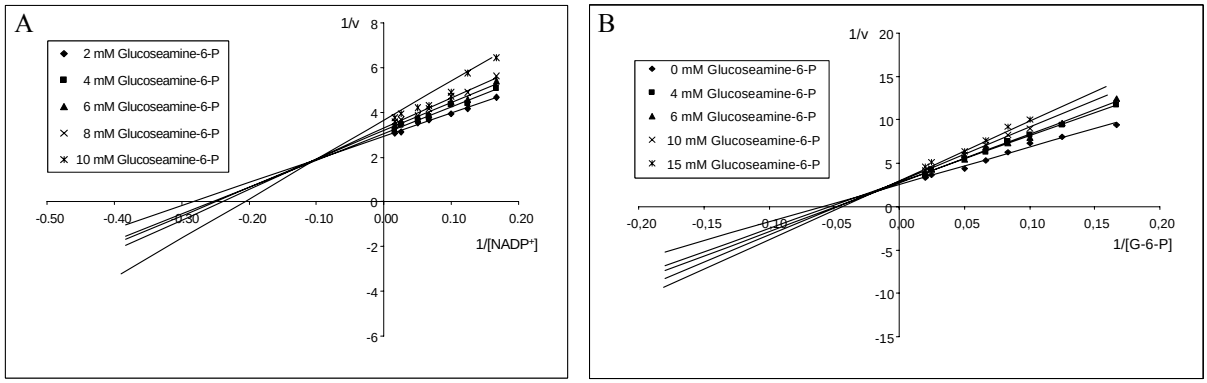

Figure 19: Glucoseamine 6-phosphate inhibition on *Pf*GluPho's G6PD. A) Glucoseamine 6-phosphate inhibition on $NADP^+$. B) Glucoseamine 6-phosphate inhibition on G6P.

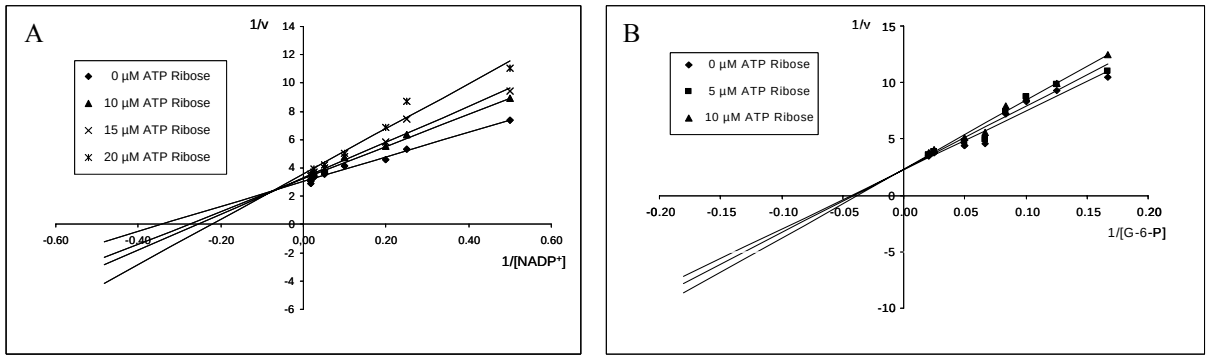

Figure 20: ATP-Ribose inhibition of *Pf*GluPho's G6PD. A) ATP-Ribose inhibition on $NADP^+$. B) ATP-Ribose inhibition on G6P.

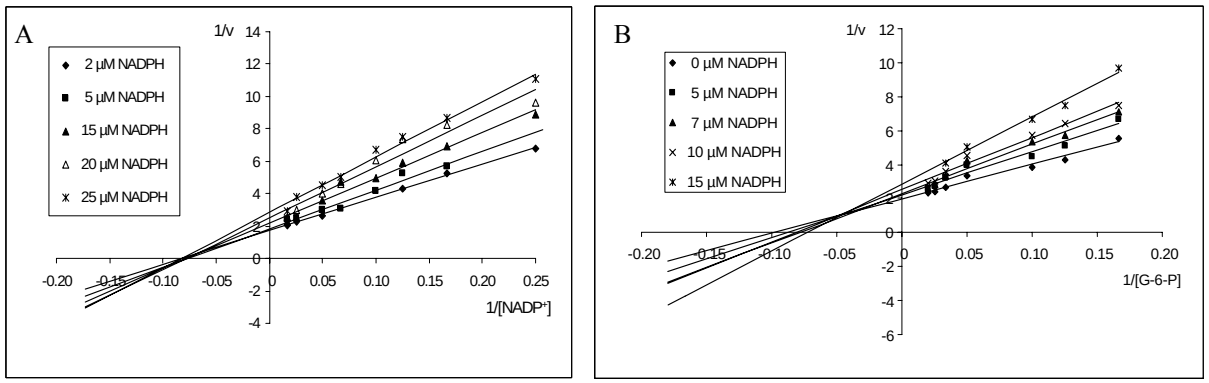

Figure 21: NADPH inhibition of *Pf*GluPho's G6PD. A) NADPH inhibition on G6P. B) NADPH inhibition on $NADP^+$.

4.1.7 *Pf*GluPho's G6PD NADPH Inhibition

Product inhibition patterns offer useful information regarding enzyme reaction mechanisms. In this case 6-phosphogluconolactone is too labile for kinetic measurements. However it is possible to determine the effects of NADPH on this reaction. NADPH was found to be a mixed inhibitor with respect to G6P and a non competitive inhibitor with respect to $NADP^+$ (Figure 21). The results imply that G6P binds to the enzyme-$NADP^+$ complex and not the free enzyme and therefore $NADP^+$ could be the leading substrate. This inhibition pattern points toward an ordered sequential mechanism with $NADP^+$ binding first to the enzyme.

4.1.8 *Pf*GluPho's G6PD Assay with GSSG, GSH and *Pf*GR

Formation of mixed disulfides between glutathione (GSSG) and the cysteines of some proteins (glutathionylation) has been suggested as a mechanism through which protein functions can be regulated by the redox status of glutathione. Experiments of the *Pf*GluPho's G6PD assay performed in the presence of any of the following: 2 mM GSH, 1 mM GSSG, *Pf*GR 10 mU/ml or in the presence of both *Pf*GR (10 mU/ml) and GSH (2 mM), showed that *Pf*GluPho is not allosterically regulated by *Pf*GR or any kind of interaction with GSSG or GSH and thus the redox status of glutathione.

4.1.9 *Pf*GluPho's G6PD Buffers, pH and Salt

Although the best buffer for *Pf*GluPho was found to be 100 mM Tris, 10 mM $MgCl_2$ and the optimum pH was found to be 7.4, our studies were able to demonstrate that the standard G6PD buffer (100 mM Tris, 0.5 mM EDTA, 10 mM $MgCl_2$, pH 8.0) could be used for further characterisation of *Pf*GluPho. This would enable us to make direct comparisons with previously published G6PD enzymes data.

4.1.10 *Pf*GluPho's 6-PGL Kinetic Analysis

*Pf*GluPho is a bifunctional enzyme composed of G6PD and 6-PGL. In reactions catalysed by G6PD glucose-6-phosphate is quickly converted to 6-phosphogluconolactone and concomitantly $NADP^+$ converted to NADPH + H^+. At the same time 6-phosphogluconolactone is quickly hydrolysed to 6-phosphogluconate by virtue of the bifunctionality of *Pf*GluPho. The 6-phosphogluconate available is converted to ribulose-5-phosphate with concomitant production of CO_2 and NADPH + H^+ in a reaction catalysed by 6-phosphogluconate dehydrogenase.

The concentration of 6-phosphogluconolactone made available to 6-PGL in a given period of time by the reaction catalysed by *Pf*GluPho's G6PD was determined as follows: Each absorbance value obtained before addition of 6-PGD at a given time t (delta A_t) corresponds to the amount of NADPH produced at time t. Since the extinction coefficient of NADPH is 6.22 l $mmol^{-1}$ cm^{-1} at 340 nm it follows that 100 µM NADPH is approximately equal to an absorbance of 0.622. A graphical plot of 6-phosphogluconolactone available against time gives a linear plot showing the amount of 6-phosphogluconolactone available at a given time (Figure 23).

The next step is to estimate the amount of 6-phosphogluconate that is produced by the reaction catalysed by *Pf*GluPho's 6-PGL and available to 6-PGD catalysed reaction. The difference in absorbance between the final absorbance readings after addition of 6-PGD (delta A_f) and the absorbance reading before addition of 6-PGD (delta A) give the corrected delta A value (delta A_c) (delta A_f – delta A = delta A_c). The calculated delta A_c was then fitted into the equation of the line of a standard curve obtained from a Lineweaver-Burk plot of the reaction performed using yeast 6-PGD in the absence of *Pf*GluPho to obtain the concentration of 6-phosphogluconate available. Thus the concentration of 6-phosphogluconate available at given

time could be calculated. A plot of 6-phosphogluconate available at given time against time gave a linear plot (Figure 23). To test for the influence of *Pf*GluPho in the reactions catalysed by yeast 6-phosphogluconate dehydrogenase, control assays of 6-phosphogluconate dehydrogenase were performed in the presence and absence of *Pf*GluPho. The results were negative which implied that *Pf*GluPho was only actively involved in the enzymatic generation of the substrate 6-phosphogluconate.

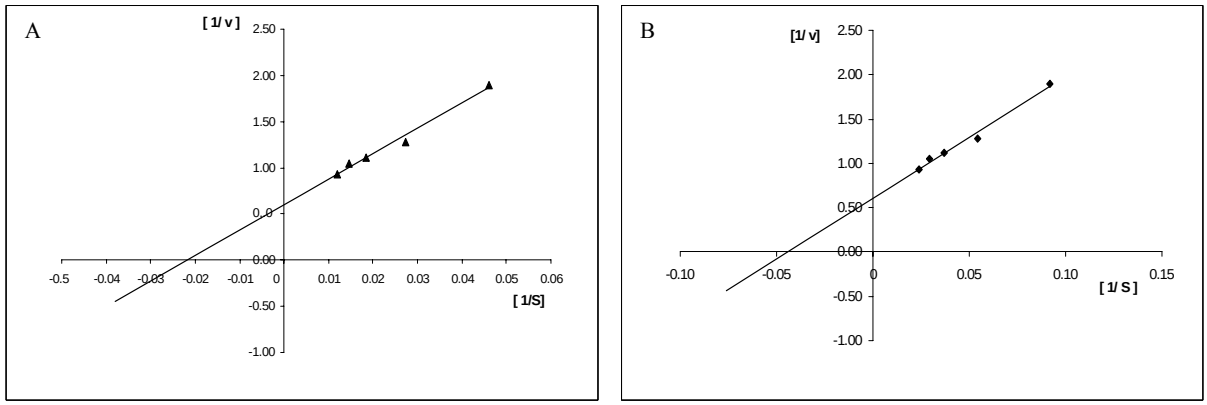

Figure 22: Lineweaver-Burk graph of *Pf*GluPho's 6-PGL and Human 6-PGL assays. A) Lineweaver-Burk graph of PfGluPho 6-PGL assays. B) Lineweaver-Burk graph of Human 6-PGL assays.

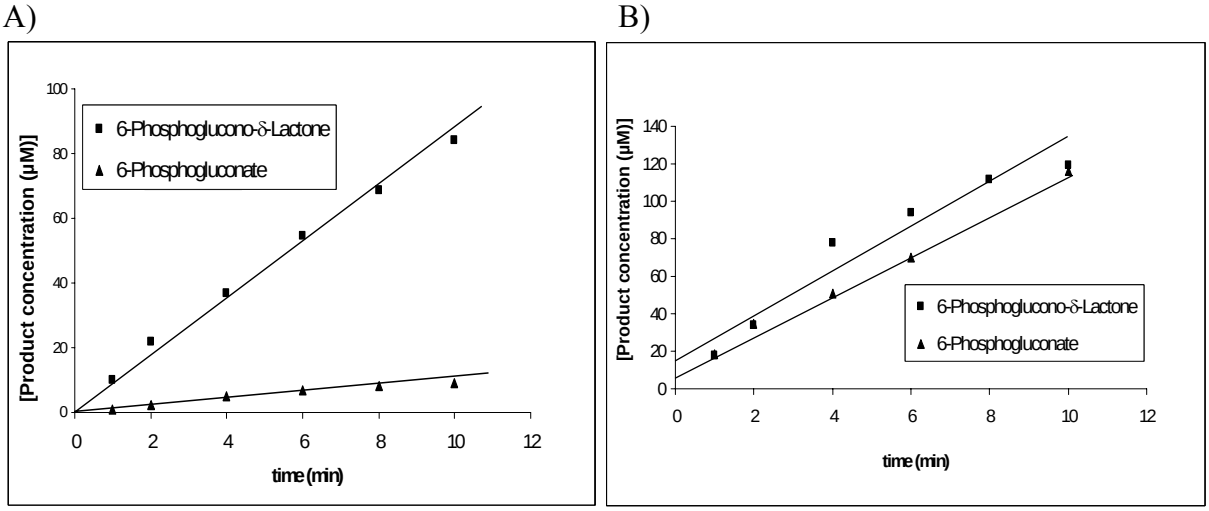

Figure 23: *Pf*GluPho's 6-PGL assay graphs. A) Graph showing the concentration of the products 6-phosphogluconolactone (6-PG-δ-L) available and the concentration of 6-phosphogluconate (6-PGn) produced by *Pf*GluPho's 6-phosphogluconolactonase. B) Graph showing the ncentration of the products 6-phosphogluconolactone (6-PG-δ-L) available and the concentration of 6-phosphogluconate (6-PGn) produced by human 6-PGL.

The K_m value for *Pf*GluPho's 6-PGL for its substrate 6-phosphogluconlactone was found to be 26.2 µM. A comparative study using the human 6-PGL showed that the human enzyme had a higher K_m value (32.5 µM) than that exhibited by *Pf*GluPho's 6-PGL. These results imply that the parasite enzyme has a higher affinity for the substrate 6-phosphogluconolactone. Comparison of the V_{max} values between the parasite enzyme and its human homologue revealed that the human enzyme V_{max} value was 5 times higher that exhibited by the parasite enzyme (712 against 71.2 U/ mg).

4.1.11 *Pf*GluPho's 6-PGL Assay in the Presence of GSSG and GSH

Formation of mixed disulfides between glutathione and cysteines in proteins (glutathionylation) has long been known to occur after oxidative stress [Brigelius *et al*., 1983]. Recently, protein glutathionylation has gained attention as a possible means of redox regulation of protein functions. We therefore tested for the possibilities of *Pf*GluPho's 6-PGL being regulated by glutathionylation. Our results demonstrate that no decrease in activity was evident in a system containing GSSG, GSH or a GSSG free reaction set up.

4.1.12 *Pf*GluPho Crystal Screening

Crystal screening trials using *Pf*GluPho have yielded crystals (Figure 24) of approximately 50 x 50 µm which can be further optimised to improve the crystal quality and thus solve the x-ray structure of *Pf*GluPho.

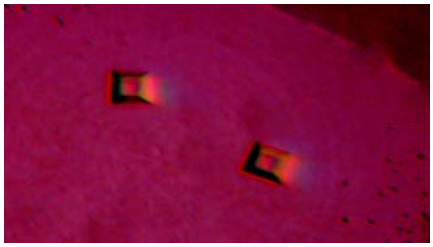

Figure 24: First *Pf*GluPho crystals

4.1.13 *Pf*GluPho Structure Prediction

4.1.13.1 Structure Prediction: Model of *Pf*GluPho's G6PD

Plasmodium falciparum GluPho (*Pf*GluPho) contains some unique structural and functional characteristics. A comparison of the C-terminal part amino acid sequence (residues 311-911) to that of human G6PD revealed only 39 % homology. The $NADP^+$ binding site as proposed by Hirono *et al*., [1989] based on clustering of mutations in G6PD genes of individuals having low affinity for $NADP^+$ is not present in *Pf*GluPho, however the region proposed by Persson *et al*., [1991] based on recognisable characteristics of the coenzyme binding site GXXGXXG/A and the β-α-β fold are present in GluPho (Figure 26). In *Pf*GluPho and in other *Plasmodium* GluPhos the final Gly of the coenzyme binding site is replaced by Phe [Clark *et al*., 2001]. The conserved Arg in this area in all other organisms is Cys (aa 363) in *Pf*GluPho although Arg 378 is conserved. The substrate (G6P) binding site IYRIDHYLGKA is highly conserved in *Pf*GluPho.

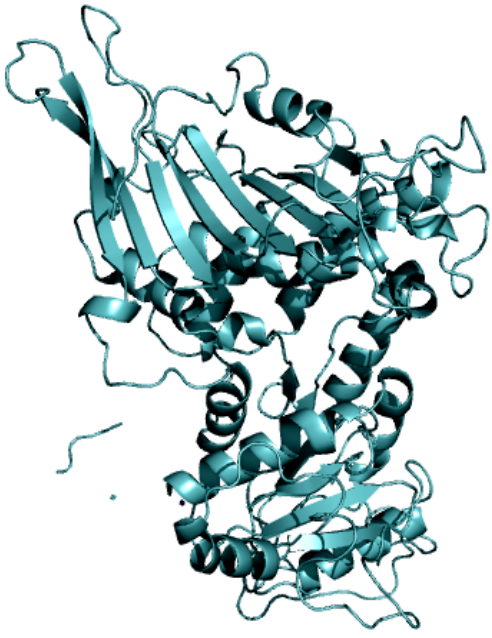

Figure 25: Model of *Pf*GluPho G6PD

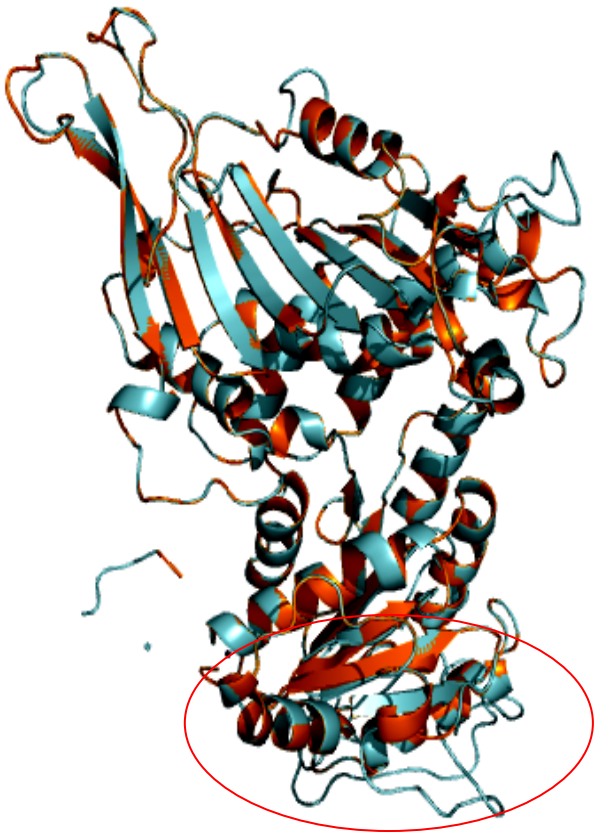

Figure 26: Overlay of the model of *Pf* GluPho's G6PD (cyan) and human G6PD (orange) differences in the *Pf* protein are marked in red.

A unique feature of *Pf*GluPho is the 62 amino acid insert (within the G6PD part) found between the structurally predicted $NADP^+$ and G6P binding site that has no similarity found to date (Figure 26). Similar inserts which differ in size and sequence are present in other *Plasmodium* GluPho and have nevertheless been demonstrated to be essential for GluPho activity [Clark *et al*., 2003]. The presence of the insert could imply that the distance between the substrate and coenzyme binding site of *Pf*GluPho may be different from that of the human G6PD and therefore there may be a difference in the efficiency of electron transfer.

A) B)

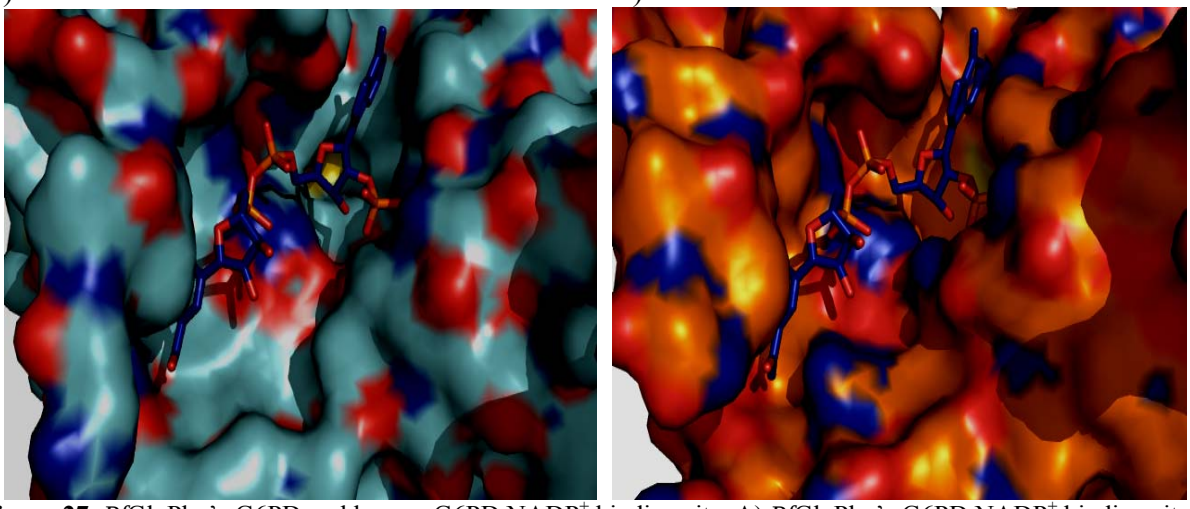

Figure 27: *Pf*GluPho's G6PD and human G6PD $NADP^+$ binding site. A) *Pf*GluPho's G6PD $NADP^+$ binding site model in complex with $NADP^+$ (light blue). B) Human G6PD $NADP^+$ binding site model in complex with $NADP^+$ (orange). Dark Blue colour patches show nitrogen, red colour patches show oxygen and yellow patches sulphur.

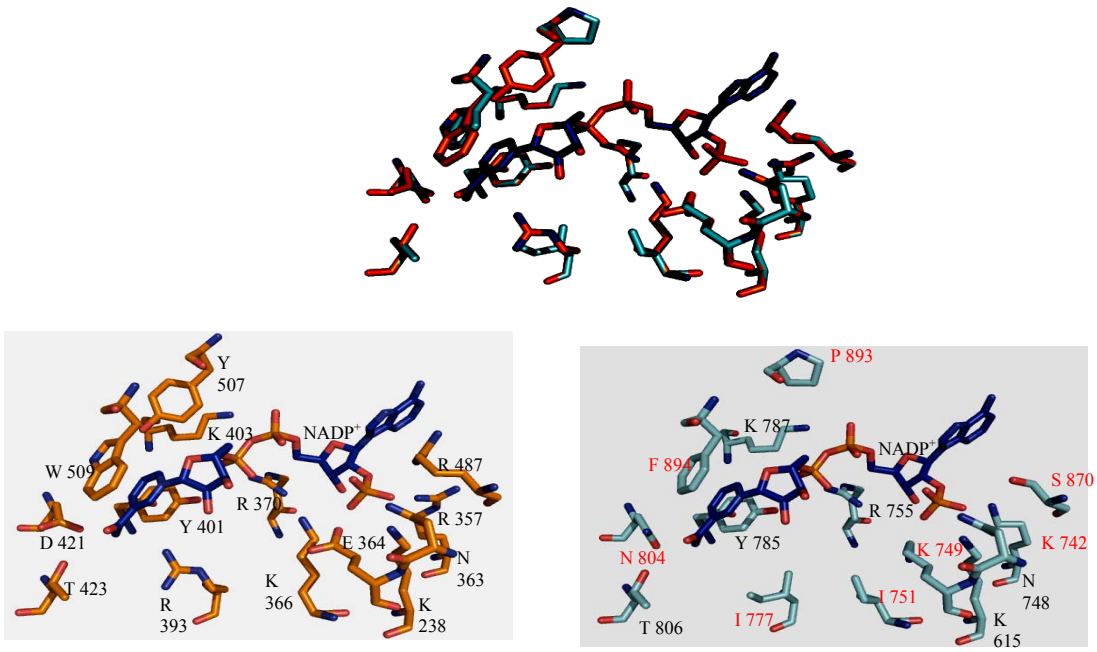

Figure 28: Comparison of the G6PD NADP$^+$ binding pocket amino acids of *Pf*GluPho's G6PD and Human G6PD. The NADP$^+$ binding pockets seem to be highly conserved except for a few differences which are marked in red in the model of the *Pf*GluPho (cyan) when compared with the human G6PDH (orange) and NADP$^+$ is shown in blue.

4.1.13.2 Structure Prediction: Model of *Pf*GluPho's 6-PGL

The structure prediction of *Pf*GluPho's 6-PGL was performed by comparing with the structure of *Thermotoga maritima*. The overall structure is very similar although *Pf*GluPho has more amino acids than *T. maritima* (Figure 29) which appear as a beta sheet (amino acid 168-190). The second observable difference is the additional alpha helix present in *Pf*GluPho but absent in *T. maritima* (Figure 29) (amino acid 263-286). Amino acids 198-208 form an alpha helix which is absent in *T. maritima* (Figure 29) where as amino acids 145-153 of *T. maritima* are present in the form of a short loop when compared to the additional *Pf*GluPho alpha helix (Figure 29) (aa 198-208).

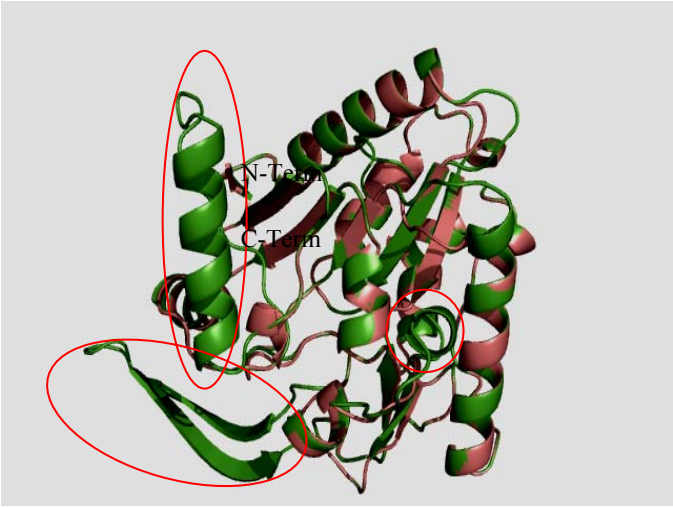

Figure 29: Overlay of the model of *Pf*GluPho's 6-PGL and 6-PGL from *T. maritima*. *Pf*GluPho's 6-PGL (green) vs. 6-PGL from *T. maritima* (1VL1; salmon), differences in the *P. falciparum* protein are marked in red.

4.1.14 Screening for *Pf*GluPho's G6PD Inhibitors

Interestingly early studies showed that many antimalarial drugs effectively inhibit commercial supplies of purified yeast G6PD [Cotton and Sutorius, 1971]. Similar studies have not been extended to *Pf*GluPho's G6PD and no known inhibitors exist to date. Identification of such inhibitors would lift the lid on probable new compounds with a different mode of action for the treatment of malaria. Screening for *Pf*GluPho's G6PD inhibitors (concentration of 5 µg/ml) from a library of 2000 compounds provided by the Hans-Knöll institute, Jena yielded 11 compounds which demonstrated an inhibition of above 60 % (Table 8). Three of these compounds (6983, 8007 and 8012) were obtained in quantities large enough for verifying the IC_{50} values as well as determining the type of inhibition. All the 3 inhibitors were found to be non-competitive with respect to G6P (K_i of 1.18, 1.65, 1.26 µM for 6983, 8007 and 8012 respectively) (Table 7) (Figure 30). In addition compound 8007 was found to be non-competitive with respect to $NADP^+$ (K_i 2.58 µM).

A) B)

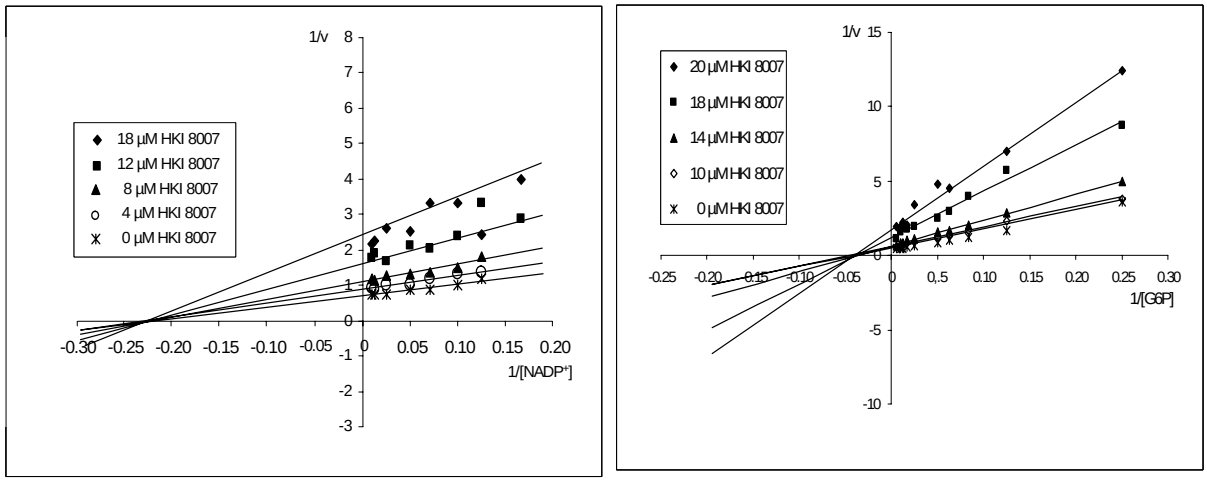

Figure 30: Non-competitive inhibition exhibited by compound 8007 on *Pf*GluPho's G6PD. A) Non-competitive inhibition pattern of compound 8007 with respect to G6P. B) Non-competitive inhibition pattern of compound 8007 with respect to $NADP^+$.

Inhibitor	K_i G6P (µM)	Type of Inhibition	K_i $NADP^+$ (µM)	Type of Inhibition
6983	1.18	Non-competitive	ND	ND
8012	1.65	Non-competitive	ND	ND
8007	1.26	Non-competitive	2.58	Non-competitive

Table 7: K_i values for *Pf*GluPho' G6PD inhibitors tested. ND stands for not determined

These results demonstrate that the inhibitors bind to another binding site other than the substrates G6P and $NADP^+$.

Inhibitor	Inhibitor Strucutre	% Inhibition at 5 µg/ml (IC_{50})
5030	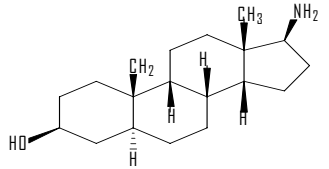	97
6465	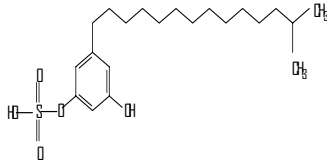	92
6983*	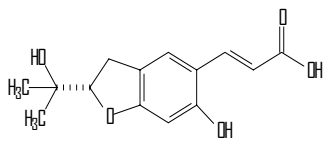	60.2 (20 µM)
7220	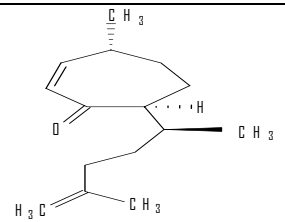	65.7
7291	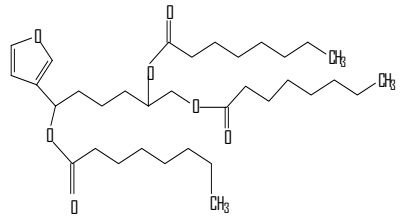	123
7593	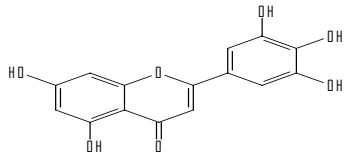	73.2

Inhibitor	Inhibitor Strucutre	% Inhibition at 5 µg/ml (IC_{50})
7604	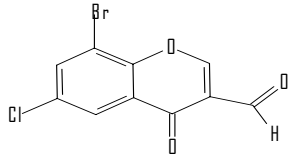	60.5
7724	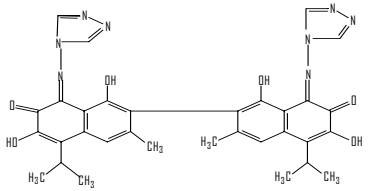	66
7868	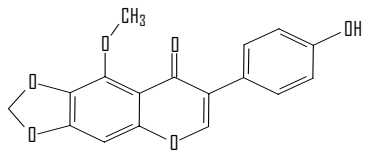	79
8012*	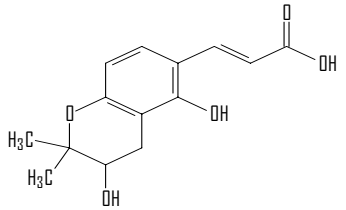	98 (14 µM)
8007*	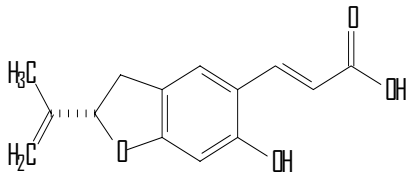	98 (18 µM)

Table 8: *Pf*GluPho's G6PD inhibitors. * are the compounds which were retrieved in larger quantities and IC_{50} were determined in enzyme assay.

4.2 Mouse IDO-1 and Mouse IDO-2

4.2.1 Heterologous Overexpression of Mouse IDO-2

The heterologous overexpression of IDO-2 protein was optimised using KRX cells. The best expression conditions were obtained using TB medium and induction with a final concentration of 0.1 % rhamnose. The expression system was supplemented with ALA, a natural precursor of heme in order to increase the heme content as reported for recombinant indoleamine 2,3-dioxygenase overexpression [Austin *et al.*, 2004] and other heme proteins [Delcart *et al.,* 2003]. Purification of the protein over a Ni-NTA column yielded 15 mg/ml protein from a litre of *E. coli* culture. The enzyme was prone to precipitation and unstable in activity. Therefore, glycerol (20-50 %) was added immediately after elution and found to enhance stability. Adding bovine serum albumin (0.05 mg/ml) or CHAPS (0.5 mM) did not enhance stability.

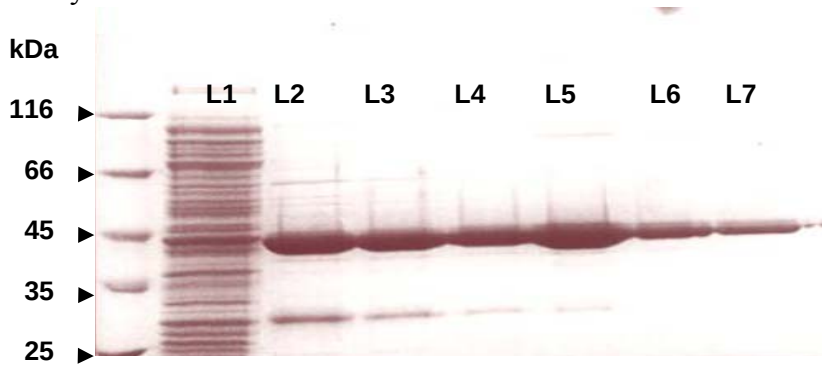

Figure 31: SDS gel showing the purification of mouse IDO-2 after the Ni-NTA column. On the left hand the molecular weight of the marker is given in kDa. L1 flowthrough fraction after binding of the protein. L2 - L7 imidazole elution concentration gradient (L2 : 50 mM, L3 : 60 mM, L4 : 75 mM, L5 & L6 : 200 mM, L7: 500 mM) in Tris buffer pH 7.4, 150 mM NaCl.

4.2.2 Optimisation of Heterologous Overexpression of Mouse IDO-1

The optimisation of heterologous overexpression of mouse IDO-1 was performed by varying various conditions as summarised in Table 9. The best expression conditions were obtained using LB medium and induction with a final concentration 0.025 mM IPTG. The expression system was supplemented with ALA just like in IDO-2 expression. Purification of the protein over a Ni-NTA column yielded 40 mg/ml protein from a litre of *E. coli* culture. Unlike IDO-2, IDO-1 was more stable and not prone to precipitation or unstable in activity.

Parameter	Condition used	Finding
IPTG Concentration	0.025 – 1.0 mM	0.025 mM was the best
Medium	LB, Terrific Broth, 2x YT	LB medium was the best
Duration of expression	3, 6 hours and overnight expression	Overnight expression was the best
E. coli cells type	BL 21, Rosetta	Rosetta cells were the best
Temperature ^{o}C	37, 30, 25, 20, room temperature	Room temperature
Supplements	Heme, δ-aminolevulininc acid (ALA) 0.1-1.0 mM	1 mM ALA

Table 9: Optimisation of the heterologous overexpression of mouse IDO-1.

4.2.3 Kinetic Assays for Mouse IDO-1 and Mouse IDO-2

The IDO-2 kinetic assays were performed using higher (0-60 mM) L-tryptophan as compared to 0-200 µM for IDO-1 and 400 µM as described by Takikawa *et al.* [1988]. At these higher concentrations L-tryptophan exhibited high absorption values by itself therefore a corresponding L-tryptophan concentration blank was always set up. The corrected assay absorption values were obtained by subtracting the value of the blank. Apart from the absorbance which could be subtracted, L-tryptophan did not influence the kynurenine calibration curve as observed in three different curves set up with 0.4, 12, and 30 mM L-tryptophan.

The values for K_m and V_{max} are characteristic properties of the enzyme and substrate system. Mouse IDO-1 exhibited a low K_m value (in the µM range) and therefore a high substrate affinity towards the substrate L-tryptophan as compared to IDO-2 which exhibited a high K_m (in the mM range) value and therefore a low affinity (Table 10).

	L-Tryptophan	
	K_m µM	**V_{max} min^{-1}**
mIDO-1[a]	28	203 ± 9
mIDO-2[a]	12000 ± 3000	0.013 ± 0.001
mIDO-2*	530 ± 100	7.7 ± 0.3

Table 10: Kinetic parameters of mouse IDO-1 and mouse IDO-2. a: done using methylene blue/ ascorbic acid method * : done using cytochrome b5/ cytochrome P450 method.

The IDO-2 K_m for the substrate L-tryptophan was found to decrease 20 fold from 12,000 to 530 µM (therefore increase in affinity for the substrate) when the assay was performed using the cytochrome b_5/ cytochrome 450 reduction method. A 590 fold improvement in the V_{max} was observed showing an improvement in L-tryptophan turnover capacity (Table 10). IDO-2 just like IDO-1 obeys Michaelis-Menten kinetics although it exhibits substrate inhibition at L-tryptophan concentration above 30 mM (Figure 32). It was also noted that for the freshly prepared IDO-2 the K_m value increased over time.

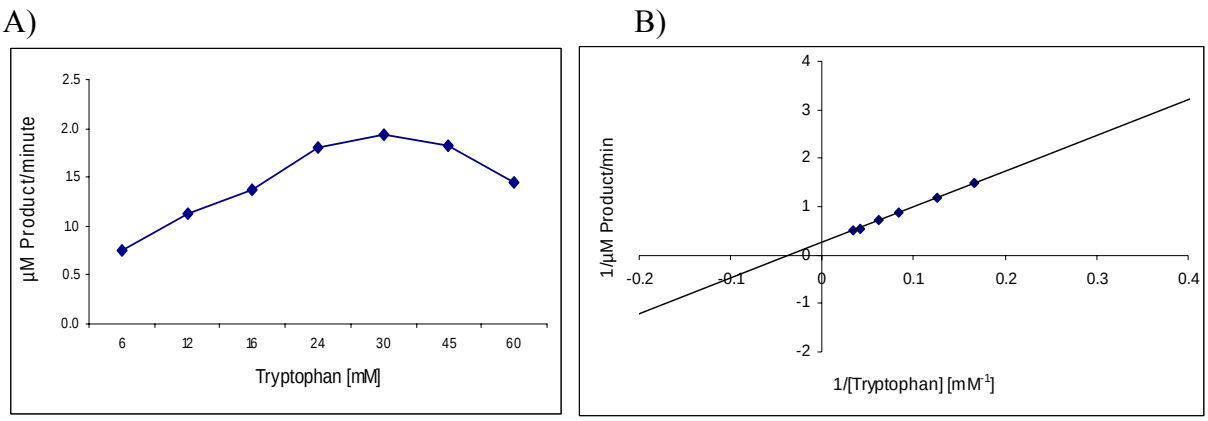

Figure 32: Michaelis-Menten and Lineweaver-Burk graph of mouse IDO-2. A) Michaelis-Menten curve of mouse IDO-2 showing substrate inhibition. B) Lineweaver-Burk graph of mouse IDO-2.

4.2.4 Test for Buffers, pH and Salt for Mouse IDO-1 and Mouse IDO-2

Several buffers were tested in order to determine the optimal mouse IDO buffer. The buffers tested were Hepes, Tricine, MES, MOPS, TEA and potassium phosphate buffer all set at a concentration of 100 mM and the pH set at the pKa value. IDO-2 recorded the best activity with 100 mM Tricine buffer pH 7.0 and IDO-1 recorded the best activity with 100 mM MOPS buffer pH 6.5 (Table 11).

Buffer	% activity IDO-2	% activity IDO-1
100 mM Hepes pH 7.2	85.3	90.1
100 mM Tricine pH 7.5	87.8	73.2
100 mM Tricine pH 7.0	100.0	97.8
100 mM MES pH 7.0	71.6	88.5
100 mM MOPS pH 7.5	98.3	88.1
100 mM MOPS pH 6.5	67.8	100.0
100 mM TEA pH 7.5	86.2	92.0
100 mM TEA pH 8.0	96.1	57.5
100 mM Potassium phosphate pH 7.4	46.7	52.62

Table 11: Mouse IDO-1 and IDO-2 test with different buffers without salt

When tests were performed using these buffers containing in addition 100 mM KCl, 100 mM TEA buffer pH 8.0 was the best buffer for IDO-2 whereas 100 mM Tricine pH 7.0 was the best buffer for IDO-1 (Table 12).

Buffer	% Activity IDO-2	% activity IDO-1
100 mM Hepes pH 7.2	78.5	83.7
100 mM Tricine pH 7.5	86.3	80.1
100 mM Tricine pH 7.0	92.0	100.0
100 mM MES pH 7	92.1	81.6
100 mM MOPS pH 7.5	91.4	74.6
100 mM MOPS pH 6.5	72.5	87.2
100 mM TEA pH 7.5	90.6	84.0
100 mM TEA pH 8.0	100.0	58.2
100 mM Potassium phosphate pH 7.4	66.0	50.2

Table 12: Mouse IDO-1 and IDO-2 test with different buffers all containing 100 mM KCl

Tests were also performed using potassium phosphate buffer pH 7.4 (a component of the standard IDO assay buffer) with varying amounts of KCl (0-300 mM). The best activities were in the presence of 100 mM KCl for IDO-2 and 50 mM KCl for IDO-1 (Table 13).

KCl conc	% Activity IDO-2	% activity IDO-1
0	93.2	99.4
50	93.4	100.0
100	100.0	89.3
150	93.4	83.0
200	89	87.4
300	77.5	91.8

Table 13: Test for different KCl concentrations in 100 mM potassium phosphate (pH 7.4) buffer

Comparing pH profiles of IDO-2 and IDO-1 revealed that whereas IDO-1 had an optimum activity at pH 6.4 - 6.5, IDO-2 had an optimum activity at pH 7.4 - 7.5 (Figure 33). Tests with various buffers showed that the 100 mM potassium phosphate buffer, pH 7.4, 100 mM KCl was the best buffer for IDO-2 and was therefore used for further analysis.

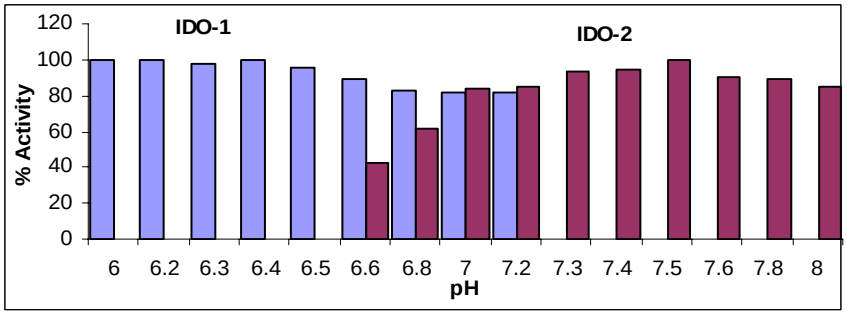

Figure 33: Mouse IDO-1 and IDO-2 pH profile

4.2.5 Spectral Characteristics of Mouse IDO-1 and Mouse IDO-2

IDO-2 protein just like IDO-1 was found to be a ferric (Fe^{+3}) type hemoprotein. Both proteins exhibit a characteristic spectrum with an absorption peak in the Soret region (406 nm) (Figure 34). Treatment of both proteins with sodium dithionite under anaerobic conditions leads to a shift in the spectra from 406 nm to 428 nm (Figure 34). This shift in the spectra strongly indicates that after purification under aerobic conditions both IDO-1 and IDO-2 are present in the Fe^{+3} oxidised state. A similar phenomenon has earlier been reported to occur for the human IDO-1 [Littlejohn *et al*., 2000].

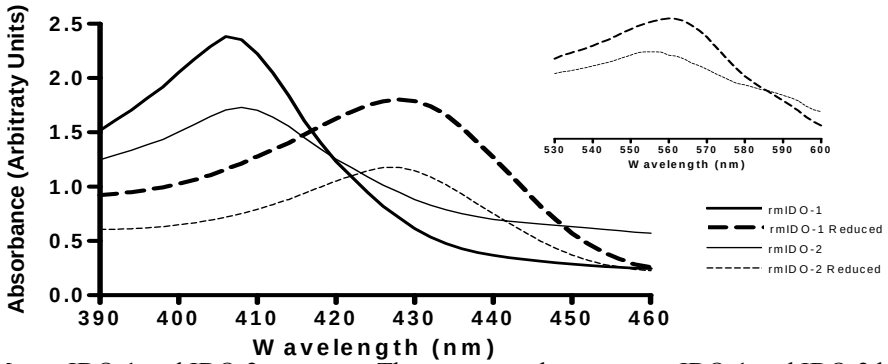

Figure 34: Mouse IDO-1 and IDO-2 spectrum. The spectrum shows mouse IDO-1 and IDO-2 before and after treatment with sodium dithionite. Inset expanded spectral region 530-600 nm

4.2.6 Oligomerisation Studies of Mouse IDO-1 and Mouse IDO-2

Oligomerisation studies carried out on IDO-2 have revealed that the mouse IDO-2 exists as both a monomer of 45 kDa (45 %) and a dimer of 90 kDa (55 %) (Figure 35). When the dimeric IDO-2 was loaded onto the FPLC column a similar pattern of monomer and dimer formation was observed. Addition of DTT to the dimeric IDO-2 form leads to the formation of monomeric IDO-2 (76 %). Addition of DTT immediately upon purification leads to the formation of about 95 % monomer of IDO-2. In the presence of H_2O_2, GSSG and GSH, IDO-2 exists predominantly as a monomer (63 %, 55 % and 78 % respectively). The existence of

IDO-2 as a monomer in the highly reductive environment of DTT and GSH could mean that dimerisation of IDO-2 involves intermolecular disulfide bonds and the enzyme could be regulated by glutathionylation or could have a redox regulated mechanism.

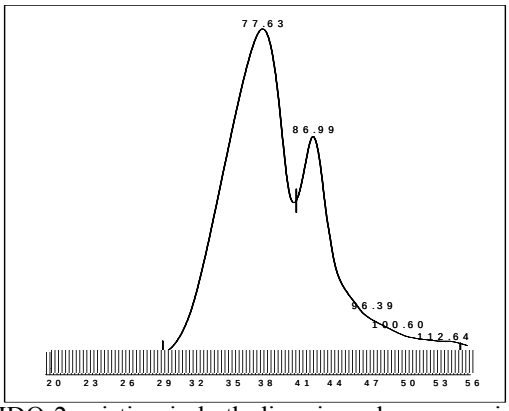

Figure 35: Mouse IDO-2 existing in both dimeric and monomeric form. 77.63 correspond to the dimeric form whereas 86.99 correspond to the monomeric form.

Measurement of activity of the monomeric IDO-2 against the dimeric form showed no difference in activity. IDO-1 on the other hand was found to predominantly exist as a monomer.

4.2.7 Crystal Screening of Mouse IDO-1 and Mouse IDO-2

The crystal screening was performed using the hanging drop method and Hampton research crystallisation kits (as described in 3.1.7). The proteins were found to precipitate very easily. Addition of DTT to the protein before crystallisation trials reduced precipitation of the protein but no crystals were obtained. Crystallisation trials were also performed using the conditions described for human IDO-1 by Sugimoto *et al*. [2006], but no crystals were obtained.

4.2.8 Structure Prediction of Mouse IDO-2

For the evaluation of the structure model of the IDO-2 from mouse an overlay with the crystal structure of human IDO1 (PDB ID: 2D0T) was made.

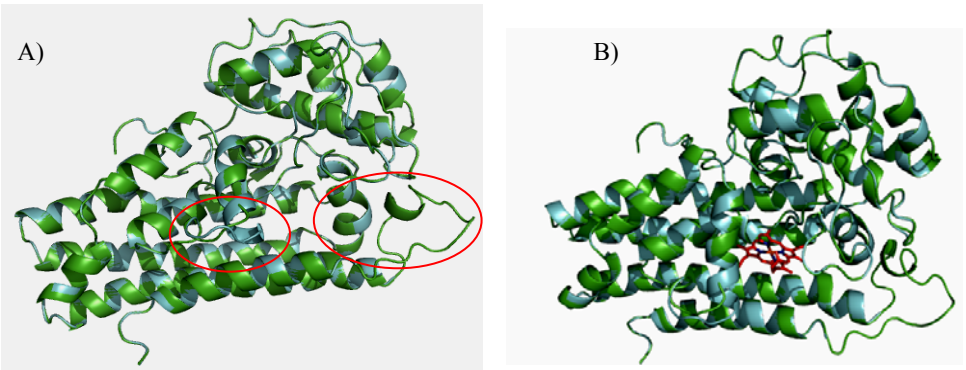

Figure 36: Mouse IDO-2 structure models. A) A) Overlay of human IDO1 (cyan) with the structure model of mouse IDO-2 (green) B) Superposition of the crystal structure of human IDO1 (cyan) with heme (red) and the modelled structure of mouse IDO-2 (green).

The overall structure was found to be identical to the structure of the human IDO1 (Figure 36), described by Sugimoto *et al*. [2006]: it folds into two domains, a large and a smaller one. The large domain consists of 13 α-helices and two 3_{10} helices. The small domain is comprised of six α-helices, two short β-sheets and three 3_{10} helices. A comparison of the amino acids 360-380 was not possible, due to disordered electron density in the crystal structure. It is assumed that the attachment of a substrate and or a ligand could lead to a conformational change in this region (the loop). The heme binding site was analyzed in detail, in order to obtain more information about the heme environment of mouse IDO-2 (Figure 37). To a large extent the same amino acids were found at identical positions and in identical conformation. An important difference in the heme environment is the exchange of the amino acids I217 and L384 of the crystal structure by a methionin (M221 and M385) in the structural model. This could cause a reinforcement of the heme binding on one hand and or a change of the oxidation state of the heme molecule within the structure on the other hand.

A) B)

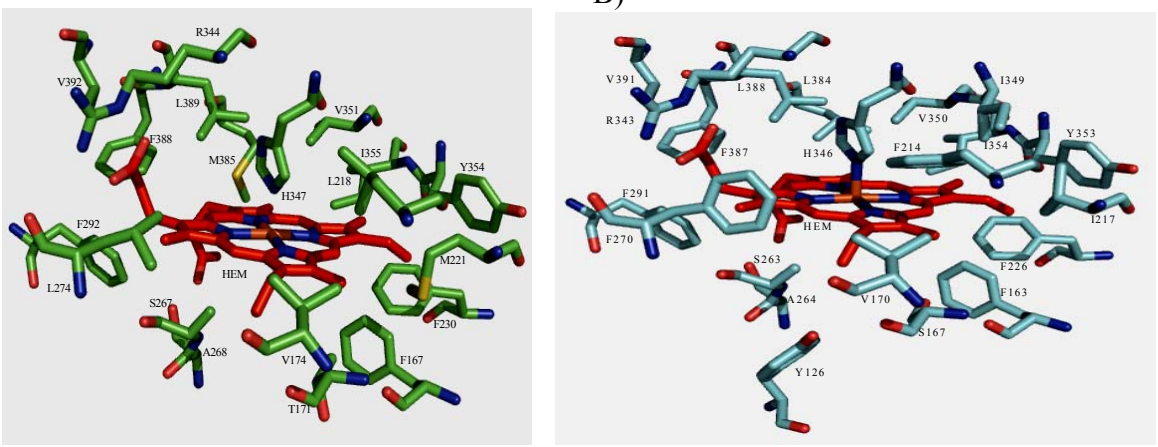

Figure 37: Heme environment of mouse IDO-2 and human IDO-1. A) Heme binding site (green) of the structure model of mouse IDO-2. B) Heme binding site (grey) of the crystal structure of human IDO1. All shown amino acids are around 4Å of heme.

All amino acid interactions for IDO-1 described by Sugimoto *et al*. [2006] could also be found in the homology model. The salt bridge, between D274 and R343 in the crystal structure (3.49 Å and 2.89 Å) is formed by similar amino acids (D278 and R344) in the structure model (3.3 Å and 2.9 Å). The crystal structure of IDO-1 implicates D274 to play a key role in the catalytic reaction, a role which could be assigned to D278 in IDO-2. This is due to their close confirmation similarities as well their similarities in terms of their position in the homology model. The described interaction between R343 of the human IDO-1 and the 6-propionate of the heme (2.63 Å and 2.9 Å) is also present in the structured model (2.63 Å and 2.57 Å), so is the interaction between S267 with 7-propionate of the heme in the homology model. Important amino acids F226, F227 and R231, which form the entrance tunnel to the heme binding pocket, were mutated to alanine by Sugimoto *et al*. [2006]. The mutations of these 3 amino acids drastically reduced the dioxygenase activity. It is accepted that F226 and R231 are directly and F227 is indirectly involved in the substrate recognition

by hydrophobic interactions. In the homology model of mouse IDO-2 F230, Y231 and R235 occupy the same positions as the aforementioned amino acids of the crystal structure (F226, R231, F227). The exchange of F227 to Y231 probably leads to a change in substrate specificity of IDO-2 in comparison to IDO-1. Analysing the entire tunnel toward the heme binding pocket reveals a bigger substrate binding pocket in IDO-1 as compared to that of IDO-2. These findings might point towards changed substrate affinity/ specificity.

4.2.9 Mouse IDO-1 and Mouse IDO-2 Inhibition Using Substrate Analogues

1-methyl-D-tryptophan and 1-methyl-L-tryptophan, which have a substitution at the indole nitrogen atom, are the best known potent substrate analog competitive inhibitors with respect to the substrates D-Trp and L-Trp for IDO. Tests performed using these inhibitors (Table 14) showed that 1-methyl-L- tryptophan was a better inhibitor for mouse IDO-1 (K_i 105 µM) as compared to1-methyl-D-tryptophan (K_i 11700 µM). 1-methyl-D-tryptophan on the other hand was found to be the best inhibitor with respect to mouse IDO-2 (K_i 2500 µM) as compared to 1-methyl-L-tryptophan (K_i 13500 µM).

	1-Methyl-L-Tryptophan	**1-Methyl-D-Tryptophan**	**Norharman**
	K_i µM	**K_i µM**	**K_i µM**
mIDO-1	105	11700	1080
mIDO-2	13500	2500	750

Table 14: Inhibition of mouse IDO-1 and IDO-2 using substrate analogues.

Norharman is a known non competitive inhibitor of IDO but a competitive inhibitor for TDO [Sono and Cady, 1989]. Tests using this inhibitor revealed that it was a better inhibitor for IDO-2 as compared to IDO-1 (Table 14).

4.2.10 Screening for Mouse IDO-1 Inhibitors

Although some IDO inhibitors are available, their inhibitory activities are relatively low at micromolar K_i values (Table 14). There is therefore need for more potent IDO inhibitors. Screening for more potent IDO specific inhibitors using a library of compounds provided by Hans-Knöll institute Jena, yielded compound 55D11 (Figure 38) which is capable of inhibiting IDO-1. This inhibitor was found to inhibit IDO-1 and not IDO-2 with an IC_{50} value of 0.02 mg/ml. We always utilised fresh preparations of enzymes for our inhibitor test and we found that the specific activity of IDO-1 varied from one preparation to another as shown in Table 15. This could be as a result of IDO-1 being very unstable. Nevertheless the K_m values remained the same or constant showing that although the enzyme might be inactivated there are some active sites which were still active.

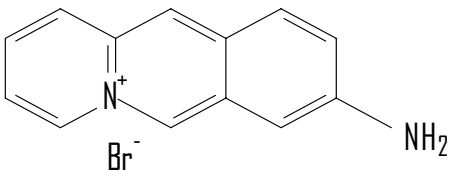

Figure 38: Structure of compound 55D11: 8-aminoacridiziniumbromide

In the presence of our inhibitor 55D11 the K_m and V_{max} values were found to decrease quite strongly (Table 15). The decrease in the K_m and V_{max} values shows that the dose dependent effect was quite strong and the data is in accordance with uncompetitive inhibition (Figure 39) with the calculated K_i value being 0.05 µM.

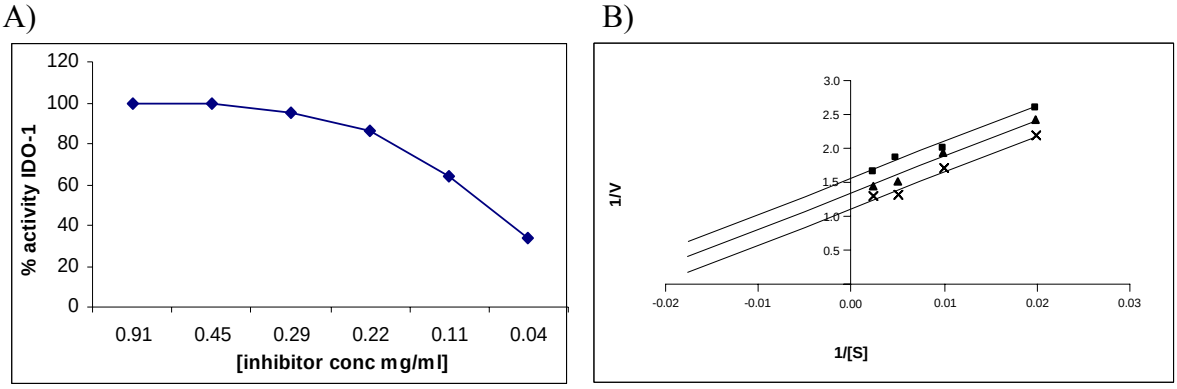

Figure 39: Inhibition of mouse IDO-1 by inhibitor 55D11. A) IC_{50} graph for mouse IDO-1 using inhibitor 55D11. B) Uncompetitive inhibition pattern exhibited by inhibitor 55D11

This inhibition pattern shows that the inhibitor can not bind to the free enzyme but binds to the enzyme-substrate complex thereby inducing a conformational change to the complex which leads to changes in V_{max} values observed.

	No inhibitor		With Inhibitor conc					
			0.9 µM		0.18 µM		0.018 µM	
Date	**K_m**	**V_{max}**	**K_m**	**V_{max}**	**K_m**	**V_{max}**	**K_m**	**V_{max}**
07.08.07	123	2.21	3.7	0.17	13.2	0.17	51.3	1.2
			0.29 µM		0.22 µM		0.11 µM	
			K_m	**V_{max}**	**K_m**	**V_{max}**	**K_m**	**V_{max}**
11.03.08	49.1	0.21	19.56	0.12	21.38	0.13	31.23	0.16
02.04.08	155.6	0.05	98	0.14	140.2	0.17	181.6	0.08
03.04.08	124.5	0.07	174.7	0.14	182.5	0.14	176.3	0.11
Average	113 ± 45	1.05 ± 0.82						

Table 15: Mouse IDO-1 inhibition by 55D11 values. K_m in µM and V_{max} in U/mg

4.2.11 Structure Activity Study of 55D11 Derivatives as Mouse IDO-1 Inhibitors

A structure activity study was undertaken to determine which elements or side chains of the inhibitor 55D11 could be modified to enhance potency. The derivatives provided by Prof Ihmels (University of Siegen) were classified into five major groups; (i) compound containg a side chain whose parent chain contains an indole ring or whose parent chains are similar to tryptophan (compounds KS 1, 4 and 16), (ii) derivative compounds having an amine side chain, and with or without a halide (compounds KS 2, 21, 22, 23 and 24), (iii) derivative compounds having a carboxylic side chain (compounds KS 5, 6 and 18), (iv) derivative compounds having an amine attached to a benzene ring (compounds KS 9, 10, 12, 13, 14, 15 and 17), (v) derivative compounds having an acetamide group (compounds KS 19 and 20) (Table 16).

Compound	Structure	% Inhibition	IC_{50} *P.f*
KS 1	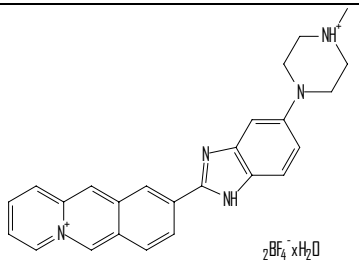	28.2	149
KS 2	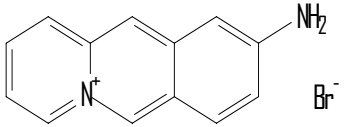	73.0	5.2
KS 3	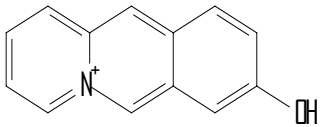	45.7	> 1000
KS 4	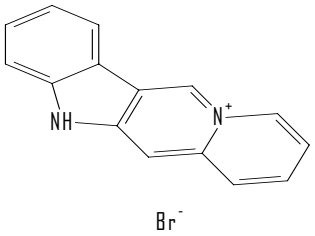	41.0	19.7
KS 5	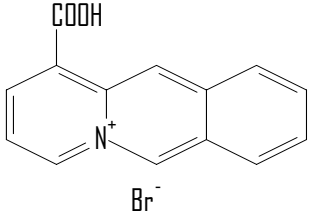	47.8	> 1000

Compound	Structure	% inhibition	IC_{50} *P.f*
KS 6	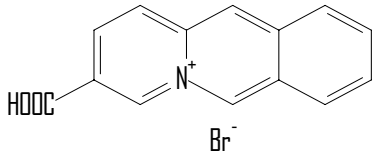	39.3	> 1000
KS 7	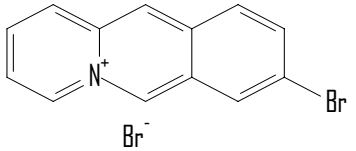	31.2	89.7
KS 8	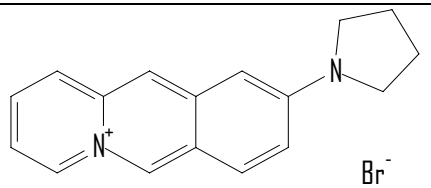	14.5	9.9
KS 9	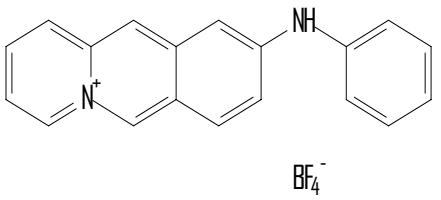	36.4	35
KS 10	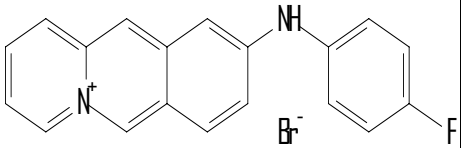	48.6	1.2

Compound	Structure	% Inhibition	IC_{50} *P.f*
KS 11	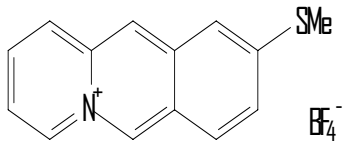	39.7	16.7
KS 12	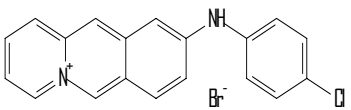	36.2	0.8
KS 13	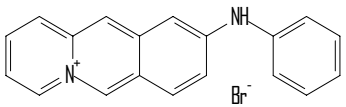	43.2	1.3
KS 14	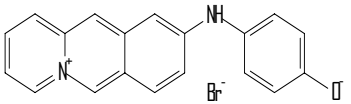	5.94	2.55
KS 15	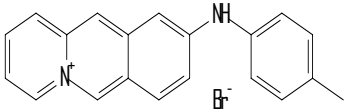	48.1	0.85
KS 16	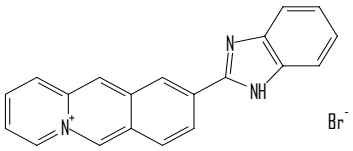	59.5	26.0
KS 17	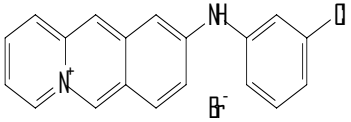	33.4	1.4

Compound	Structure	% Inhibition	IC_{50} *P.f*
KS 18	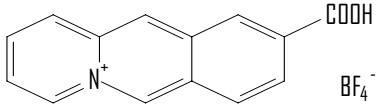	47.4	1000
KS 19	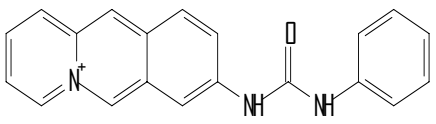	45.7	9.8
KS 20	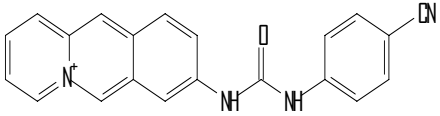	46.3	43.4
KS 21	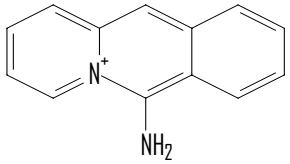	47.6	> 1000
KS 22	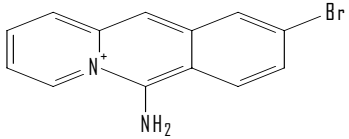	54.1	207
KS 23	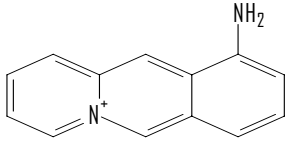	-29.0	99.8
KS 24	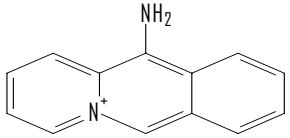	49.6	63

Table 16: Derivatives of inhibitor 55D11. Percent inhibiton on IDO determined using an inhibitor concentration of 5µg/ml. IC_{50} also determined in *P. falciparum* cell culture. *P.f* means *P. falciparum* 3D7 IC_{50} in ng/ml.

4.3 Thioredoxin Networks

Members of the thioredoxin superfamily mediate thiol disulphide exchange reactions, and can transfer reducing equivalents to other proteins. First, Trx induces the conformational change of the targe t protein and facilitates the reduction of the disulphide bridge in the molecule [Brandes *et al*., 1993; Stumpp *et al*., 1999]. Then Trx and its target protein form a mixed disulphide intermediate at the first reactive cysteine in the reactive site CxxC [Brandes *et al*., 1993]. This intermolecular disulphide bond is attacked by the second cysteine of Trx, hereby the target protein is reduced and the reduced form of Trx is oxidized. The substitution of the second cysteine to serine can interrupt this reduction process at the stage of the formation of the mixed disulphide intermediate. This basic concept of Trx affinity chromatography was first applied by Verdoucq *et al*., [1999] to capture the interacting partner protein of Trx in yeast. The strategy that was applied was conceptually similar to this work. However, in this study the *Pf*Plrx mutant was immobilized on the gel surface and the gel was used for the affinity chromatography [Motohashi *et al*., 2001]. When the protein pool of *P. falciparum* proteins was incubated with this gel, potential *Pf*Plrx target proteins having an accessible disulphide bond should form a mixed disulphide intermediate with the immobilized *Pf*Plrx mutant on the resin. This intermediate complex should be stable under the experimental conditions, i.e. in the absence of any reductants. In order to remove non-specifically bound proteins the gel was washed with high concentrations of NaCl (500 mM). After repeated washing, the captured proteins were then eluted from the gel using 10 mM dithiothreitol (DTT), a concentration sufficient to reduce the mixed disulphide bond formed (Figure 40). By this procedure several potential *Pf*Plrx target proteins were captured and it was possible to identify some of these proteins by N-terminal sequencing as summarised in Table 17 [Motohashi *et al*., 2001].

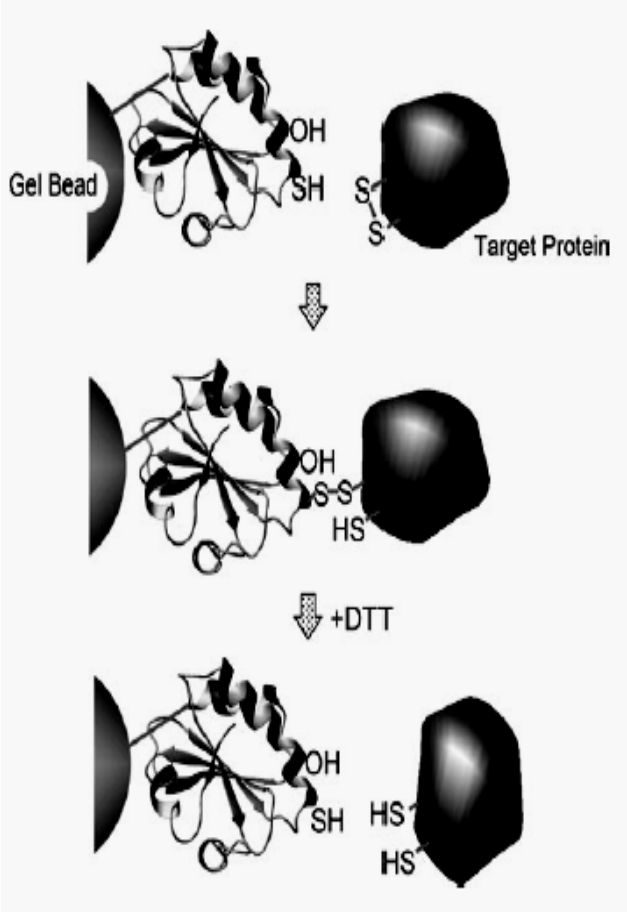

Figure 40: *Pf*Plrx affinity chromatography [Motohashi *et al*., 2001]. The second cysteine of Plrx was mutated to serine. The mutant protein was immobilised on CNBr activated sepharose according to manufacturer's instructions. The prepared resin was incubated with protein mixture for 2 hours at room temperature. After repeated washings captured proteins were eluted from the resin using 10 mM DTT.

Protein Name	Accession number		Protein MW [kDa]	Protein Isoelectric point	Protein Coverage [%]	Masses Matched
	Swiss-Prot/ GenBank	PlasmoDB				
40S ribosomal protein S12	O97249	PFC0295C	15.4	4.91	23	3
Acyl carrier protein, putative	Q7KWJ1	PFB0385w	15.8	8.87	19	3
14-3-3 protein homologue, putative	Q8IB17	MAL8P1.69	29.5	4.96	20	4
Co-chaperone GrpE, putative	Q8IIB6	PF11_0258	34.5	8.8	20	4
14-3-3 Protein, putative	Q8ID86	MAL13P1.309	35.1	7.08	17	3
Glyceraldehyde-3-phosphate dehydrogenase	Q8IKK7	PF14_0598	36.6	7.59	30	7
Hypothetical protein	Q8IJX6	PF10_0065	37.8	8.67	16	4
Ribonucleotide reductase small subunit	Q8IM38	PF14_0053	40.6	5.37	14	4
S-adenosylmethionine synthetase	Q7K6A4	PFI1090w	44.8	6.28	20	5
Conserved GTP-binding protein, putative	Q8IBM9	MAL7P1.122	45.2	6.88	35	9
Ornithine aminotransferase	Q6LFH8	PFF0435w	46.1	6.47	22	8
Endonuclease iii homologue, putative	Q6LFC2	PFF0715c	49.2	9.37	11	4
HAP protein/Plasmepsin III	Q8IM15	PF14_0078	51.7	8.04	18	8
Hypothetical protein	Q8ILQ4	PF14_0190	54.7	5.53	9	3
Hexokinase	Q6LF74	PFF1155w	55.3	6.72	11	4
Disulfide isomerase, putative	Q8I6S6	MAL8P1.17	55.5	5.56	9	3
Pyruvate kinase, putative	Q6LF06	PFF1300w	55.7	7.5	28	9
Heat shock protein	Q8I2X4	PFI0875w	72.4	5.18	9	6
Heat shock 70 kDa protein	Q8IB24	PF08_0054	73.9	5.5	28	12
Heat shock protein 86	Q8IC05	PF07_0029	86.2	4.94	13	8
Elongation factor 2	Q8IKW5	PF14_0486	93.5	6.35	10	5

Table 17: Potential plasmoredoxin target proteins identified in *Plasmodium falciparum*

Analysis using the Biacore system with immobilised S-adenosyl-L-homocysteine hydrolase (SAHH) sensor chip CM5 and *Pf*Plrx showed an association between SAHH and *Pf*Plrx. Although the interaction between the SAHH and the wild type *Pf*Plrx was stronger than that between SAHH and *Pf*Plrx^{C63S} (Figure 41) the binding was not affected by the flow of the buffer over the chip which indicates the presence of a covalent interaction. The dissociation of the interaction of SAHH and the analytes (*Pf*Plrx and *Pf*Plrx^{C63S}) in the presence of 10 mM DTT confirms that the interaction takes place through formation of disulfide bonds.

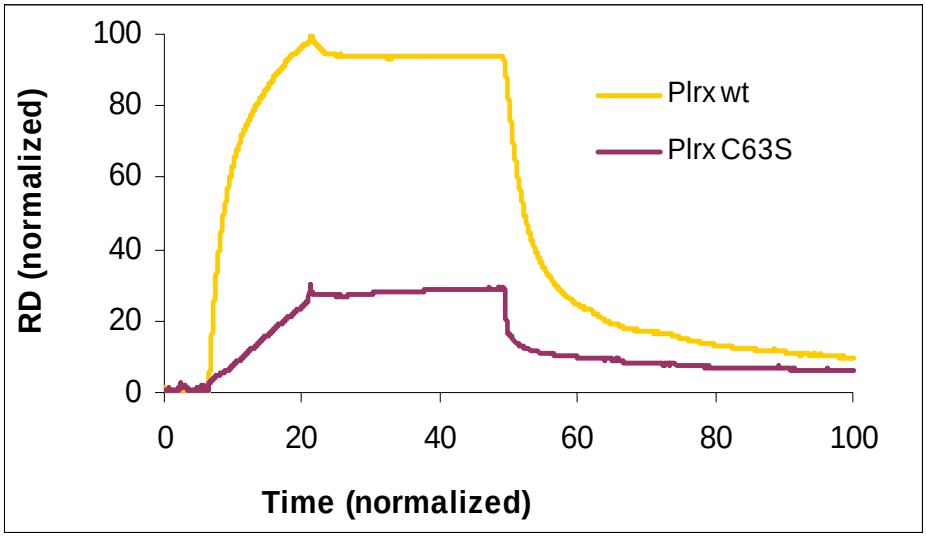

Figure 41: Sensogram of interaction between SAHH and *Pf*Plrx or *Pf*Plrx^{C63S}.

5 Discussion

5.1 *Pf*GluPho's G6PD

Using our optimised method of expression and purification we have been able to heterologously overexpress and purify *Pf*GluPho to homogenity. It was impossible to purify the enzyme using 2' 5' ADP Sepharose 4B material a phenomenon which had been earlier reported by Kurdi-Haidar and Luzzatto [1990]. Since we overexpressed our protein with a His-tag it was possible to use the Ni-NTA column for the first purification step followed by a size exclusion chromatography using gel filtration which yielded a homogenous pure protein. Typically 1 mg of purified enzyme could be obtained from 1 litre of *E. coli* culture. This unique bifunctional enzyme from *P. falciparum* has for the first time been successfully cloned, heterologously overexpressed and purified.

Antibodies specific for different parts of *Pf*GluPho were produced in rabbits. Using these antibodies recombinant *Pf*GluPho as well as the native protein in *P. falciparum* whole cell extracts could be identified by Western blot. The results confirm that *Pf*GluPho is present as a bifunctional enzyme in *P. falciparum* parasites and that the recombinant protein is *Pf*GluPho.

Earlier studies on the oligomeric structure of *Pf*GluPho were rather contradictory. Kurdi-Haidar and Luzzatto [1990] estimated the molecular weight of *Pf*GluPho to be 450 kDa and predicted that it was an octamer of an "ordinary size" consisting of 8 subunits of 50-60 kDa each. O'Brian *et al*. [1994] on the other hand disputed this finding and predicted that *Pf*GluPho was a tetramer of "oversized" subunits. Molecular studies of G6PD have indicated that the dimer is the minimal catalytically active structure and often aggregates to form tetramers [Levy, 1979] but since *Pf*GluPho exhibits high substrate affinities, this implies that the enzyme does not exist as a tetramer. Our data clearly indicates that *Pf*GluPho has a molecular weight of 636 kDa with a subunit molecular weight of 106 kDa which does not differ from the predicted molecular weight of 107 kDa. *Pf*GluPho therefore exists as a hexamer and not an octamer or an oversized tetramer.

When comparing *Pf*GluPho K_m values with those documented for the human G6PD (Table 5) [Birke *et al*., 1989; Wang *et al*., 2002], *Pf*GluPho was found to be more active and exhibits substrate affinities that favour turnover by the parasite enzyme (K_m values for G6P differ by a factor of 3) in comparison to the human G6PDH. This implies that in infected RBC where G6P and particularly $NADP^+$ concentrations are lower than K_m values of human G6PD, *Pf*GluPho utilises most of the G6P and $NADP^+$ present for the generation of NADPH through the PPP. This high substrate affinity of *Pf*GluPho makes the *Plasmodium* enzyme unique amongst G6PD enzymes characterised so far and also from other protozoa (Table 16). The discrepancy between the *Pf*GluPho K_m values from our study and those from earlier studies could be due to reliance on *Pf*GluPho obtained from parasitised cells which contains a large excess of RBC G6PD (homogeneity of the enzyme used).

Assays with the substrate analogue 2-deoxyglucose-6-phosphate revealed that *Pf*GluPho had a low affinity for the analogue (K_m 2.5 mM), when compared to the affinity of G6P (K_m 18.1 µM) this affinity differs by a factor of 138. When compared to the human G6PD (K_m 1.67 mM) [Wang *et al*., 2002], which has a better affinity to the analogue compared to *Pf*GluPho, the affinity for the substrate analogue differs by a factor of 1.5 in favour of the human G6PD.

	K_m (µM)		
Organism	**G6P**	**$NADP^+$**	**Reference**
Giardia 3 isolates	360	2.4	Bertram *et al*., 1983
	691	2.1	
	565	2.3	
Leishmania	150	12	Walter, 1979
Trypanosoma cruzi	300	87	Funayama *et al*., 1977
P. falciparum	11	0.8	Yoshida and Roth, 1987
P. falciparum	27	4.5	Kurdi-Haidar and Luzzatto, 1990
P. falciparum	18	5.1	Present study

Table 18: Summary of biochemical properties of G6PD from protozoa

The initial rate studies yielded double reciprocal plots suggesting a sequential (ternary complex) mechanism in which both substrates must first bind to the enzyme before product formation can occur. Product inhibition studies are among the most useful methods of elucidating the order of binding of substrates and the release of products which serve as an independent test that helps to differentiate between an ordered and random sequential mechanism. NADPH was found to be a mixed inhibitor with respect to G6P and a non-competitive inhibitor with respect to $NADP^+$. This inhibition pattern points toward an ordered sequential mechanism with $NADP^+$ binding first to the enzyme.

The dead end inhibitor glucoseamine 6-phosphate was found to be a mixed inhibitor with respect to both substrates G6P and $NADP^+$. This indicates that the inhibitor binds to the enzyme-$NADP^+$ binary complex and not to the free enzyme. Since glucoseamine 6-phosphate is an analogue of G6P, it seems likely that this inhibition pattern confirms that G6P binds only to the enzyme-$NADP^+$ complex and that *Pf*GluPho follows an ordered sequential mechanism. Tests using the NADP fragment ATP-ribose further confirmed the existence of an ordered sequential mechanism.

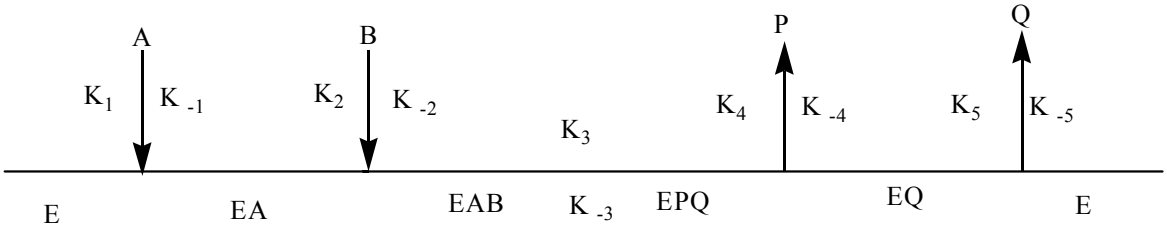

Figure 42: Schematic representation of an ordered sequential mechanism where E is the enzyme, A and B are the leading and following substrates.

An independent test of the mechanism may be applied using the Dalziel parameters (Table 6). For a compulsory order mechanism with substrate X binding first to the enzyme, $\Phi_{XY}/\ \Phi_Y$ gives K_d the dissociation constant for substrate X leaving the binary enzyme complex EX. This value should not change if an alternative substrate is used. Similarly the values of Φ_X and $\Phi_{XY}/\Phi_X\Phi_Y$ should remain unchanged regardless of the nature of substrate Y even though there may be changes in the individual values of $\Phi_{0,}\ \Phi_{Y,}\ \Phi_{XY}$ [Dalziel, 1957; Fromm, 1979]. There is a corresponding relationship if Y is the leading substrate. The relationship was tested for G6P by the alternative substrate 2-DeoxyG6P. If $NADP^+$ is the leading substrate the $\Phi_{\ NADP\ G6P}\ /\ \Phi_{G6P}$ should be equal to $\Phi_{\ NADP\ 2\text{-}DeoxyG6P}\ /\ \Phi_{2\text{-}DeoxyG6P}$. The mean values obtained were 5.1 for both cases (Table 6). The $\Phi_{\ NADP}$ with G6P as the substrate is 0.025 µMs and $\Phi_{\ NADP}$ with 2-DeoxyG6P as the substrate is 0.027 µMs which are quite similar. The mean values for $\Phi_{XY}/\Phi_X\Phi_Y$ ($\Phi_{\ NADP\ 2\text{-}DeoxyG6P}\ /\ \Phi_{2\text{-}DeoxyG6P}\ \Phi_{\ NADP}$ and $\Phi_{\ NADP\ G6P}\ /\ \Phi_{G6P}\ \Phi_{\ NADP}$) were found to be 190 against 204 s^{-1} (Table 6) which are almost similar. The results confirm that *Pf*GluPho exhibits a compulsory order mechanism with $NADP^+$ as the leading substrate.

Using a similar relationship Wang *et al*. [2002] were able to test for the possibility of the human G6PD exhibiting an ordered sequential mechanism with $NADP^+$ being the leading substrate. The $\Phi_{\ NADP\ G6P}\ /\ \Phi_{G6P}$ and $\Phi_{\ NADP\ 2\text{-}DeoxyG6P}\ /\ \Phi_{2\text{-}DeoxyG6P}$ were found to be very similar, 6.8 against 6.6 µM [Table 6]. The $\Phi_{\ NADP}$ with G6P as the substrate was 0.042 µM.s which was 6.6 fold lower than $\Phi_{\ NADP}$ with 2-DeoxyG6P as the substrate (0.28 µM.s). Consequently $\Phi_{XY}/\Phi_X\Phi_Y$ ($\Phi_{\ NADP\ 2\text{-}DeoxyG6P}\ /\ \Phi_{2\text{-}DeoxyG6P}\ \Phi_{\ NADP}$ and $\Phi_{\ NADP\ G6P}\ /\ \Phi_{G6P}\ \Phi_{\ NADP}$) also revealed very different values for the two sugar phosphate substrates (161 s^{-1} vs. 25 s^{-1}). A compulsory order mechanism with $NADP^+$ as the leading substrate was therefore ruled out for the human G6PD. Wang *et al*. [2002] went ahead to demonstrate that the human G6PD exhibits a rapid equilibrium random order mechanism.

The reaction of *Pf*GluPho's G6PD follows an ordered sequential mechanism as compared to the random order sequential mechanism found in the human G6PD. Comparing the catalytic efficiency (k_{cat}/K_m) between *Pf*GluPho's G6PD and the human G6PD (Table 5) demonstrates that *Pf*GluPho's G6PD is a more efficient in conversion of its substrates G6P (1.14 x 10^7 $M^{-1}S^{-1}$) and $NADP^+$ (3.98 x 10^7 $M^{-1}S^{-1}$) to products than its human homologue (G6P 2.9 x 10^6 $M^{-1}S^{-1}$ and $NADP^+$ 2.3 x 10^7 $M^{-1}S^{-1}$). These findings imply that *Pf*GluPho's G6PD is more efficient in the production of NADPH as compared to its human counterpart.

Atamna *et al*. [1994] demonstrated an increase in the PPP activity with parasite maturation from ring to trophozoite stage and suggested that this upregulation could be a consequence of increased parasite biomass and upregulation of the PPP enzymes (the increase in PPP is even larger than the increase in parasite biomass). In the light of our findings we would like to suggest that the upregulation of the PPP is due partly to the high efficiency in the production of NADPH by *Pf*GluPho which catalyses the first step of the PPP and not necessarily due to an up regulated synthesis of PPP enzymes.

5.1.2 *Pf*GluPho's 6-PGL

Time dependent assays for 6-PGL have been described earlier by Rakitzis and Papandreou, [1995], Bauer *et al*., [1983] and Schofield and Sols, [1976]. We modified the method in order to measure the 6-phosphogluconolactone available and the amount of 6-phosphogluconolactone consumed by the reaction catalysed by *Pf*GluPho's 6-PGL. Our modified method differs mainly from other methods in the way the experimental data was generated and analysed. The generation of 6-phosphogluconolactone by the action of an excess of G6PD, and subsequent determination of the amount of 6-phosphogluconolactone hydrolysed by the addition of an excess of 6-PGD has been employed by Schofield and Sols [1976] and also by Bauer *et al*. [1983]. However to this end Schofield and Sols [1976] have determined initial rate constants rather than the utilisation of reaction time course thereby introducing a methodological error [Rakitzis and Papandreou, 1995]. Bauer *et al*. [1983] have used log residual 6-phosphogluconolactone against reaction time plots to determine the rate constants of the uncatalysed hydrolysis of 6-phosphogluconolactone without using the end point of the reaction. In 6-PGL activity determinations, Bauer *et al*. [1983] have used two identical 6-phosphogluconolactone / 6-PGD solutions in one of which the 6-PGL preparation was added. Enzyme activity was then determined by subtracting concurrent absorbance values of the enzyme containing solution and the control solution. Rakitzis and Papandreou [1995] have on the other hand performed a time course study on the hydrolysis of 6-phosphogluconolactone with the change in absorbance being recorded and analysed. In this study involving *Pf*GluPho's 6-PGL, a time course study of 6-PGL activity was performed by monitoring the concentration of 6-phosphogluconolactone formed after the reaction catalysed by G6PD and 6-phosphogluconate formed after 6-PGL assay.

The principles of the method employed rest on two assumptions:

(1) That all the 6-phosphogluconolactone produced by action of *Pf*GluPho's G6P is immediately available to *Pf*GluPho's 6-PGL.

(2) The activity of 6-PGD is not influenced by the assay parameters and therefore not rate limiting in any way.

The plots of 6-phosphogluconolactone available against time and plots of 6-phosphogluconate against time gave linear plots. The K_m value for *Pf*GluPho's 6-PGL for its substrate 6-phosphogluconolactone was found to be 26.2 μM which is 1.45 times higher that exhibited by *Pf*GluPho's G6PD for its substrate G6P (18.1 μM). The V_{max} on the other hand was found to be 74.9 U/mg for *Pf*GluPho's 6-PGL compared to 116 U/mg exhibited by *Pf*GluPho's G6PD for G6P. The V_{max} differed by a factor of 1.5 in favour of G6PD. The catalytic efficiency (k_{cat}/K_m) was found to be 206 s^{-1} and 133 s^{-1} for *Pf*GluPho's G6PD and 6-PGL respectively, which implies that *Pf*GluPho's G6PD is catalytically more efficient than the lactonase.

Comparing the activity of *Pf*GluPho's 6-PGL to its human homologue revealed that although *Pf*GluPho's 6-PGL had a higher affinity for its substrate (K_m 26.2) when compared

to the human enzyme (K_m 32.5). The human enzyme on the other hand had a higher rate of substrate turnover (344 s^{-1}) as well as catalytic efficiency (1.0 x 10^7 $M^{-1}s^{-1}$) when compared to *Pf*GluPho's 6-PGL (133 s^{-1} and 5.08 x 10^6 $M^{-1}s^{-1}$).

Under conditions of oxidative stress, formation of mixed disulfides between glutathione and cysteines in proteins (glutathionylation) has not only been known to occur but implicated as a mechanism through which protein functions can be regulated by the redox status [Brigelius *et al*., 1983]. Glutathionylation takes place by thiol-disulfide exchange between protein sulfhydryls and oxidized glutathione (GSSG), a reversible process that can be catalyzed by glutaredoxin. The GSH/GSSG ratio is an indicator of the redox status of the cell, and the extent of protein glutathionylation will vary accordingly: a higher ratio will promote glutathionylation; a lower ratio will result in deglutathionylation/release of glutathione. Tests for *Pf*GluPho's 6-PGL assay in the presence of either GSSG or GSH in the presence or absence or glutaredoxin showed that *Pf*GluPho's 6-PGL activity was neither inhibited nor influenced any way. These findings imply that *Pf*GluPho's 6-PGL is not allosterically influenced or regulated by glutathionylation a finding that conforms to that found for other 6-phopshogluconolactonases [Hofer and Bauer, 1987]; although the activity of 6-PGL prepared from red blood cell lysates has been shown to be inactivated by GSSG [Fratelli *et al*., 2002].

One of the major aims of this study was to identify *Pf*GluPho's G6PD inhibitors as a strategy for rational drug development against malaria. We have been able to characterise fully the inhibition of compound 8807 against G6P and $NADP^+$. Compound 8807 was found to be non-competitive with respect to both the substrates. This implies that the inhibitor is able to bind to the enzyme-substrate complex. However the enzyme-substrate-inhibitor complex does not proceed to form product. The non-competitive phenomenom exhibited by compound 8807 has the advantage of not being overcome by increase in the concentration of the substrate.

The notion that different performance requirements may mediate natural selection for the high activity of different enzymes in a pathway and the realisation of the importance of the intrinsic chemical properties of metabolic intermediates helps to elucidate a puzzling but recurrent finding in *P. falciparum* evolutionary history and its adaptation towards overcoming oxidative stress. Namely adaptation of *P. falciparum* PPP to conditions that require very high rates of NADPH production is accompanied by a large increase in the substrate affinities namely G6P and $NADP^+$ by *Pf*GluPho's G6PD at the same time not being inhibited by its product NADPH but being rather more efficient in its production.

In the battle to eradicate malaria, effective drug targets are needed. An essential feature for a molecule to be considered as a potential drug target is that it must be distinguishable from its counterpart in the human host. The enzyme *Pf*GluPho might prove valuable in this respect, as mammals do not express this bifunctional enzyme, do not express insertion sequences within their two homologues and the enzymes differ in their mechanism of action. Besides *Pf*GluPho occupies position 75 of the TDR targets database against

neglected tropical diseases [http://tdrtargets.org]. In summary this study offers the first clear documentation of the cloning, heterologous expression and biochemical as well as kinetic characterisation of the bifunctional enzyme *Pf*GluPho.

5.2 Mouse IDO-1 and Mouse IDO-2

At least 3 forms of IDO have been thought to exist from the experiments of Shizu *et al*. [1978] but until recently only one form of IDO (IDO-1) has been heavily investigated. The identification of IDO-2 in man and mouse and the demonstration of its capacity using heterologously overexpressed protein to metabolise tryptophan along the kynurenine pathway adds a new dimension to the understanding of how this pathway is regulated under normal and abnormal physiological conditions. IDO-1 and TDO are two phylogenetically unrelated genes that have evolved to have a similar function (i.e. catalysing the first step in tryptophan catabolism). Although there are differences in enzyme activity with regard to substrates other than L-tryptophan, the major difference between IDO-1, IDO-2 and TDO that may play a role during the generation of functional diversity is the different expression patterns of the proteins. TDO is the enzyme responsible for tryptophan metabolism in the liver, but it is also expressed in the brain and epididymis [Haber *et al*., 1993; Britan *et al*., 2006]. IDO-1 is expressed in the intestines, kidney and reproductive system, including the epididymis, and is also induced in many tissues in response to stimuli such as inflammatory mediators. The overlapping expression of IDO-2 with the other two enzymes in the kidney, epididymis and liver might be taken to indicate some redundancy, but the different cellular localisation of the enzymes also suggests a distinct role for each of the enzymes [Ball *et al*., 2007].

	Mouse IDO-1	**Mouse IDO-2**
Molecular mass	45,335 Da	45,255 Da
pI	5.94	6.21
Amino acids	424	405
ε_{280} nm (assuming all Cys are reduced)	48220 M^{-1} cm^{-1}	40680 M-1 cm^{-1}
ε_{280} nm (assuming all Cys are oxidized)	48820 M^{-1} cm^{-1}	41280 M^{-1} cm^{-1}

Table 19: Comparison of other properties of mouse IDO-1 and IDO-2

Using the methylene blue/ ascorbic acid method IDO-2 exhibited K_m values which were approximately 300 fold higher than those exhibited by mouse IDO-1. Using a similar method (methylene blue/ ascorbic acid) the human IDO-2 protein as well as IDO-2 like proteins from lower vertebrates, such as Xenopus, have been reported to also exhibit L-tryptophan K_m values which are approximately 500–1000-fold higher than those of their corresponding IDO-1 enzymes [Yuasa *et al*., 2007]. When compared to the cytochrome b_5/ cytochrome P450 method a 20 fold decrease in the K_m value which was accompanied by 590 fold improvement in the V_{max} value was observed which implied that the enzyme had an improved substrate affinity as well as turnover capacity under the cytochrome b_5/ cytochrome P450 method. Substrate inhibition observed for IDO-2 at relatively high concentrations of L-tryptophan could be due to the formation of a low spin ferric enzyme complex with L-

tryptophan. A similar phenomenon had earlier been reported for IDO-1 by Sono [1989]. The substrate analogue inhibitor 1-methyl-D-tryptophan was found to inhibit IDO-2 whereas 1-methyl-L- tryptophan inhibited IDO-1. Similar IDO inhibition by substrate analogues has been reported by Metz *et al*. [2007].

Oligomerisation studies carried out on IDO-2 have revealed that the mouse IDO-2 exists as both a monomer of 45 kDa (45 %) and a dimer of 90 kDa (55 %). In the presence of DTT and GSH IDO-2 was found to exist predominantly as a monomer. The existence of IDO-2 as a monomer in the highly reductive environment of DTT and GSH could mean that dimerisation of IDO-2 involves intermolecular disulfide bonds and the enzyme could be regulated by glutathionylation or could have a redox regulated mechanism. These results could also imply that in the dimeric structure of IDO-2, the relative configuration of each monomer in the dimerized form might be changed by the association or dissociation of O_2 thus triggering a conformational change or signal transduction. This interpretation was based on the R-T transition of haemoglobin. Although we do not know what kind of cellular response is affected by IDO-2, it is very interesting to note that the redox state of the environment could determine the oligomeric structure of the enzyme. It is most likely that the redox sensing by IDO-2 leads to a conformational change which could be associated with the O_2 dissociation from the heme iron. The conformational change could initiate a signal transduction. The activities of IDO-1 as well as IDO-2 have been reported to be responsible for triggering signalling pathways such as phosphorylation of the translation initiation factor eIF-2α and translation of liver enriched inhibitory protein (LIP), an inhibitory isoform of CEPBβ transcription factor (Metz *et al*., 2007).

The induction of IDO has been implicated in cerebral malaria and many other diseases. Suppression of IDO activity by use of IDO inhibitors alone or in combination with other chemotherapeutics might provide another tool in the cerebral malaria armamentarium. Strikingly almost all IDO inhibitors known so far, whether competitive or non-competitive, retain the indole ring of the natural substrate tryptophan [Muller *et al*., 2005; Malachowski *et al*., 2005]. The compound 55D11 and its derivatives do not contain the indole ring of the natural substrate tryptophan and therefore it is not necessary for its inhibition activity. Currently the most potent IDO inhibitor reported is 3-butyl-β-carboline, a non-competitive inhibitor with a K_i of 3.3 μM [Peterson *et al*., 1993]. However the most commonly used inhibitor is 1-methyl-Trp, a commercially available compound with a K_i of 34 μM. Our inhibitor has a lower K_i of 0.05 μM compared to the 2 mostly known IDO inhibitors.

Cerebral malaria is the most severe complication of *P. falciparum* infection therefore an inhibitor with the capabilities to inhibit IDO and at the same time have some anti-malaria activity would be a big boost in the fight against cerebral malaria. Tests of compound 55D11 did not show significant antimalarial activity in the mouse model, parasitemia or survival of the mouse model [Austin and Hunt, personal communication]. This could be due to the compound being rapidly renally eliminated in the mouse model.

Further structure activity relationships using derivatives of 55D11 were done with the aim of discovering more potent IDO inhibitors. Compound KS 2 which is structurally similar to 55D11 was the most potent derivative with a percent inhibition value of 73.02 (at 5 µg/ml inhibitor concentration) for IDO. A clear structure function relationship was also observed in the inhibition of *P. falciparum* cell culture. However reproducibility of the inhibition assays was limited due to the instability of the enzyme and the compounds which were light sensitive. Nevertheless the inhibitory activity demonstrated by 55D11 and derivative KS 2 create new opportunities for further inhibitor development that avoids the pharmacological liabilities of the indole ring and leverage the wealth of chemical methods for benzene substitution.

5.3 Thioredoxin Networks

The redox-active protein plasmoredoxin which is unique and highly conserved among *Plasmodium* species was first described by Becker *et al*, [2003]. The physiological function of *Pf*Plrx is still unknown and the protein seems not to be essential for the survival of the parasite under conditions of oxidative stress as shown very recently by Buchholz *et al*, [2008]. One of the factors limiting the understanding of *Pf*Plrx function is the lack of information on target proteins and enzymes that interact with it. The present findings suggest that *Pf*Plrx participates in the regulation of at least 8 known metabolic functions and 2 other unknown functions (Table 20) in *P. falciparum* parasites. Although *Pf*Plrx has been reported to reduce ribonucleotide reductase [Becker *et al*., 2003], *Pf*Plrx could also be involved in other physiological capacities some of which are highlighted in Table 20.

Transcription/Translation
Elongation factor 2
40S ribosomal protein S12
Protein folding
Heat shock protein
Heat shock 70 kDa protein
Heat shock protein 86
Co-chaperone GrpE, putative
Disulfide isomerase, putative
Carbohydrate metabolism
Hexokinase
Pyruvate kinase, putative
Glyceraldehyde-3-phosphate dehydrogenase
Signal transduction
14-3-3 protein homologue, putative
14-3-3 Protein, putative
Conserved GTP-binding protein, putative
Polyamine metabolism
Ornithine aminotransferase
S-adenosylmethionine synthetase
Lipid metabolism
Acyl carrier protein, putative
Hemoglobin catabolism
HAP protein/Plasmepsin III
DNA synthesis and repair
Endonuclease iii homologue, putative
Ribonucleotide reductase small subunit
Others
Hypothetical protein
Hypothetical protein

Table 20: Functional clusters of *Pf*Plrx target proteins captured in the present study.

S-adenosyl-L-homocysteine hydrolase (SAHH) catalyzes the hydrolysis of S-adenosyl-L-homocysteine, produced from S-adenosyl-L-methionine dependent methylation reactions, into L-homocysteine and adenosine. Surface plasmon resonance analyses were carried out (Figure 41) in order to identify the cysteine(s) of the three redox-active proteins which are responsible for the interaction with SAHH. The study using *Pf*Plrx demonstrates that the C-terminal active site cysteine (Cys 63) is obviously involved in complex formation since its mutation into a serine significantly impairs binding to SAHH (Figure 41). This might be the reason why SAHH was not captured by the *Pf*Plrx affinity column.

From the study its evident that *Pf*Plrx could be playing a role in a wide variety of pathways. Further studies are required to elucidate the modes and functional consequences of these interactions.

References

Allison A C, Clyde D F. **(1961)**. Malaria in African children with deficient erythrocyte glucose-6-phosphate dehydrogenase. *BMJ*, **1**: 1346.

Allison A C. **(1960)**. Glucose 6-phosphate dehydrogenase deficiency in red blood cells of East Africans. *Nature*, **186**: 531.

Atamna H, Pascarmona G, Ginsburg H. **(1994)**. Hexose monophosphate shunt activity in intact *Plasmodium falciparum* infected erythrocytes and in free parasites. *Mol Biochem Parasitol*, **67**: 79–89.

Au S W N, Gover S, Lam V M S, Adams J M. **(2000)**. Human G6PD: the crystal structure reveals a structural $NADP^+$ molecule and provides insight into enzyme deficiency. *Structure*, **8**: 293-303.

Austin C J D, Astelbauer F, Kosim-Satyaputra P, Ball H J, Willows R D, Jamie J F, Hunt N H. **(2008)**. Mouse and human indoleamine 2,3-dioxygenase display some distinct biochemical and structural properties. *Amino acids* in press.

Austin C J D, Mizdrak J, Matin A, Sirijovski N, Kosim-Satyaputra P, Willows R D, Roberts T H, Truscott R J W, Polekhina G, Parker M W, Jamie J F. **(2004)**. Optimised expression and purification of recombinant human indoleamine 2,3-dioxygenase. *Protein Expression and Purification*, **37**: 392–398.

Ball H J, Sanchez-Perez A, Weiser S, Austin C J, Astelbauer F, Miu J, McQuillan J A, Stocker R, Jermiin L S, Hunt NH. **(2007)**. Characterization of an indoleamine 2,3 dioxygenase like protein found in humans and mice. *Gene*, **396**: (1) 203–213.

Ball H J, Yuasa H J, Austin C J D, Weiser S, Hunt N H. **(2008)**. Molecules in focus: Indoleamine 2,3 dioxygenase-2; a new enzyme in the kynurenine pathway. *Int. J. Biochem & Cell Biol* in press.

Barnes K I, Durrheim D N, Little F, Jackson A, Mahta U, Allen E, Dlamini S S, Tsoka J, Bredenkamp B, Mthembu D J, White N J, Sharp B L. **(2005)**. Effect of artemether-lumefantrine policy and improved vector control on malaria burden in KwaZulu-Natal, South Africa. *PLoS Med*, **2**:e330.

Battistuzzi G, D'Urso M, Toniolo D, Persico G M, Luzzatto L.**(1985)**. Tissue specific levels of G6PD correlate with methylation at the 3´ end of the gene. *Proc. Natl. Acad. Sci.USA*, **82**: 1465-69.

Bauer H P, Srihari T, Jochims J C, Hofer H W. **(1983)**. 6-phosphogluconolactonase. Purification, Properties and Activities in Various Tissues. *Eur. J. Biochem*, **133**: 163-168.

Bayoumi R A, Nur-E-Kamal M S, Tadayyon M, Mohamed K K, Mahboob B H, Qureshi M M, Lakhani M S, Awaad M O, Kaeda J, Vulliamy T J, Luzzatto L. **(1996)**. Molecular characterization of erythrocyte glucose-6-phosphate dehydrogenase deficiency among school boys of Al-Ain district, United Arab Emirates. *Hum Hered*, **46**: 136–41.

Becker K, Kanzok S M, Iozef R, Fischer M, Schirmer R H, Rahlfs S. **(2003)**. Plasmoredoxin, a novel redox active protein unique for malarial parasites. *Eur. J. Biochem*, **270**: 1057–1064.

Becker K, Koncarevic S, Hunt N H. **(2005)** Oxidative stress and antioxidant defence in malaria parasites, pp. 365-383. *In* Sherman I W (Ed.), *Molecular Approaches to Malaria*. ASM Press, Washington, D.C.

Becker K, Rahlfs S, Nickel C, Schirmer R H. **(2003)**. Glutathione function and metabolism in the malarial parasite *Plasmodium falciparum*. *Biol. Chem*, **348**: 551–566.

Becker K, Tilley L, Vennerstrom J L, Roberts D, Rogerson S, Ginsburg H. **(2004)** Oxidative stress in malaria parasite infected erythrocytes: host parasite interactions. *Int. J. Parasitol*, **34**: 163–189.

Bender D A. **(1989)**. The kynurenine pathway of tryptophan metabolism. In: Stone, T.W. Ed., *Quinolinic Acid and the Kynurenines*. CRC Press, Boca Raton, FL, pp. 3–24.

Bertram M A, Meyer E A, Lile J D, Morse S A. **(1983)**. A comparison of isoenzymes of five axenic Giardia isolates. *J. Parasitol*, **69**: 793-801.

Beutler E, Yeh M, Fairbanks V F. **(1962)**. The normal human female as a mosaic of X chromosome activity: studies using the genes of G6PD deficiency as a marker. *Proc. Natl. Acad. Sci.USA*, **48**: 9–16.

Beutler E. **(1984)**. Red cell metabolism: *A manual of biochemical methods*, 3rd edn. Grune and Stratton New York.

Beutler E. **(1994)**. G6PD deficiency. *Blood*, **84**: 3613–36.

Bhattarai A, Ali A S, S. Patrick Kachur P S, Mårtensson A, . Abbas A K, Rashid Khatib R, Al-mafazy A, Ramsan M, Rotllant G,. Gerstenmaier J F, Fabrizio Molteni F, Abdulla S, Montgomery S M, Kaneko A, Björkman A. **(2007)**. Impact of artemisinin based combination therapy and insecticide-treated nets on malaria burden in Zanzibar. *PLoS Med*, **4**: (11) 309.

Bienzle U, Ayeni O, Lucas A O, Luzzatto L. **(1972)**. Glucose-6-phosphate dehydrogenase and malaria: greater resistance of females heterozygous for enzyme deficiency and of males with non-deficient variant. *Lancet*, **1**: 107–10.

Bienzle U, Lucas A O, Ayeni 0, Luzzatto L. **(1972)**. Glucose-6-phosphate dehydrogenase and malaria. Greater resistance of females heterozygous for enzyme deficiency and of males with non-deficient variant. *Lancet*, **1**: 107.

Birke S, Kim H W, Periclou A, Schorsch B, Grouse D, Craney C. **(1989)**. Kinetics of human erythrocyte glucose-6-phosphate dehydrogenase dimmers. *Biochim. Biophys. Acta*, **999**: 243-247.

Bradford M M. **(1976)**. A rapid and sensitive method for the quantitation of microgram quantities of protein utilising the principle of protein dye binding. *Anal. Biochem*, **72**: 248-254.

Brandes H K, Larimer F W, Geck M K, Stringer C D, Schurmann P, Hartman F C. **(1993)**. Direct identification of the primary nucleophile of thioredoxin f. *J. Biol. Chem*, **268**: 18411–18414.

Brigelius R, Muckel C, Akerboom T P, Sies H. **(1983)**. Identification and quantitation of glutathione in hepatic protein mixed disulfides and ist relationship to glutathione disulfide. *Biochem Pharmacol*, **32**: 2529–2534.

Britan A, Maffre V, Tone S, Drevet J R. **(2006)**. Quantitative and spatial differences in the expression of tryptophan metabolizing enzymes in mouse epididymis. *Cell Tissue Res*, **324**: 301–310

Brito I. **(2001)**. Eradicating malaria: high hopes or a tangible goal? *Health Policy at Harvard*, **2**: 61–66.

Buchholz K, Rahlfs S, Schirmer RH, Becker K, Matuschewski K. **(2008)**. Depletion of *Plasmodium berghei* plasmoredoxin reveals a non-essential role for life cycle progression of the malaria parasite. *PLoS ONE*, **3**: e2474.

Cabrera V M, González P, Salo W L. **(1996)**. Human enzyme polymorphism in the Canary Islands: VII—G6PD Seattle in Canarians and north African Berbers. *Hum Hered*, **46**: 197–200.

Campanale N, Nickel C, Daubenberger C, Wehlan D, Gorman J, Foley M, Becker K, Tilley L. **(2003)**. Identification and characterisation of a series of haem-interacting proteins of the malaria parasite, *Plasmodium falciparum*. *J. Biol. Chem*, **278**: 27354–27361.

Cappadoro M, Giribaldi G, O'Brien E, Turrini F, Mannu F, Ulliers D, Simula G, Luzzatto L, Arese P. **(1998)**. Early phagocytosis of glucose-6-phosphate dehydrogenase (G6PD) deficient erythrocytes parasitized by *Plasmodium falciparum* may explain malaria protection in G6PD deficiency. *Blood*, **92**: 2527–34.

Cappellini M D, Fiorelli G. **(2008)** Glucose-6-phosphate dehydrogenase deficiency. *Lancet*, **371**: 64–74.

Cappellini M D, Martinez di Montemuros F, De Bellis G, De Bernardi S, Dotti C, Fiorelli G. **(1996)**. Multiple G6PD mutations are associated with clinical and biochemical phenotype similar to that of G6PD Mediterranean. *Blood*, **87**: 3953–58.

Cappellini M D, Sampietro M, Toniolo D, Carandina G, Martinez di Montemuros F, Tavazzi D, Fiorelli G. **(1994)**. G6PD Ferrara I has the same two mutations as G6PD A (–) but a distinct biochemical phenotype. *Hum Genet*, **93**: 139–42.

Clark I A, Cowden W B, Hunt N H, Maxwell L E, Mackie E J. **(1984)**. Activity of divicine in *Plasmodium vinckei* infected mice has implications for treatment of favism and epidemiology of G-6-PD deficiency. *Br J Haematol*, **57**: 479.

Clarke J L, Scopes D A, Sodeinde O, Mason P J. **(2001)**. Glucose-6-phosphate dehydrogenase 6-phosphogluconolactonase: A novel bifunctional enzyme in malaria parasites. *Eur J Biochem*, **268**: 2013–2019.

Clarke J L, Sodeinde O, Mason P J. **(2003)**. A unique insertion in *Plasmodium berghei* glucose-6-phosphate dehydrogenase-6-phosphogluconolactonase: evolutionary and functional studies. *Mol Biochem Parasitol*, **127**: 1–8.

Clarke S E, Bøgh C, Brown R C, Pinder M, Walraven G E L, Lindsay S W. **(2001)**. Do untreated bednets protect against malaria? *Transactions of the Royal Society of Tropical Medicine and Hygiene*, **95**: 457–462.

Cooper D W, Irwin P H. **(1968)**. Glucose-6-phosphate dehydrogenase: evidence for tetrameric structure in doves (*Streptopelia*). *Proc. Natl. Acad. Sci.USA*, **61**: 979-981.

Cosgrove M S, Gover S, Naylor C E, Vandeputte-Rutten L, Adams J M, Levy R H. **(2000)**. An examination of the role of Asp-177 in the His-Asp catalytic dyad of *Leuconostoc mesenteroides* Glucose-6-phosphate dehydrogenase: X-ray structure and pH dependence of kinetic parameters of the D177N mutant enzyme. *Biochemistry*, **39**: 15002-15011.

Cosgrove M S, Naylor C E, Paludan S, Adams J M, Levy R H. **(1998)**. On the mechanism of the reaction catalysed by Glucose-6-phosphate dehydrogenase. *Biochemistry*, **37**:15002-15011.

Cotton D W K, Sutorius A H M. **(1971)**. Inhibiting effects of some antimalarial substances on glucose-6-phosphate dehydrogenase. *Nature*, **233**: 197.

Crooke A, Diez A, Mason J P, Bautista J M. **(2006)**. Transient silencing of *Plasmodium falciparum* glucose-6-phosphate dehydrogenase-6-phosphogluconolactonase. *FEBS*, **273**: 1537-1546.

Daily J P. **(2006)**. Antimalarial drug therapy: the role of parasite biology and drug resistance. *J. Clinical Pharmacol*, **46**:1487-1497.

Daubener W, Spors B, Hucke C, Adam R, Stins M, Kim K S, Schroten H. **(2001)**. Restriction of *Toxoplasma gondii* growth in human brain microvascular endothelial cells by activation of indoleamine 2,3-dioxygenase. *Infect. Immun*, **69**: 6527–6531.

Davies J, Jacob F. **(1968)**. Genetic mapping of the regulator and operator genes of lac operon. *J. Mol. Biol*, **36**: 469-518.

De Vita G, Alcalay M, Sampietro M, Cappellini M D, Fiorelli G, Toniolo D. **(1989)**. Two point mutations are responsible for G6PD polymorphism in Sardinia. *Am J Hum Genet*, **44**: 233–40.

Delarue M, Duclert-Savatier N, Miclet E, Haouz A, Giganti D, Ouazzani J, Lopez P, Nilges M, Stoven V. **(2007)**. Three dimensional structure and implications for the catalytic mechanism of 6-phosphogluconolactonase from *Trypanosom brucei*. *J. Mol. Biol*, **366**: 868-881.

Delcarte J, Fauconnier M, Jacques P, Matsui K, Thonart P, Marlier M. **(2003)**. Optimization of expression and immobilized metal ion affinity chromatographic purification of recombinant (His) 6-tagged cytochrome P450 hydroperoxide lyase in *Escherichia coli*. *Biomed. Life Sci*, **786**: 229–236.

Desjardins R E, Canfield C J, Heynes J D, Chulay J D. **(1979)**. Quantitative assessment of antimalarial activity *in vitro* by semi automated microdilution technique. *Antimicrob Agents Chemother*, **16**: 710-718

Eckman J, Eaton J W. **(1979)**. Dependence of *Plasmodium* glutathione metabolism on the host cell. *Nature,* **278**: 754-756.

Egan T J, Combrinck J M, Egan J, Hearne G R, Marques H M, Ntenteni S, Sewell B T, Smith P J, Taylor D, van Schalkwyk D A, Walden J C. **(2002)**. Fate of haem iron in the malaria parasite *Plasmodium falciparum*. *Biochem Journal,* **365**: 343–347.

Fairall L, Schwabe J W, Chapman L, Finch J T, Rhodes D. **(1993)**. The crystal structure of a two zinc-finger peptide reveals an extension to the rules for zinc-finger/DNA recognition. *Nature,* **366** (6454): 483-7.

Fernandes A P, Holmgreen A. **(2004)**. Glutaredoxins: glutathione dependent redox enzymes with functions far beyond a simple thioredoxin backup system. *Antioxid Redox Signal*, **6**: 63-74

Fernstrom J D, Wurtman R J, **(1972)**. Brain serotonin content: physiological regulation by plasma neutral amino acids. *Science*, **178**: 414–416.

Fidock D A, Rosenthal P J, Croft S L, Brun R, Nwaka S. **(2004)**. Antimalarial drug discovery: efficacy models for compound screening: http://www.mmv.org/Files Upld/164.pdf

Fiorelli G, Manoussakis C, Sampietro M, Pittalis S, Guglielmino C R, Cappellini M D. **(1989)**. Different polymorphic variants of glucose-6-phosphate dehydrogenase (G6PD) in Italy. *Ann Hum Genet*, **53**: 229–36.

Fivelman Q L, Adagu I S, Warhurst D C. **(2004)**. Modified fixed ratio isobologram method for studying *in-vitro* interactions between atovaquone and proguanil or dihydroatemisinin against drug resisitant strains of *Plasmodium falciparum*. *Antimicrob Agents Chemother*, **48**: 4097-4102.

Fletcher K A, Canning M V, Theakston R D G. **(1977)**. Electrophoresis of glucose-6- phosphate and 6-phosphogluconate dehydrogenase in erythrocytes from malaria infected animals. *Ann. Trop. Med. Parasitol*, **71**: 125-130.

Frank J E. **(2005)**. Diagnosis and management of G6PD deficiency. *Am Fam Physician*, **72**: 1277–82.

Fratelli M, Demol H, Puype M, Casagrande S, Eberini I, Salmona M, Bonetto V, Mengozzi M, Duffieux F, Miclet E, Bachi A, Vandekerckhove J, Gianazza E, Ghezzi P. **(2002)**. Identification by redox proteomics of glutathionylated proteins in oxidatively stressed human T lymphocytes. *Proc. Natl. Acad. Sci.USA*, **99**: (6) 3505–3510.

Fraternali F, Van Gunstern W F. **(1996)**. An efficient mean solvation force for use in molecular dynamics simulation of proteins in aqueous solution. *J. Mol. Biol*, **256**: (5) 939-948.

Frumento G, Rotondo R, Tonetti M, Damonte G, Benatti U, Ferrara G B. **(2002)**. Tryptophan derived catabolites are responsible for inhibition of T and natural killer cell proliferation induced by indoleamine 2,3-dioxygenase. *J. Exp. Med*, **196**: 459–468.

Fujigaki S, Saito K, Sekikawa K, Tone S, Takikawa O, Fujii H, Wada H, Noma A, Seishima M. **(2001)**. Lipopolysaccharide induction of indoleamine 2,3-dioxygenase is mediated dominantly by an IFN-gammaindependent mechanism. *Eur. J. Immunol*, **31**: 2313–2318.

Funayama S, Ito I Y, Veiga L A. **(1977)**. Trypanosoma cruzi: kinetic properties of glucose-6-phosphate dehydrogenase. *Exp. Parasitol*, **43**: 376-381.

Gaetani G D, Parker G C, Kirkman H N. **(1974)**. Intracellular restraint: a new basis for the limitation in response to oxidative stress in human erythrocytes containing low activity variants of glucose-6-phosphate dehydrogenase. *Proc. Natl. Acad. Sci.USA*. **71**: 3584–87.

Ganczakowski M, Town M, Kaneko A, Bowden D K, Cleg J B, Luzzatto L. **(1995)**. Multiple glucose-6-phosphate dehydrogenase deficient variants correlate with malaria endemicity in the Vanuatu archipelago (South-Western Pacific). *Am J Hum Genet*, **56**: 294–301.

Gardner M J, Hall N, Fung E, White O, Berriman M, Hyman R W, Carlton J M, Pain A, Nelson K E, Bowman S, Paulsen I T, James K, Eisen J A, Rutherford K, Salzberg S L, Craig A, Kyes S, Chan M S, Nene V, Shallom S J, Suh B, Peterson J, Angiuoli S, Pertea M, Allen J, Selengut J, Haft D, Mather M W, Vaidya A B, Martin D M A, Fairlamb A H, Fraunholz M J, Roos D S, Ralph S A, McFadden G I, Cummings L M, Subramanian G M, Mungall C, Venter C J, Carucci D J, Hoffman S L, Newbold C, Davis R W, Fraser C M, Barrell B.**(2002)**. Genome sequence of the human malaria parasite *Plasmodium falciparum*. *Nature*, **419**: 498–511.

Gilles H M, Fletcher K A, Hendrickse R G, Lindner R, Reddy S, Allan N. **(1967)**. Glucose-6-Phosphate dehydrogenase deficiency, sickling, and malaria in African children in South Western Nigeria. *Lancet,* **1**: 138.

Ginsburg H, Famin O, Zhang J, Krugliak M. **(1998)**. Inhibition of glutathione dependent degradation of heme by chloroquine and amodiaquine as a possible basis for their antimalarial mode of action. *Biochem. Pharmacol*, **56**: 1305–1313.

Golenser J, Miller J, Spira D T, Kosower N S, Vande waa, J A, Jensen J B. **(1988)**. Inhibition of intraerythrocytic development of *Plasmodium falciparum* in glucose-6-phosphate dehydrogenase deficient erythrocytes is enhanced by oxidants and crisis form factor. *Trop Med Parasitol*, **39**: 272-276.

Gould B J and Goheer M A. **(1976)**. Kinetic mechanism from steady state kinetics of the reaction catalysed by baker's Yeast Glucose 6-phosphate dehydrogenase in solution and covalently attached to sepharose. *Biochem Journal*, **157**: 389 – 393.

Greene L S. **(1993)**. G6PD deficiency as protection against *falcipurum* malaria: An epidemiologic critique of population and experimental studies. *Yearbook Phys Anthropol*, **17**: 153, (suppl 3).

Greenwood B M, Fidock D A, Kyle D E, Kappe S H I, Alonso P L, Collins H F, Duffy P E. **(2008)**. Malaria: progress, perils, and prospects for eradication. *J. Clinical Investigation*, **118**: (4) 1266-76.

Guggenmoos-Holzmann I, Bienzle U, Luzzatto L. **(1981)**. *Plasmodium falciparum* malaria and human red cells: II red cell genetic traits and resistance against malaria. *Int J Epidemiol*; **10**: 16–22.

Haber R, Bessette D, Hulihan-Giblin B, Durcan M J, Goldman D. **(1993)**. Identification of tryptophan 2,3-dioxygenase RNA in rodent brain. *J. Neurochem*, **60**: 1159–1162.

Harwaldt P, Rahlfs S, Becker K. **(2002)**. Glutathione S-transferase of the malarial parasite *Plasmodium falciparum*: characterization of a potential drug target. *Biol. Chem*, **383**: 821–830.

Hawley W A, Phillips-Howard P A, ter Kuile F O, Terlouw D J, Vulule J M, Ombok M, Nahlen B L, Gimnig J E, Kariuki S K, Kolczak M S, Hightower A W. **(2003)**. Community wide effects of permethrin-treated bed nets on child mortality and malaria morbidity in western Kenya. *Am J Trop Med Hyg*, **68**: 121-127.

Hayaishi O, Yoshida R, Takikawa O, Yasui H, **(1984)**. Indoleamine dioxygenase a possible biological function. pp. 33–42 *In*: Schlossberger H G, KochenW, Linzen B, Steinhart H. (Eds). *Progress in Tryptophan and Serotonin Research*. De Gruiter, W. Berlin.

Hempelmann E, Wilson R J M. **(1981)**. Detection of glucose-6-phosphate dehydrogenase in malaria parasites. *Mol. Biochem. Parasitol*, **2**: 197-204.

Heyes M P, Brew B J, Martin A, Price A M, Salazar A M, Sidtis J J, Yergey J A, Mouradian M M, Sadler A E, Keilp J, Rubinow D, Markey S P. **(1991)**. Quinolinic acid in cerebrospinal fluid and serum in HIV-1 infection: relationship to clinical and neurologic status, *Ann. Neurol*, **29**: 202-209.

Hirata H, Hayaishi O, **(1975)**. Studies on Indoleamine 2,3-dioxygenase. Superoxide anion as substrate. *J. Biol. Chem*, **250**: 5960–5966.

Hirono A, Fujii H, Takano T, Chiba Y, Azuno Y, Miwa S. **(1997)**. Molecular analysis of eight biochemically unique glucose-6-phosphate dehydrogenase variants found in Japan. *Blood*, **89**: 4624–27.

Hirono A, Kuhl W, Gelbart T, Forman L, Fairbanks V F, Beutler E. **(1989)**. Identification of the binding domain for NADP+ of human glucose-6-phosphate dehydrogenase by sequence analysis of mutants. *Proc. Natl. Acad. Sci. USA,* **86**: 10015-10017.

Hofer H W, Bauer H P. **(1987)**. 6-Phosphogluconolactonase. *Cell Biochem and function*, **5**: 97-99.

Hoffman S L, Rustama D, Punjabi N H, Surampaet B, Sanjaya B, Dimpudus A J, McKee K T Jr, Paleologo F P, Campbell J R, Marwoto H. **(1998)**. High-dose dexamethasone in quinine-treated patients with cerebral malaria: a doubleblind, placebo-controlled trial. *J Infect Dis*, **158**: 325-331.

Janney S K, Joist J H, Fitch C D. **(1986)**. Excess release of ferrriheme in G6PD-deficient erythrocytes: possible cause of haemolysis and resistance to malaria. *Blood*, **67**: 331-333.

Jeffery J, Persson B, Wood I, Bergman T, Jeffery R, Jornvall H. **(1993)**. Glucose 6-phosphate dehydrogenase structure function relationships and the *Pichia jadinii* enzyme structure. *Eur. J. Biochem*, **212**: 41-49.

Kanzok S M, Schirmer R H, Turbachova I, Iozef R, Becker K. **(2000)**. The thioredoxin system of the malaria parasite Plasmodium falciparum. Glutathione reduction revisited. *J. Biol. Chem,* **275**: 40180–40186.

Kar S, Seth S, Seth P K. **(1992)**. Prevalence of malaria in Ao Nagas and its association with G6PD and HbE. *Hum Biol*, **64**: 187.

Karimi M, Martinez di Montemuros F, Danielli M G, Farjadian S, Afrasiabi A, Fiorelli G, Cappellini M D. **(2003)**. Molecular characterization of glucose-6-phosphate dehydrogenase deficiency in the Fars province of Iran. *Haematologica*, **88**: 346–47.

Kidson C, Gorman J G. **(1962)**. A challenge to the concept of selection by malaria in glucose-6-phosphate dehydrogenase deficiency. *Nature*, **196**: 49.

Killeen G F, Smith T A, Ferguson H M, Mshinda H, Abdulla S, Lengeler C, Kachur S P. **(2007)**. Preventing childhood malaria in Africa by protecting adults from mosquitoes with insecticide treated nets. *PLoS Medicine*, **4**: (7):e229.

Knox W E. **(1966)**. The regulation of tryptophan pyrrolase activity by tryptophan. *Adv. Enzyme Regul,* **4**: 287–297.

Kotake Y, Masayama T. **(1937)**. Uber den mechanismus der kynurenine-bildung aus tryptophan. Hoppe-Seyler's Z. *Physiol. Chem*, **243**: 237–244.

Kuby S A, Wu J T, Roy R N. **(1974)**. Glucose 6-phosphate dehydrogenase from brewers yeast. *Arch. Biochem. Biophys*, **165**: 153-178.

Kurdi-Haidar B, Luzzatto L. **(1990)**. Expression and characterization of glucose-6-phosphate dehydrogenase of *Plasmodium fulcipurum*. *Mol. Biochem. Parasitol*, **41**: 83.

Kurdi-Haidar B, Mason P J, Berrebi A, Ankra-Badu G, al-Ali A, Oppenheim A, Luzzatto L.**(1990)**. Origin and spread of G6PD variant (G6PD Mediterranean) in the Middle East. *Am J Hum Genet*, **47**: 1013–19.

Laemmli U K. **(1970)**. Cleavage of structural proteins during assembly of the head of bacteriophage T4. *Nature*, **227**: 680-685.

Lambros C, Vanderberg J P. **(1979)**. Synchronisation of *Plasmodium falciparum* erythrocytic stages in culture. *J Parasitol*, **65**: 418-420.

Langer B W, Phisphumvidhi P, Friedlander Y. **(1967)**. Malaria parasite metabolism: the pentose cycle in *Plasmodium berghei*. *Exp.Parasitol*, **20**: 68-76.

Lengeler C. **(2000)**. Insecticide-treated bednets and curtains for preventing malaria. *Cochrane Database of Systematic Reviews*, (2):CD000363 (update Cochrane Database of Systematic Reviews, 2004,(2): CD000363).

Levy, H R. **(1979)**. Glucose-6-phosphate dehydrogenase. *Adv. Enzymol*, **48**: 97-192.

Lim F, Wulliamy T, Abdalla S H. **(2005)**. An Ashkenazi Jewish woman presenting with favism. *J Clin Pathol*, **58**: 317–19.

Ling I T, Wilson R J M. **(1988)**. Glucose 6-phosphate-dehydrogenase activity of the malaria parasite *Plasmodium falciparum*. *Mol. Biochem. Parasitol*, **31**: 47-56.

Looareesuwan S, Wilairatana P, Vannaphan S, Wanaratana V, Wenisch C, Aikawa M, Brittenham G, Graninger W, Wernsdorfer W H. **(1998)**. Pentoxifylline as an ancillary treatment for severe *falciparum* malaria in Thailand. *Am J Trop Med Hyg*, **58**: 348-353.

Loria P, Miller S, Foley M, Tilley L. **(1999)**. Inhibition of the peroxidative degradation of haem as the basis of action of chloroquine and other quinoline antimalarials. *Biochem Journal*, **339**: 363–370.

Luzzatto L, Battistuzzi G. **(1985)**. Glucose-6-phosphate dehydrogenase, in Harris H, Hirschhorn K. (Eds): *Advances in Human Genetics*, New York, NY, Plenum, p 217.

Luzzatto L, Bienzle U. **(1979)**. The malaria/G6PD hypothesis. *Lancet*, **1**: 1183–84.

Luzzatto L, Metha A, Vulliamy T. **(2001)** Glucose 6-phosphate dehydrogenase deficiency. In: Scriver C R, Beaudet A L, Sly W S, Eds. *The metabolic and molecular bases of inherited disease*, 8th edn. Columbus: McGraw-Hill, 4517–53.

Luzzatto L, O'Brien S, Usanga E, Wanachiwanawin W. **(1986)** Origin of G6PD polymorphism: Malaria and G6PD deficiency, in Yoshida A, Beutler E. (Eds): *Glucose-6-Phosphate Dehydrogenase*, Orlando, FL, Academic, , p 181.

Luzzatto L, Usanga E A, Reddy S. **(1969)**. Glucose 6-phosphate dehydrogenase deficient red cells: Resistance to infection by malarial parasites. *Science*, **164**: 839.

MacKenzie C R, Heseler K, Muller A, Daubener W. **(2007)**. Role of indoleamine 2,3-dioxygenase in antimicrobial defence and immuno-regulation: tryptophan depletion versus production of toxic kynurenines. *Curr. Drug Metab*, **8**: (3), 237–244.

Maghzal G J, Thomas S R, Hunt N H, Stocker R. **(2008)**. Cytochrome b5, not superoxide anion radical, is a major reductant of indoleamine 2,3-dioxygenase in human cells. *J. Biol. Chem*, **283**: (18) 12014-12025

Malachowski W P, Metz R, Prendergast G C, Muller A J. **(2005)**. A review of IDO mechanism, inhibition and therapeutic applications. *Drugs Future*, **30**: 897.

Marsh K, English M, Crawley J, Peshu N. **(1996)**. The pathogenesis of severe malaria in African children. *Ann Trop Med Parasitol*, **90**: 395-402.

Martin S K, Miller L H, Alling D, Okoye V C, Esan G J, Osunkoya B O, Deane M. **(1979)**. Severe malaria and glucose-6-phosphate-dehydrogenase deficiency: a reappraisal of the malaria/ G6PD hypothesis. *Lancet*, **1**: 524–26.

Martin S K. **(1980)**. Modified G-6-PD/ malaria hypothesis. *Lancet*, **1**: 5l.

Martinez di Montemuros F, Dotti C, Tavazzi D, Fiorelli G, Cappellini M D. **(1997)**. Molecular heterogeneity of glucose-6-phosphate dehydrogenase (G6PD) variants in Italy. *Haematologica*, **82**: 440–45.

Mason P J, Sonati M F, MacDonald D, Lanza C, Busutil D, Town M, Corcoran C M, Kaeda J S, Stevens D J, AI-Ismail S, Altay C, Hatton C, Lewis D S, McMullin M F, Meloni T, Paul B, Pippard M, Prentice A G, Vulliamy T J, Luzzatto L. **(1995)**. New glucose 6-phosphate dehydrogenase mutations associated with chronic anaemia. *Blood*, **85**: 1377–80.

Metz R, Duhadaway J B, Kamasani U, Laury-Kleintop L, Muller A J, Prendergast G C. **(2007)**. Novel tryptophan catabolic enzyme IDO2 is the preferred biochemical target of the antitumor indoleamine 2,3-dioxygenase inhibitory compound D-1-methyltryptophan. *Cancer Res*, **67**: (15) 7082–7087.

Miller J, Golenser J, Kullgren B, Spira D T. **(1984)**. *Plasmodium falciparum*: thiol status and growth in normal and deficient human erythrocytes. *Exp Paraasitol*, **57**: 239-247.

Miroux B, walker J E. **(1996)**. Over production of proteins in Escherichia coli: mutant host that allow synthesis of some membrane proteins and globular proteins at high levels. *J Mol Biol*, **260**: 289-298.

Motohashi K, Kondoh A, Stumpp M T, Hisabori T. **(2001)**. Comprehensive survey of proteins targeted by chloroplast thioredoxin. *Proc. Natl. Acad. Sci. USA*, **98**: 11224–11229.

Motulsky A G. **(1961)**. Glucose-6-phosphate dehydrogenase deficiency haemolytic disease of the newborn, and malaria. *Lancet*, **1**: 1168.

Muller A J, Malachowski W P, Prendergast G C. **(2005)**. Indoleamine 2,3-dioxygenase in cancer: targeting pathological immune tolerance with small molecule inhibitors. *Exp. Opin. Ther. Targets*, **9**: 831-849.

Muller S. **(2004)**. Redox and antioxidant systems of the malaria parasite *Plasmodium falciparum*. *Eur. J. Biochem*, **268**: 1404-1409.

Munn D H, Shafizadeh E, Attwood J T, Bondarev I, Pashine A, Mellor A L. **(1999)**. Inhibition of T cell proliferation by macrophage tryptophan catabolism. *J. Exp. Med*, **189**: 1363–1372.

Murphy S C, Breman J G. **(2001)**. Gaps in the childhood malaria burden in Africa: cerebral malaria, neurological sequelae, anemia, respiratory distress, hypoglycemia, and complications of pregnancy. *Am J Trop Med Hyg*, **64**: 57-67.

Murray M F. **(2007)**. The human indoleamine 2,3-dioxygenase gene and related human genes. *Curr. Drug Metab*, **8**: (3), 197–200.

Nyarango P M, Gebremeskel T, Mebrahtu G, Mufunda J, Abdulmumini U, Ogbamariam A, Kosia A, Gebremichael A, Gunawardena D, Ghebrat Y, Okbaldet Y. **(2006)**. A steep decline of malaria morbidity and mortality trends in Eritrea between 2000 and 2004: the effect of combination of control methods. *Malar. J*, **5**: 33 (April 2006).

O'Brien E, Kurdihaidar B, Wanachiwanawin W, Carvajal J.L, Vulliamy T. J, Cappadoro M, Mason P J, Luzzatto L. **(1994)**. Cloning of the glucose 6-phosphate dehydrogenase gene from *Plasmodium falciparum*. *Mol. Biochem. Parasitol*, **64**: 313-326.

Oo M, Tin-Shwe, Marlar-Than, O'Sullivan W J. **(1995)** Genetic red cell disorders and severity of *falciparum* malaria in Myanmar. *Bull World Health Organ*; **73**: 659–65.

Peitsch M C, Wells T N, Stampf D r, Sussman J L. **(1995)**. The swiss 3D image collection and PDB-Browser on the world wide web. *Trends Biochem Sci*, **20**: (2) 82-84.

Perkins M N, Stone T W. **(1982)**. Specificity of kynurenic acid as an antagonist of synaptic transmission in rat hippocampal slices. *Neurosci.Lett*, **18**: 432–436.

Perng L, Chiou S-S, Liu T C, Chang J G. **(1992)**. A novel C to T substitution at nucleotide 1360 of cDNA which abolishes a natural HhaI site accounts for a new G6PD deficiency gene in Chinese. *Hum Mol Genet*, **1**: 205–08.

Persson B, Jornvall H, Wood I, Jeffrey J. **(1991)**. Functionally important regions of glucose-6-phosphate dehydrogenase defined by the *Saccharomyces cerevisiae* enzyme and its differences from the mammalian and insect forms. *FEBS Lett*, **198**: 485-491.

Pfefferkorn E R. **(1984)**. Interferon gamma blocks the growth of *Toxoplasma gondii* in human fibroblasts by inducing the host cells to degrade tryptophan. *Proc. Natl. Acad. Sci. USA*, **81**: 908–912.

Rahlfs S, Becker K. **(2001)**. Thioredoxin peroxidases of the malarial parasite *Plasmodium falciparum. Eur. J. Biochem*, **268**: 1404–1409.

Rahlfs S, Fischer M, Becker K. **(2001)**. *Plasmodium falciparum* possesses a classical glutaredoxin and a second, glutaredoxin-like protein with a PICOT homology domain. *J. Biol. Chem*, **276**: 37133–37140.

Rahlfs S, Schirmer R H, Becker K. **(2002)**. The thioredoxin system of *Plasmodium falciparum* and other parasites. *Cell. Mol. Life Sci*, **59**: 1024–1041.

Rahlfs S, Nickel C, Deponte M, Schirmer R H, Becker K. **(2003)**. *Plasmodium falciparum* thioredoxins and glutaredoxins as central players in redox metabolism. *Redox Rep*, **8**: 246-250.

Rakitzis E T, Papandreou P. **(1995)**. Kinetic analysis of 6-phosphogluconolactone hydrolysis in hemolysates. *Biochem. Mol. Biol. Int*, **37**: (4) 747-755

Riddle M S, Jackson J L, Sanders J W, Blazes D L. **(2002)**. Exchange transfusion as an adjunct therapy in severe *Plasmodium falciparum* malaria: a meta-analysis. *Clin Infect Dis*, **34**: 1192-1198.

Roberts D R, Manguin S, Mouchet J. **(2000)**. DDT house spraying and re-emerging malaria. *Lancet*, **356**: 330–332.

Roth E F Jr. Raventos-Suarez C, Rinaldi A, Nagel R L. **(1983)**. Glucose-6-phosphate dehydrogenase deficiency inhibits in vitro growth of *Plasmodium falciparum*. *Proc. Natl. Acad. Sci.USA*, **80**: 298.

Roth E Jr, Schulman S. **(1988)**. The adaptation of *Plasmodium falciparum* to oxidative stress in G6PD deficient human erythrocytes. *Br J Haematol*, **70**: 363.

Ruwende C, Hill A. **(1998)**. Glucose-6-phosphate dehydrogenase deficiency and malaria. *J Mol Med*, **76**: 581–88.

Ruwende C, Khoo S C, Snow R W, Yates S N R, Kwiatkowski D, Gupta S, Warn P, Allsopp C E M, Gilbert S C, Peschu N, Newbold C I, Greenwood B M, Marsh K, Hill A V S. **(1995).** Natural selection of hemi and heterozygotes for G6PD deficiency in Africa by resistance to severe malaria. *Nature*; **376**: 246–49.

Saito K, Nowak T S, Markey S P, Heyes M P. **(1993)**. Mechanism of delayed increase in kynurenine pathway metabolism in damaged brain regions following transient cerebral ischemia. *J Neurochem*, **60**: 180-192.

Sanni L A, Thomas S R, Tattam B N, Moore D E, Chaudhri G, Stocker R, Hunt N H, **(1998)**. Dramatic changes in oxidative tryptophan metabolism along the kynurenine pathway in experimental cerebral and noncerebral malaria. *Am. J. Pathol*, **152**: 611–619.

Schimke R T, Sweeney E W, Berlin C M. **(1965)**. The roles of synthesis and degradation in the control of rat liver tryptophan pyrrolase. *J. Biol. Chem*, **240**: 322–331.

Schofields P J, Sols A. **(1976)**. Rat liver 6-phosphogluconolactonase: a low Km enzyme. *Biochem. Biophys. Res. Comm*, **71**: 1313-1318.

Schroten H, Spors B, Hucke C, Stins M, Kim K S, Adam R, Daubener W. **(2001)**. Potential role of human brain microvascular endothelial cells in the pathogenesis of brain abscess: inhibition of Staphylococcus aureus by activation of indoleamine 2,3-dioxygenase. *Neuropediatrics*, **32**: 206–210.

Schurr A, Rigor B M. **(1993)**. Quinolinate potentiates the neurotoxicity of excitatory amino acids in hypoxic neuronal tissue in vitro. *Brain Res*, **617**: 76–80.

Schutz G, Chow E, Feigelson P. **(1972)**. Regulatory properties of hepatic tryptophan oxygenase. *J. Biol. Chem*, **247**: 5333–5337.

Schwarcz R, Whetsell W O, Mangano R M. **(1983)**. Quinolinic acid: an endogenous metabolite that produces axon-sparing lesions in rat brain. *Science,* **219**: 316–318.

Scopes D A, Bautista J M, Vulliamy T J, Mason P J. **(1997)**. *Plasmodium falciparum* Glucose-6-Phosphate dehydrogenase the N-terminal portion is homologous to a predicted protein encoded near to Glucose-6-Phosphate dehydrogenase in *Haemophilus Influenzae. Mol. Microbiol*; **23**: 847-848.

Seitz R, Egbring R, Gaus W, Hogel J, Hassemer M, Nawroth P P, Kern P, Dietrich M. **(1997)**. Supportive pentoxifylline in *falciparum* malaria: no effect on tumor necrosis factor alpha levels or clinical outcome: a prospective, randomized, placebo-controlled study. *Am J Trop Med Hyg*, **56**: 397-403.

Shahabuddin M, Rawlings D J, Kaslow D C. **(1994)**. A novel glucose 6-phosphate dehydrogenase in *Plasmodium falciparum*: cDNA and primary protein structure. *Biochim. Biophys. Acta*, **1219**: 191-194.

Shane T R, Stocker R. **(1999)**. Redox reactions related to indoleamine 2,3-dioxygenase and tryptophan metabolism along the kynurenine pathway. *Redox Rep*, **4**: 199–220.

Shaw A, McRee D E, Vacquier V D, Stout C D. **(1993)**. The crystal structure of lysin, a fertilization protein. *Science*, **262** (5141): 1864-7. (McRee, **1993**)

Sherman I W. **(1979)**. Biochemistry of *Plasmodium* (malaria parasites). *Microbiol. Rev*, **43**: 453-495.

Shimizu T, Nomiyama S, Hirata F, Hayaishi O. **(1978)**. Indoleamine 2,3-Dioxygenase: Purification and some properties. *J. Biol. Chem*, **253**: 4700–4706.

Sidransky H. **(1976)**. Nutritional disturbances of protein metabolism in the liver. *Am. J. Pathol*, **84**: 649–668.

Singh B, Sung K L, Matusop A, Radhakrishnan A, Shamsul S S G, Cox-Singh J, Thomas L, Conway D J. **(2004)**. A large focus of naturally acquired *Plasmodium knowlesi* infections in human beings. *Lancet*, **363**: 1017–1024.

Siniscalco M, Bemini L, Filippi G, Lane B, Meera-Khan P, Piomelli S, Rattazzi M. **(1966)**. Population genetics of haemoglobin variants, thalassaemia and G-6-PD deficiency, with particular reference to the malaria hypothesis. *Bull WHO*, **34**: 379.

Siniscalco M, Bemini L, Latte B, Motulsky A G. **(1961)**. Favism and thalassaemia in Sardinia and their relationship to malaria. *Nature*, **190**: 1179.

Slater A F, Cerami A. **(1992)**. Inhibition by chloroquine of a novel haem polymerase enzyme activity in malaria trophozoites. *Nature,* **355**: 167–169.

Snow R W, Guerra C A, Noor A M, Myint H Y, Hay S I. **(2005).** The global distribution of clinical episodes of *Plasmodium falciparum* malaria. *Nature*, **434**: 214-217.

Snow R W, Korenkromp E L, Gouws E. **(2004)**. Pediatric mortality in Africa: *Plasmodium falciparum* malaria as a cause or risk. *Am J Trop Med Hyg*, **71** (Suppl. 2), 16–24.

Snow R W, Trape J F, Marsh K. **(2001)**. The past, present and future of childhood malaria mortality in Africa. *Trends Parasitol*, **17**: 593–597.

Sono M. **(1989)**. Enzyme kinetics and spectroscopic studies of inhibitor and effector interactions with indoleamine 2, 3-dioxygenase. 2. Evidence for existence of another binding site in the enzyme for indole derivative effectors. *Biochemistry*, **28**: 5400-5407.

Sono M, Cady S G. **(1989)**. Enzyme kinetics and spectroscopic studies of inhibitor and efector interactions with Indoleamine 2,3-dioxygenase. 1. Norharman and 4-Phenylimidazole binding to the enzyme inhibitors and heme ligands. *Biochemistry*, **28**: 5392-5399.

Stone T W, Behan W M, Jones P A, Darlington L G, Smith R A. **(2001)**. The role of kynurenines in the production of neuronal death, and the neuroprotective effect of purines. *J. Alzheimers Dis*, **3**: 355–366.

Stone T W, Mackay G M, Forrest C M, Clark C J, Darlington L G, **(2003)**. Tryptophan metabolites and brain disorders. *Clin. Chem. Lab. Med*, **41**: 852–859.

Stumpp M T, Motohashi K, Hisabori T. **(1999)**. Chloroplast thioredoxin mutants without active-site cysteines facilitate the reduction of the regulatory disulphide bridge on the gamma subunit of chloroplast ATP synthase. *Biochem. J*, **341**:157–163.

Su X, kirkman L A, Fujioka H, Wellems T E. **(1997)**. Complex polymorphisms in a ~330kDa protein are linked to chloroquine resistant *P. falciparum* in Southeast Asia and Africa. *Cell*, **91**: 593-603.

Sugimoto H, Oda S, Otsuki T, Hino T, Yoshida T, Shiro Y. **(2006)**. Crystal structure of human indoleamine 2,3-dioxygenase: Catalytic mechanism of O_2 incorporation by a heme-containing dioxygenase. *Proc. Natl. Acad. Sci.USA*, **103**: (8) 2611–2616.

Sztajer H, Gamain B, Aumann K D, Slomianny C, Becker K, Brigelius-Flohe´, R, Flohe´ L. **(2001)**. The putative glutathione peroxidase gene of *Plasmodium falciparum* codes for a thioredoxin peroxidase. *J. Biol. Chem*, **276**: 7397–7403.

Takikawa O, Tagawa Y, Iwakura Y, Yoshida R, Truscott R J. **(1999)**. Interferon gamma dependent/ independent expression of indoleamine 2,3-dioxygenase. Studies with interferon gamma knockout mice. *Adv. Exp.Med. Biol*, **467**: 553–557.

Takikawa O, Kuroiwa T, Yamazaki F, Kido R. **(1988)**. Mechanism of interferon-gamma action characterization of indoleamine 2,3-dioxygenase in cultured human-cells induced by interferongamma and evaluation of the enzyme-mediated tryptophan degradation in its anticellular activity. *J. Biol. Chem*, **263**:2041–2048

Tilley L, Loria P, Foley M. **(2001)**. Chloroquine and other quinoline antimalarials, pp. 87–122. *In* Rosenthal P J. (Ed.), *Antimalarial Chemotherapy*, Humana Press, Totowa, NJ.

Towbin H, Staehelin T, Gordon J. **(1979)**. Electrophoretic transfer of proteins from polyacrylamide gels to nitrocellulose sheets: procedure and some applications. *Proc. Natl. Acad. Sci.USA*. **76**: 4350-4354

Trager W, Jensen J B. **(1976)**. Human malaria parasites in continous culture. *Science*, **193**: 673-679.

Turrini F, Schwarzer E, Arese P. **(1993)**. The involvement of hemozoin toxicity in depression of cellular immunity. *Parasitol today*, **9**: 297-300.

Usanga E A, Luzzatto L. **(1985)**. Adaptation of *Plasmodium falciparum* to glucose 6-phosphate dehydrogenase deficient host red cells by production of parasite-encoded enzyme. *Nature*, **313**: 793.

van Hensbroek M B, Palmer A, Onyiorah E, Schneider G, Jaffar S, Dolan G, Memming H, Frenkel J, Enwere G, Bennett S, Kwiatkowski D, Greenwood B. **(1996)**. The effect of a monoclonal antibody to tumor necrosis factor on survival from childhood cerebral malaria. *J Infect Dis*, **174**: 1091-1097.

Verdoucq L, Vignols F, Jacquot J P, Chartier Y, Meyer Y. **(1999)**. In vivo characterization of a thioredoxin h target protein defines a new peroxiredoxin family. *J. Biol. Chem*, **274**: 19714–19722.

Vulliamy T J, Kaeda J S, Ait-Chafa D, Mangerini R, Roper D, Barbot J, Mehta A B, Athanassiou-Metaxa M, Luzzatto L, Mason P J. **(1998)**. Clinical and haematological consequences of recurrent G6PD mutations and single new mutation causing chronic non spherocytic haemolytic anaemia. *Br J Haematol*, **101**: 670–75.

Walter R D. **(1979)**. Purification and properties of glucose-6-phosphate dehydrogenase from *Leishmania tropica* promastigotes. *Tropen med. Parasitol*, **30**: 3-8.

Warrell D A, Looareesuwan S, Warrell M J, Kasemsarn P, Intaraprasert R, Bunnag D, Harinasuta T. **(1982)**. Dexamethasone proves deleterious in cerebral malaria: a double blind trial in 100 comatose patients. *N Engl J Med*, **306**: 313-319.

Watanabe Y, Yoshida R, Sono M, Hayaishi O, **(1981)**. Immunohistochemical localization of indoleamine 2,3-dioxygenase in the argyrophilic cells of rabbit duodenum and thyroid gland. *J. Histochem. Cytochem*, **29**: 623–632.

Weiwei H, Wang Y, Liu W, Zhou C Z. **(2007)**. Crystal structure of Saccharomyces ceravisiae 6-phosphogluconate dehydrogenase Gnd l. *BMC Structural Biology*, **7**: 38.

White N J, Nosten F, Looareesuwan S, Watkins W M, Marsh K, Snow R W, Kokwaro G, Ouma J, Hien T T, Molyneux M E, Taylor T E, Newbold C I, Ruebush T K 2nd,Danis M, Greenwood B M, Anderson R M, Olliaro P. **(1999)**. Averting a malaria disaster. *Lancet*, **353**: 1965–1967.

WHO. **(1989)**. Glucose-6-phosphate dehydrogenase defi ciency. *Bull World Health Organ*; **67**: 601–11.

WHO. **(1999)**. Making a difference. The World Health Report 1999. *Health Millions*, **25**:3-5.

WHO. **(2007)**. WHO releases new guidance on insecticide-treated mosquito nets: Recent data from Kenya "ends the debate" about how to deliver the nets. http://www.who.int/mediacentre/news/releases/2007/pr43/en/index.html

Wong J T, Hanes C S. **(1962)**. Kinetic formulations for enzymatic reactions involving two substrates. *Can. J. Biochem. Physiol*. **40**: 763–804.

World Health Organization, Communicable Diseases Cluster **(2000)**. Severe *falciparum* malaria. *Trans R Soc Trop Med Hyg,* **94** (suppl 1):S1-S90.

Yoshida A, Roth Jr E F. **(1987)**. Glucose-6-phosphate dehydrogenase of Malaria parasite *Plasmodium falciparum*. *Blood*, **69** (5) 1528-1530.

Yoshida R, Hayaishi O. **(1987)**. Indoleamine 2,3-dioxygenase. *Meth. Enzymol*, **142**: 188–195.

Young S N, Leyton M, **(2002)**. The role of serotonin in human mood and social interaction. Insight from altered tryptophan levels. *Pharmacol. Biochem.Behav*, **71**: 857–865.

Yuasa H J, Takubo M, Takahashi A, Hasegawa T, Noma H, Suzuki T. **(2007)**. Evolution of vertebrate indoelamine 2,3-dioxygenases. *J. Mol. Evol*, **65**: (6) 705–714.

Zhang F, Schmidt W G, Hou Y, Williams A F, Jacobson K. **(1992)**. Spontaneous incorporation of the glycosyl-phosphatidylinositol-linked protein Thy-1 into cell membranes. *Proc. Natl. Acad. Sci. USA,* **89**: 5231–5235.

Zucker J R. **(1996)**. Changing patterns of autochthonous malaria transmission in the United States: a review of recent outbreaks. *Emerg. Infect. Dis*, **2**:37–43.